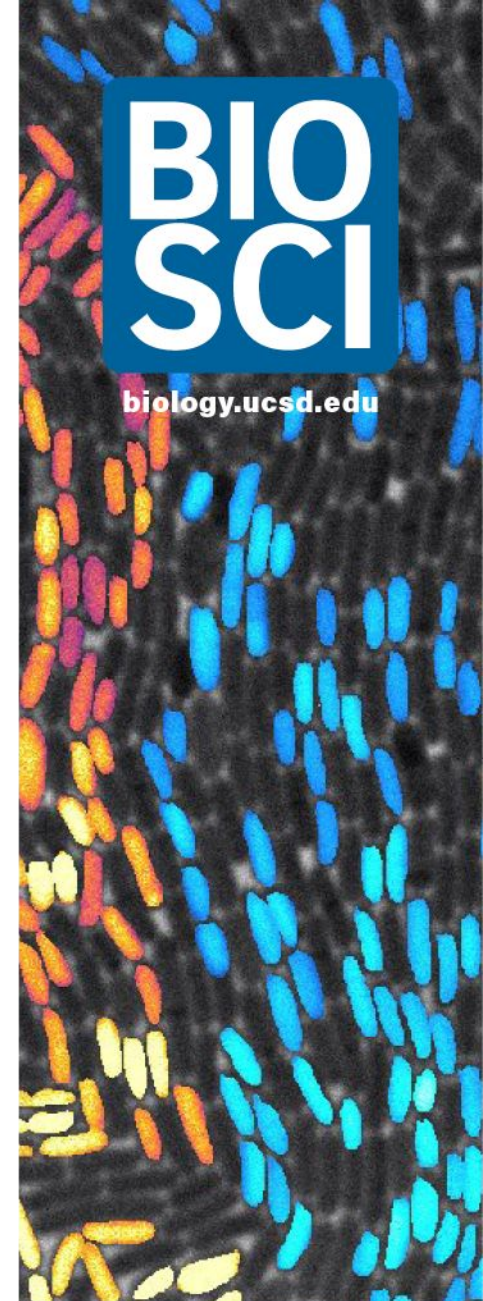


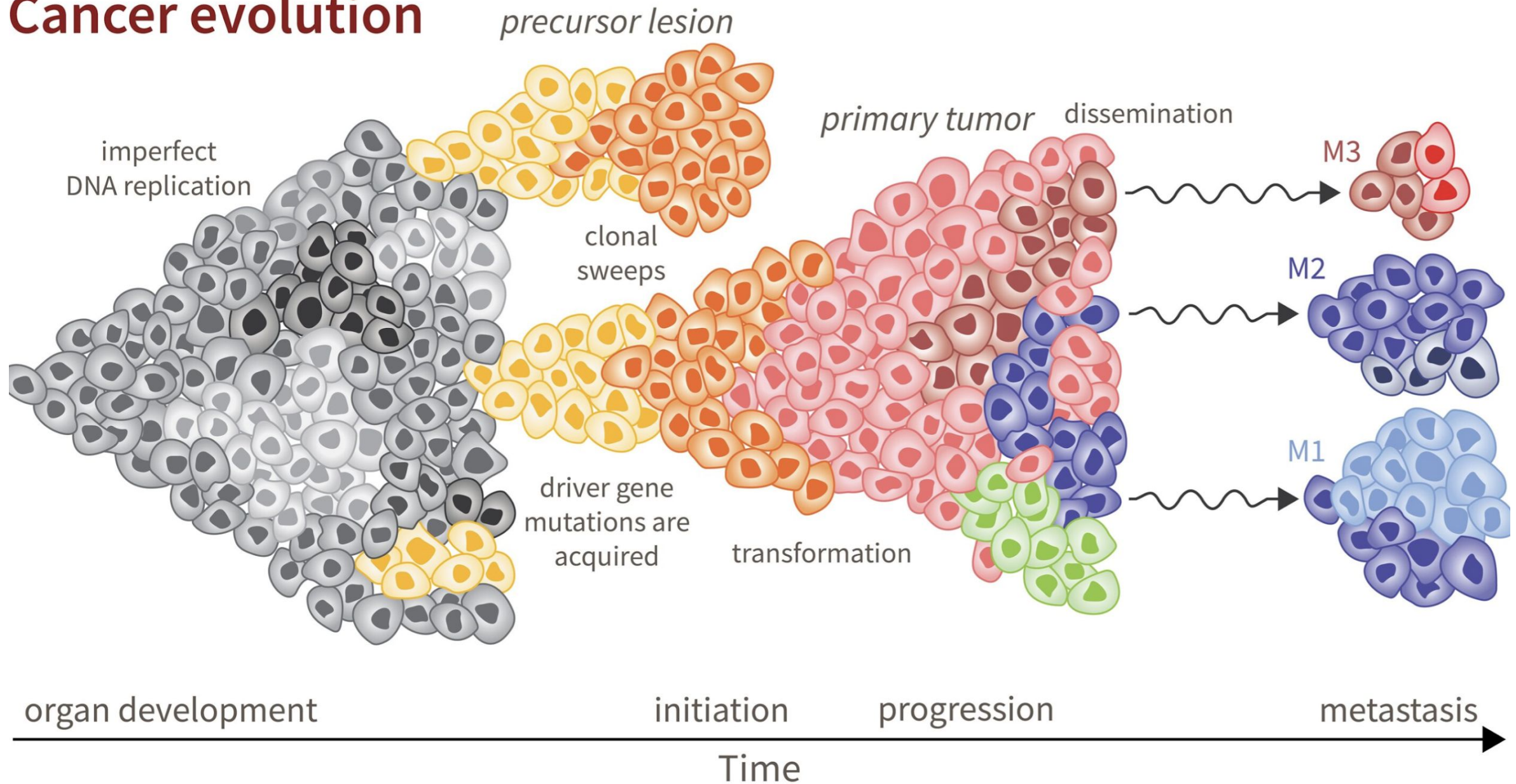
Cancer Dynamics, Evolution, and Spatial Structure

1. Basic concepts in cancer biology and cancer evolution
2. Modeling cell evolution in pre-malignant tissue
3. Evolutionary dynamics in spatially structured cell populations

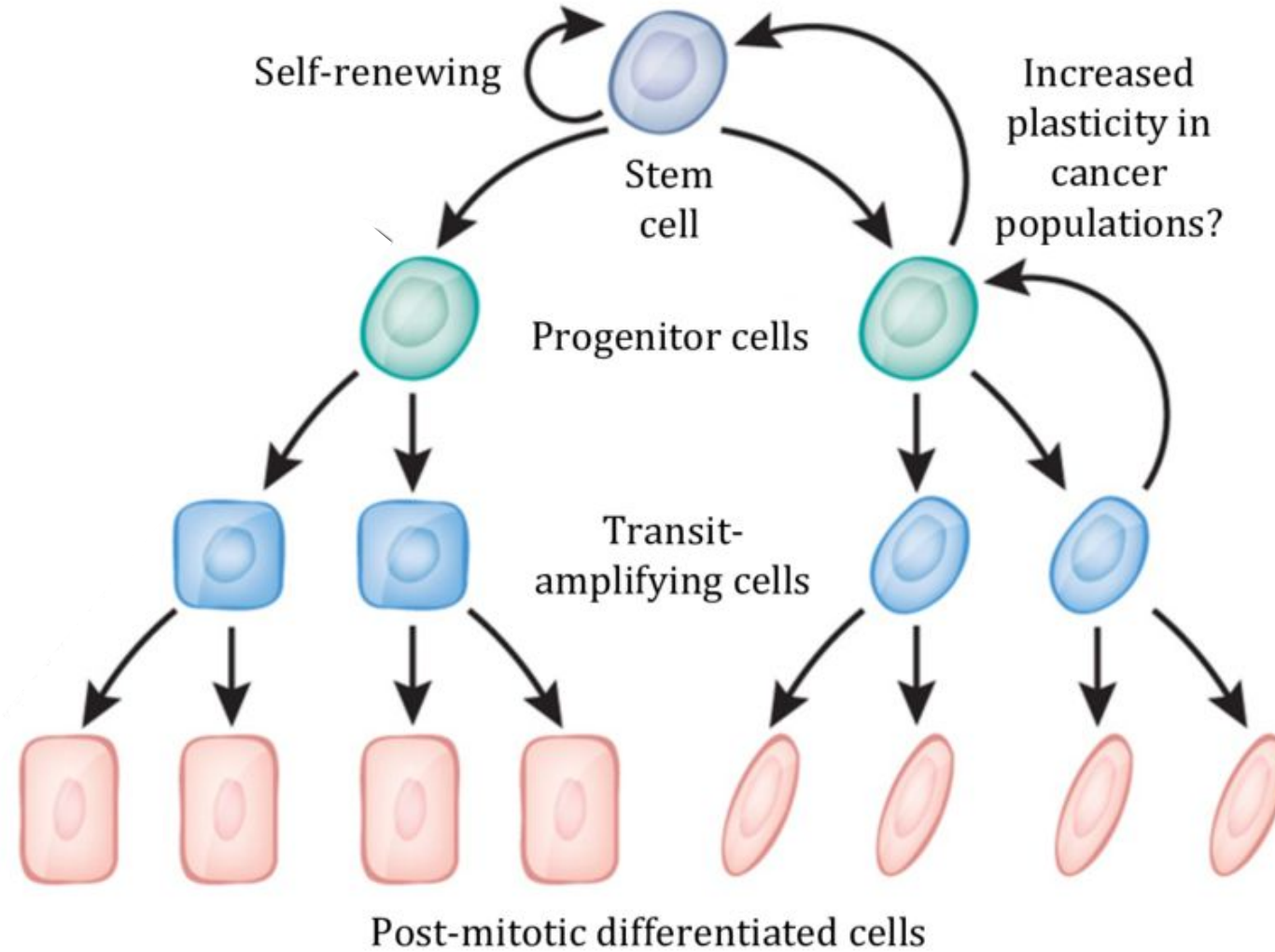
Dominik Wodarz
Dept. of Ecology, Behavior & Evolution
dwodarz@ucsd.edu



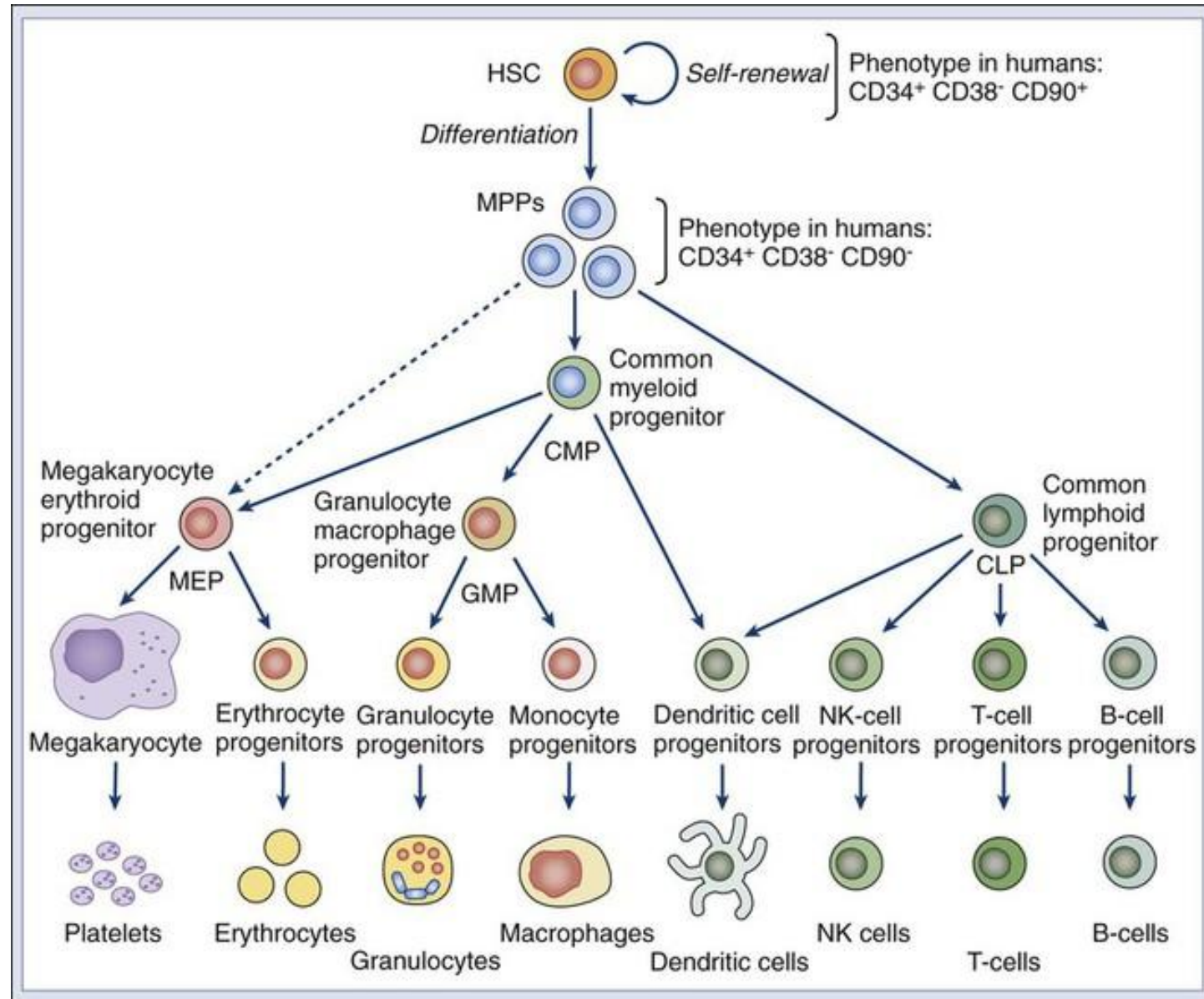
1. Cancer evolution



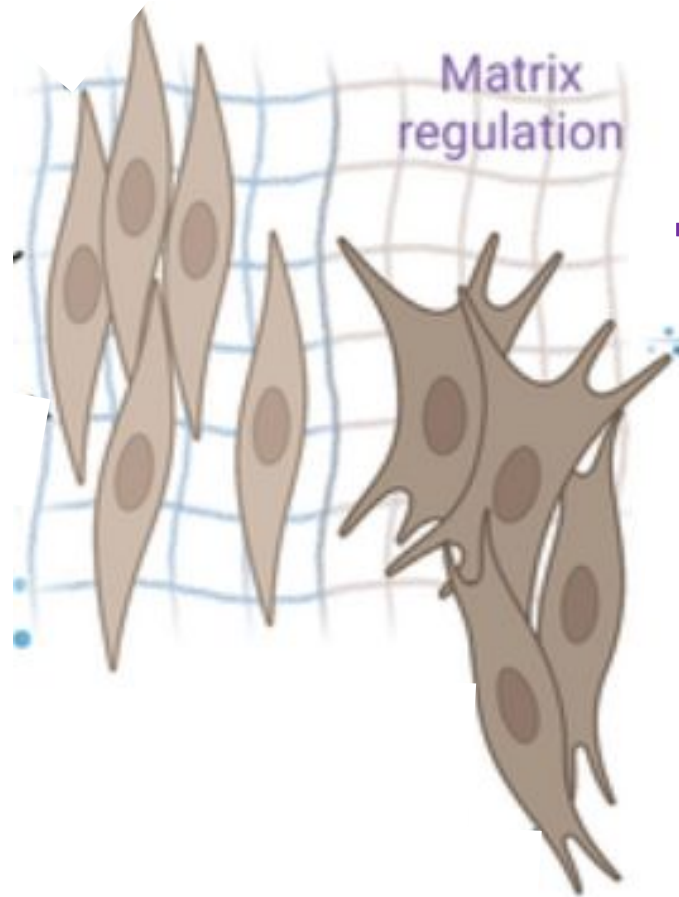
Healthy tissue architecture and homeostasis



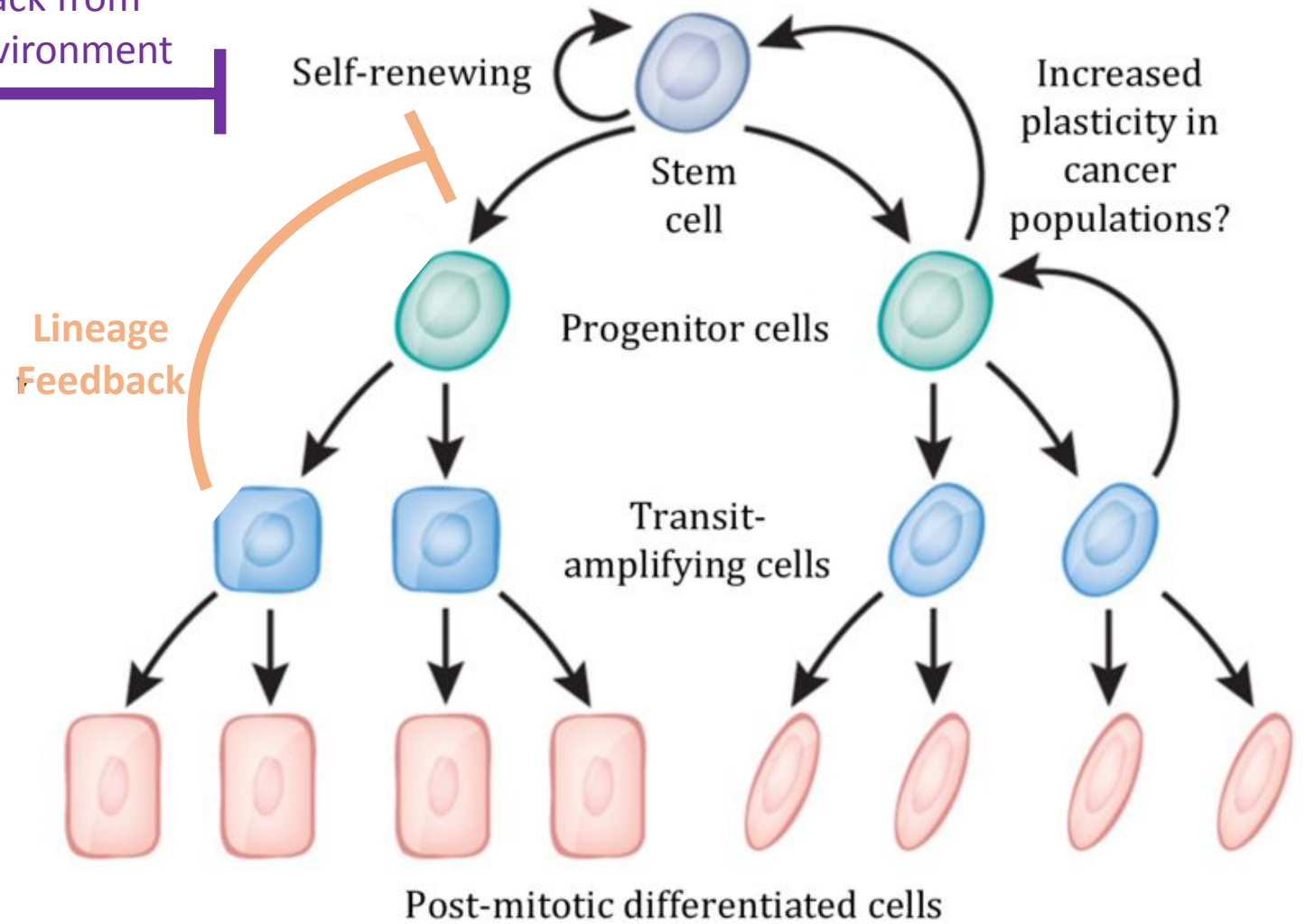
For example: Blood



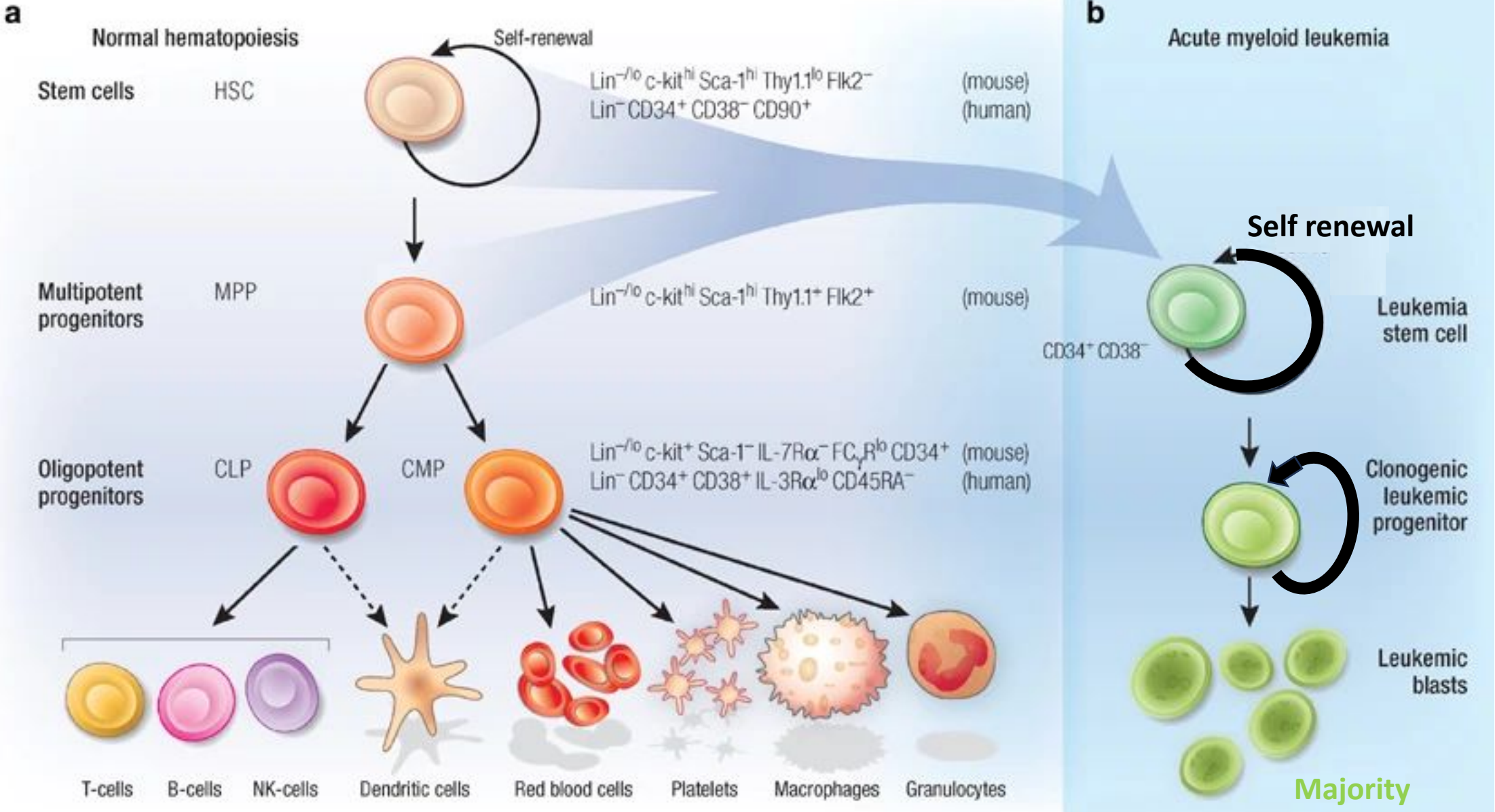
Homeostasis



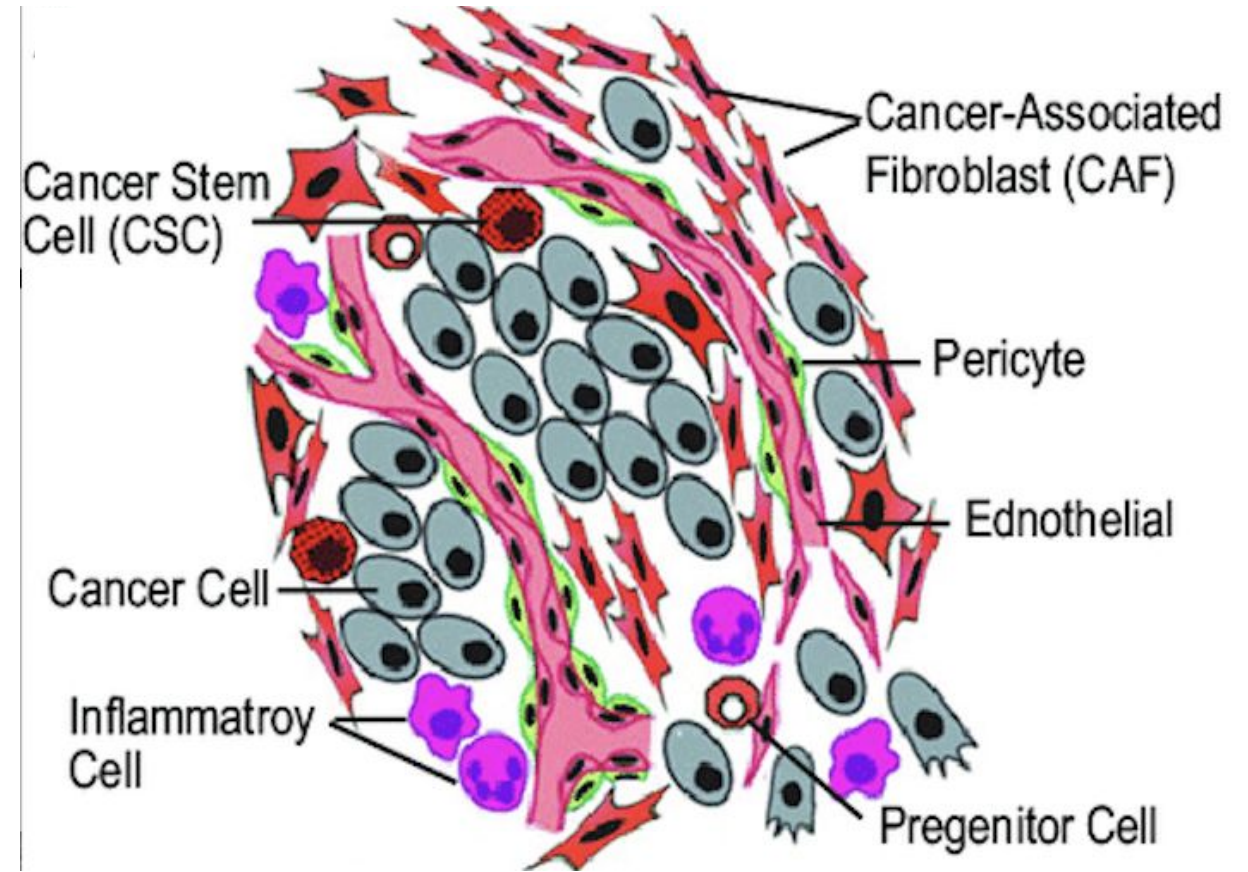
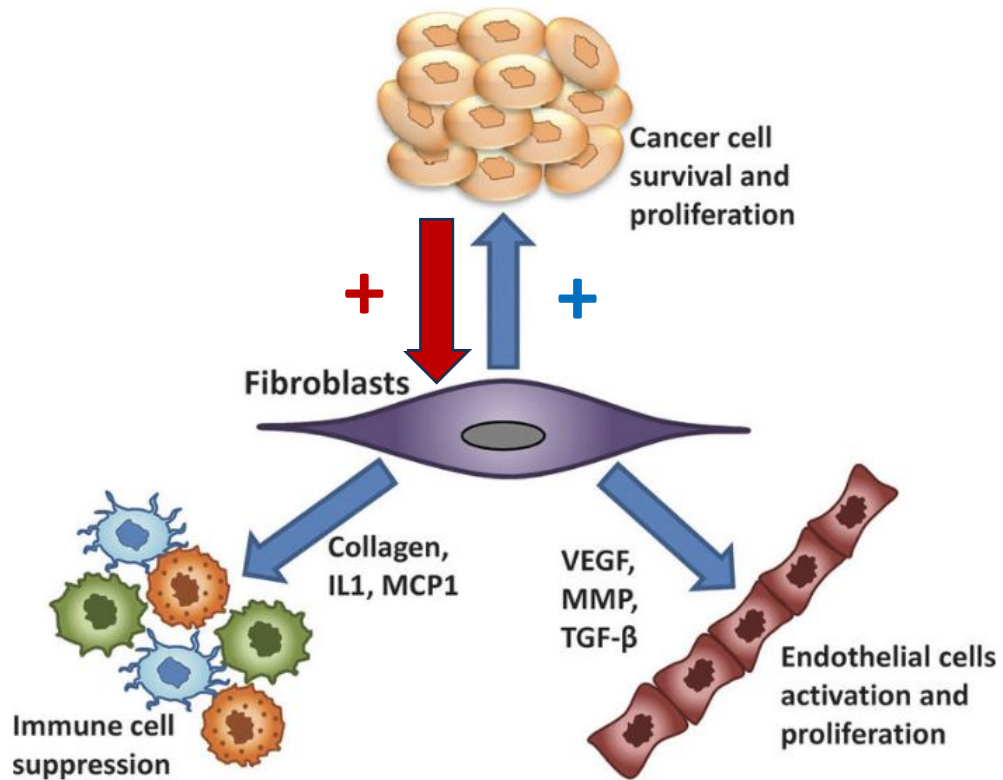
Feedback from microenvironment



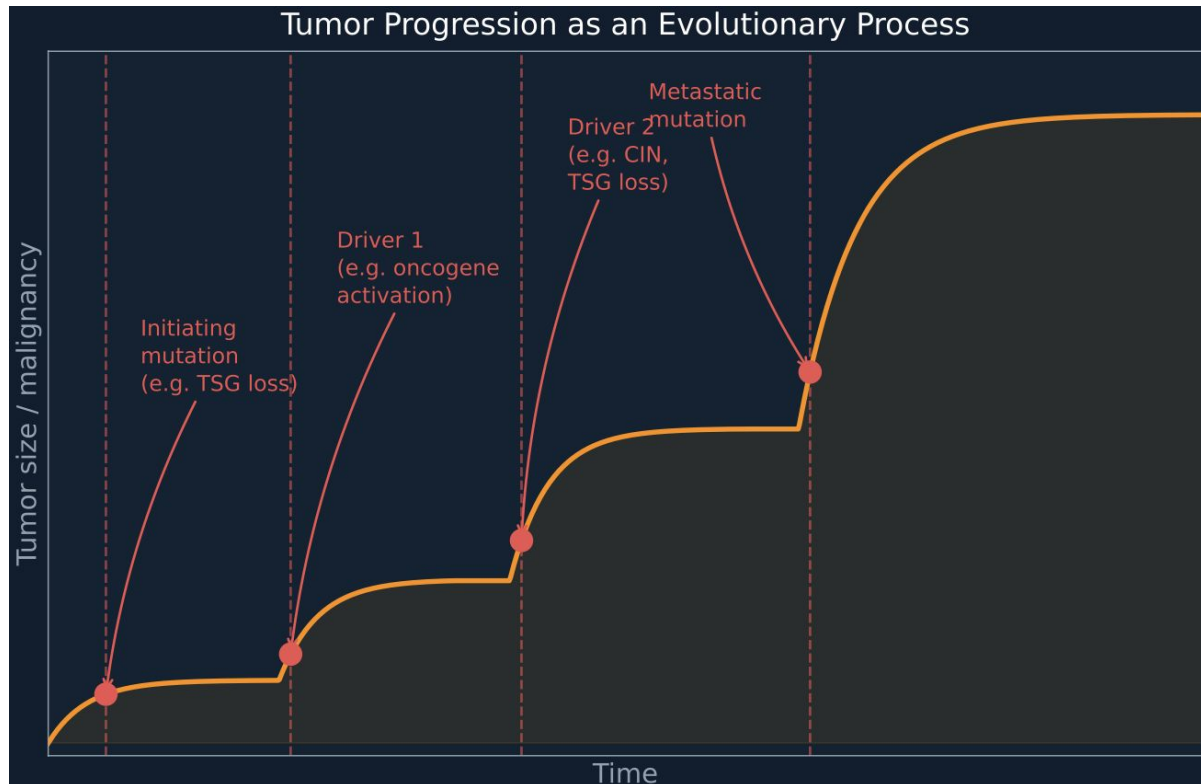
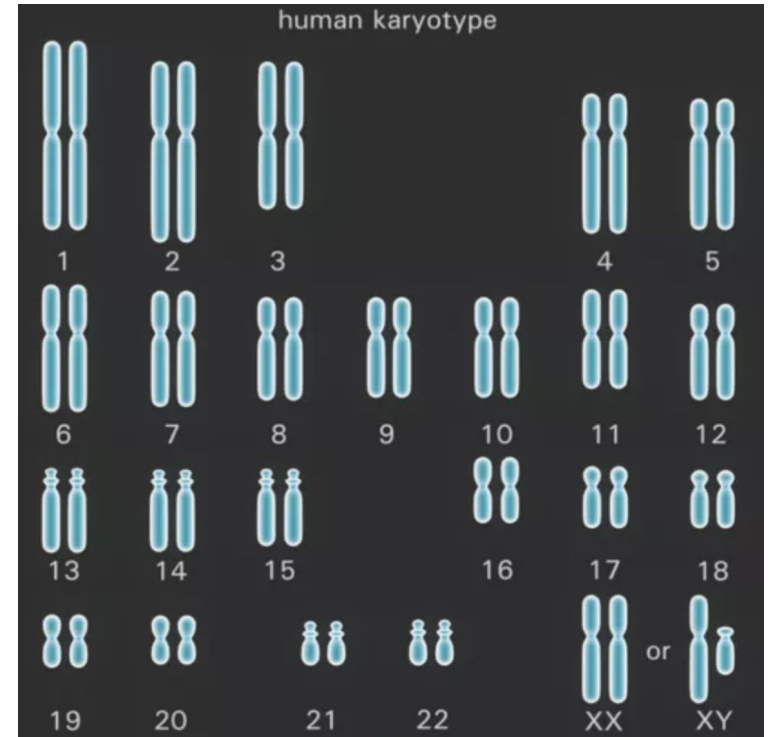
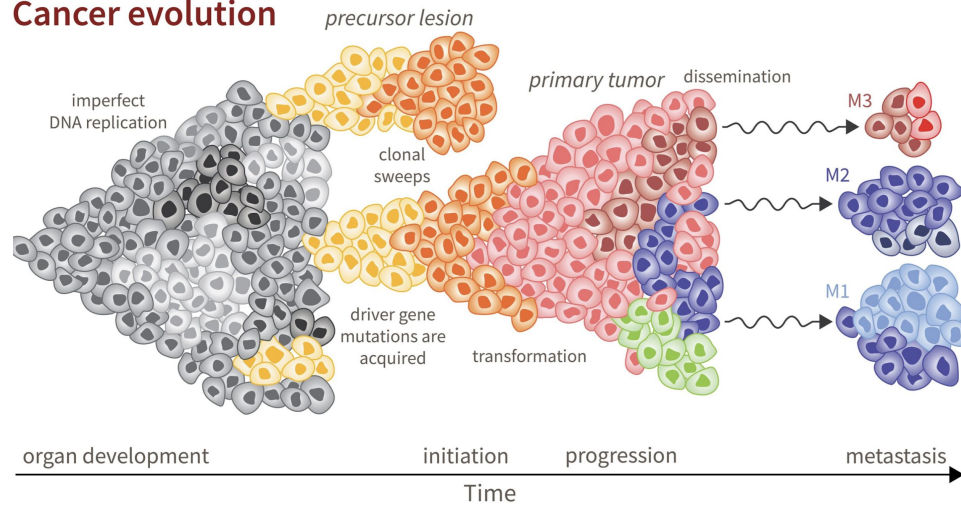
Cancer is a tissue gone wrong: characterized by the same tissue architecture



Cancer – Microenvironment interactions



Cancer evolution



Cancer Evolution: Driver Mutations & Gene Classes

Cancer is driven by mutations in three key gene classes

Oncogenes

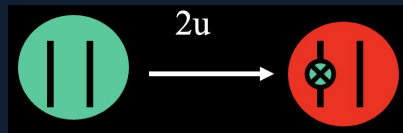
"Accelerator"

Normally promote cell growth

Gain-of-function mutations

One mutant copy sufficient

Examples: RAS, MYC, BCR-ABL



Stuck 'ON' -- uncontrolled growth

Tumor Suppressor Genes (TSGs)

"Brakes"

Normally inhibit cell growth

Loss-of-function mutations

Both copies often needed

Examples: TP53, RB, APC



Both brakes cut -- growth unchecked

DNA Repair Genes

"Caretakers"

Maintain genome integrity

Loss elevates mutation rate

Accelerates driver acquisition

Examples: BRCA1/2, MMR genes

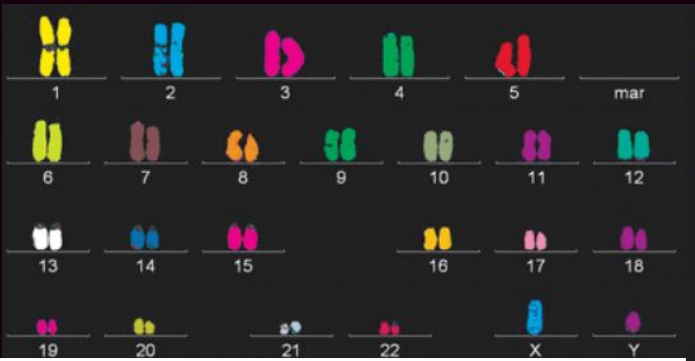
More mutations -- faster evolution

Genetic Instability: Accelerating Evolution

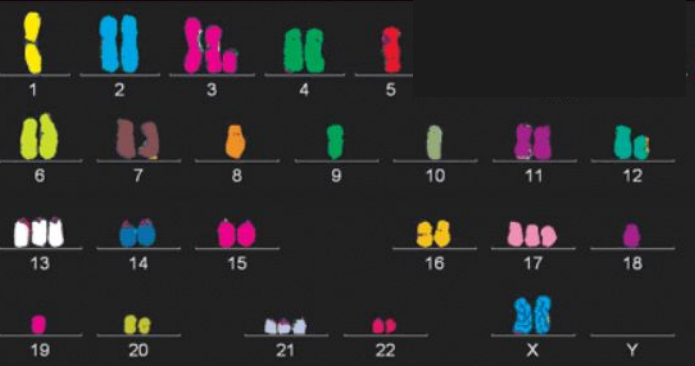
Defective genome maintenance --> elevated mutation rate --> faster evolution

Chromosomal Instability (CIN)

large-scale genetic changes



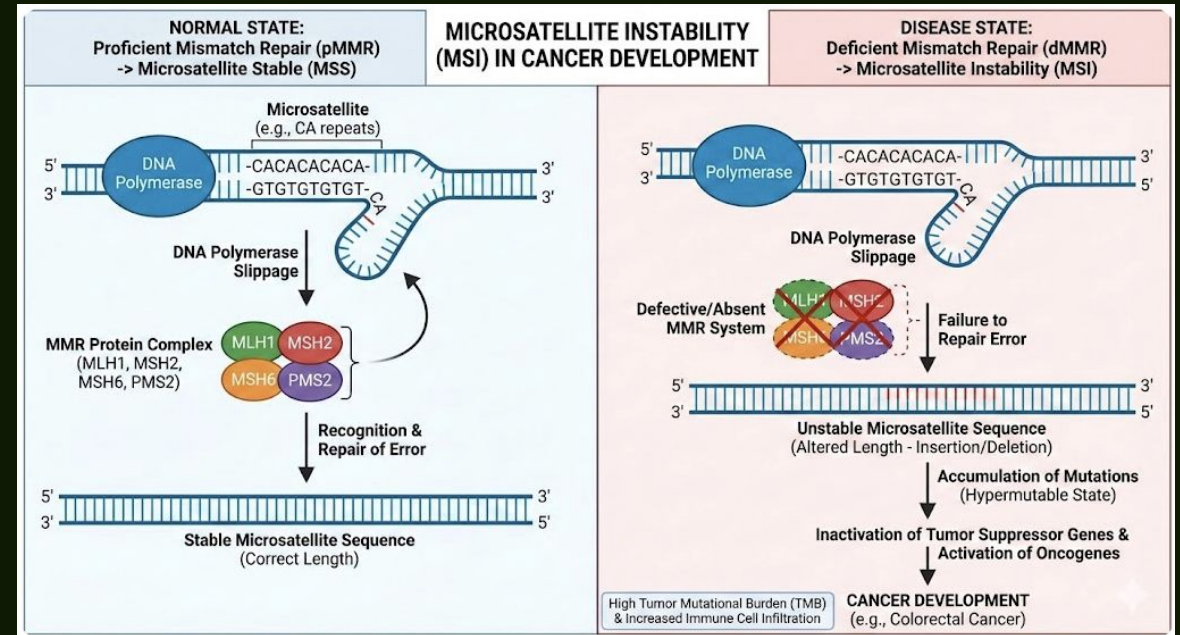
normal cell



cancer cell

Microsatellite Instability (MSI)

small-scale genetic changes



Key insight: Genetic instability is an 'enabler' -- it accelerates acquisition of driver mutations

Cancer Therapy: Major Approaches

Traditional Chemotherapy

Cytotoxic agents kill rapidly dividing cells

DNA-damaging agents
(cisplatin, doxorubicin)

Mitotic inhibitors
(taxanes, vinca alkaloids)

Antimetabolites
(5-FU, methotrexate)

Affects all dividing cells --> toxicity

Targeted Therapy (Small Molecules)

Inhibit specific molecular drivers of cancer

Tyrosine kinase inhibitors
(imatinib in CML, BCR-ABL)

EGFR inhibitors
(erlotinib, lung cancer)

BRAF inhibitors
(melanoma)

Higher specificity but resistance common

Immunotherapy

Harness the immune system against cancer

Immune checkpoint inhibitors
(PD-1, CTLA-4)

CAR-T cell therapy

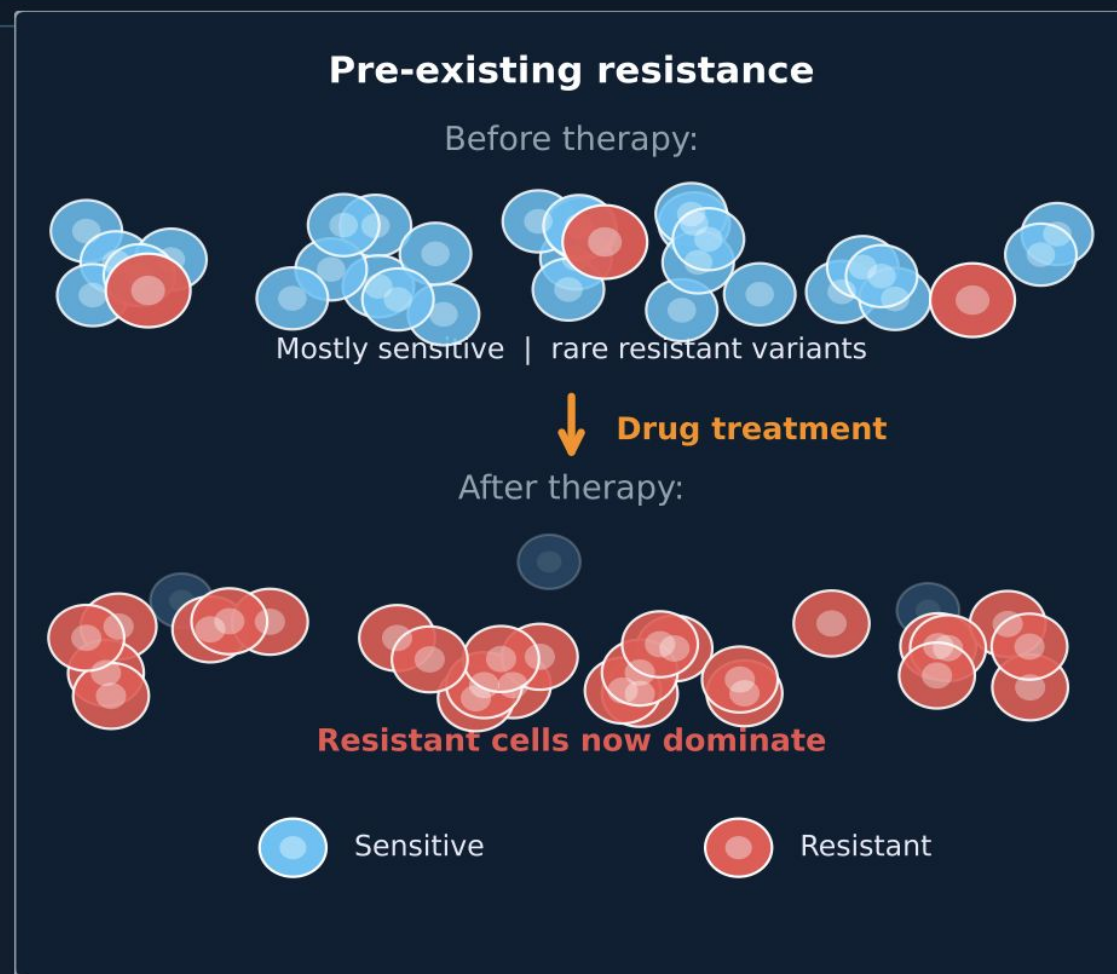
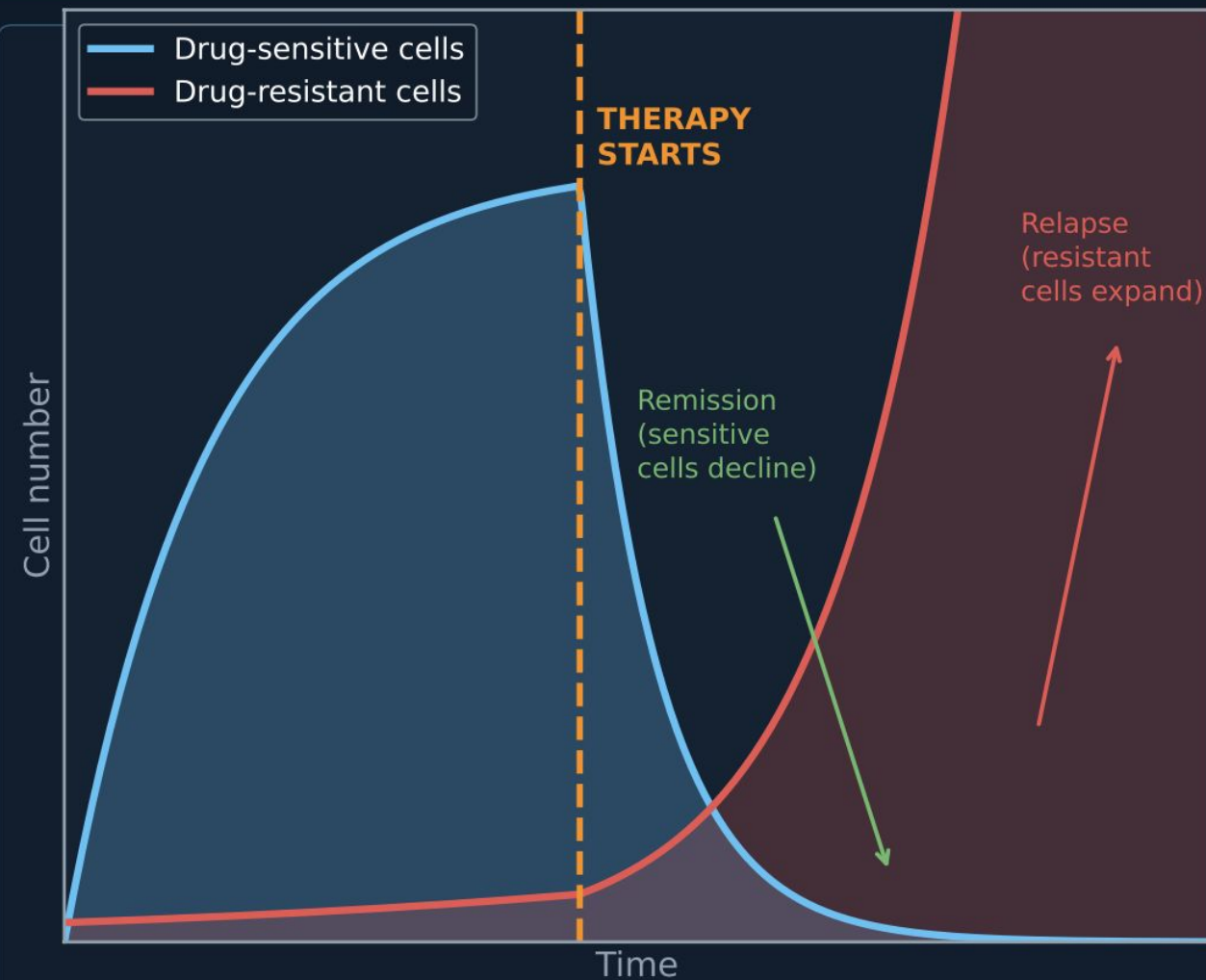
Cancer vaccines

Bispecific antibodies

Durable responses in some patients

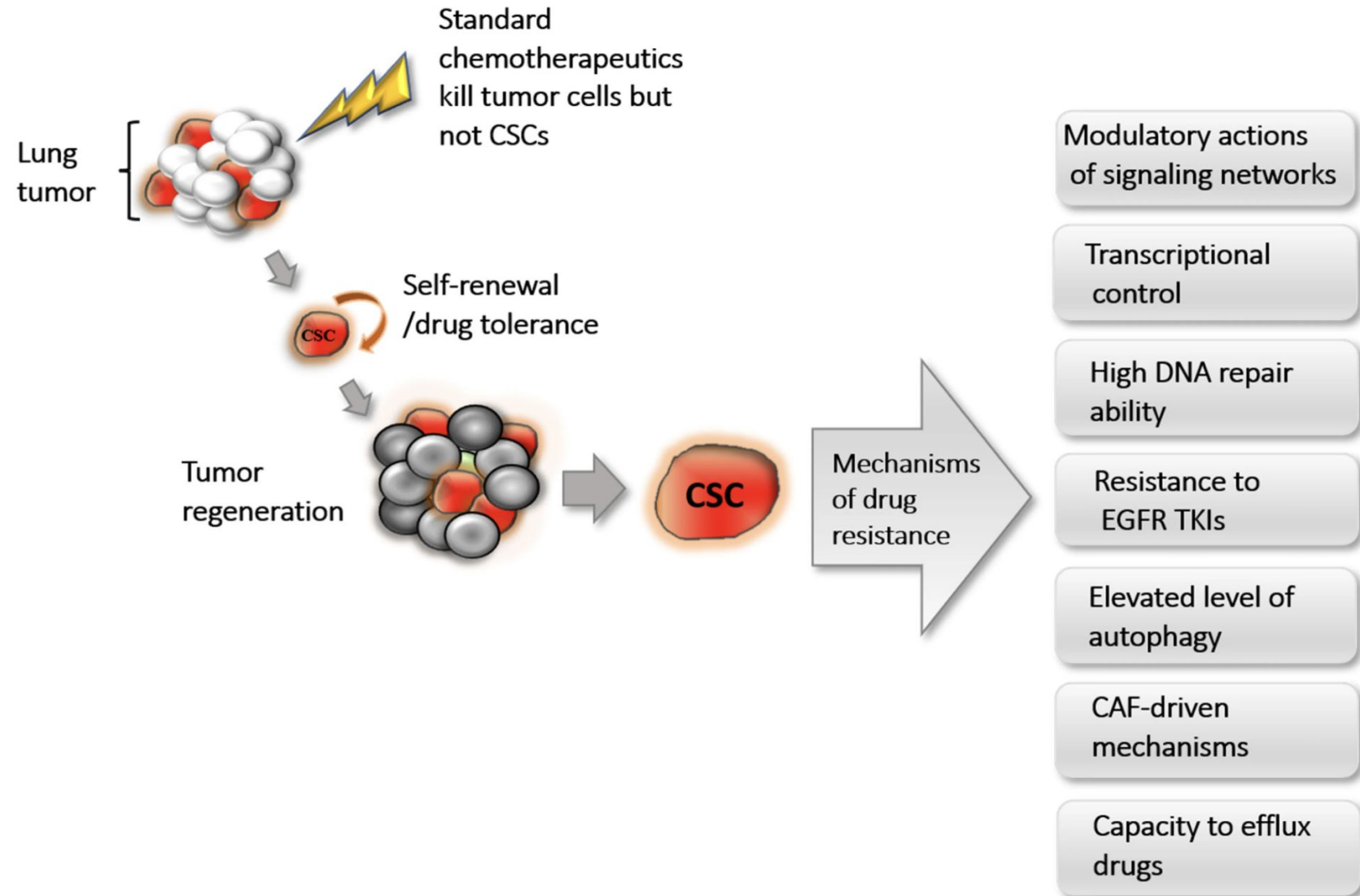
Landmark: Imatinib (Gleevec) targets BCR-ABL in CML -- transformed a lethal disease into a manageable chronic condition

Drug Resistance: Evolution in Action



Key insight: Resistant cells PRE-EXIST as rare variants before therapy starts. Therapy selects for them -- combination therapy targeting multiple pathways is more effective at preventing resistance.

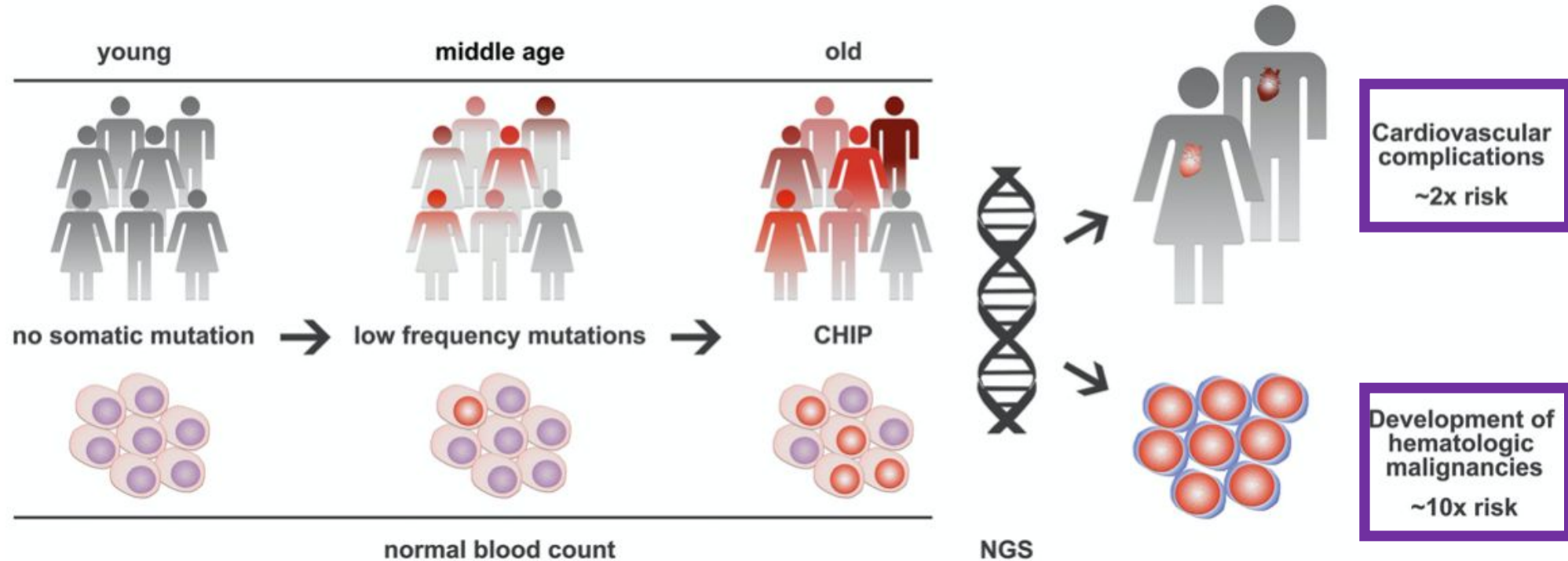
Drug resistance can also be based on cancer stem cell persistence (no resistant mutations)



2. Modeling tissue and tumor cell evolution

- Consider pre-malignant cell evolution in the blood
- Show how simple ordinary differential equation models can provide biological insights

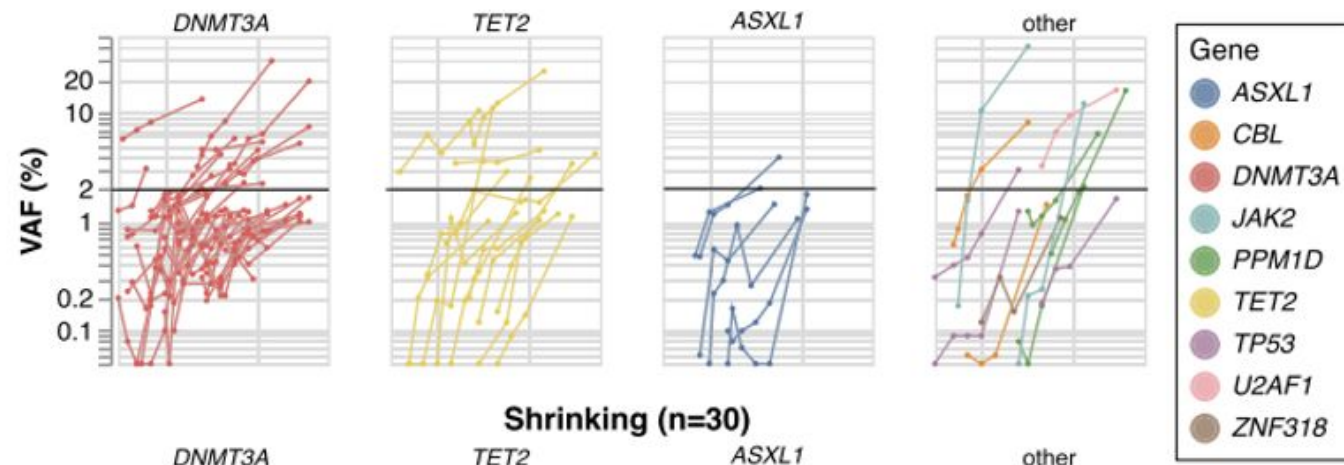
Pre-cancer evolution in healthy tissue: Clonal hematopoiesis of indeterminate potential in the blood



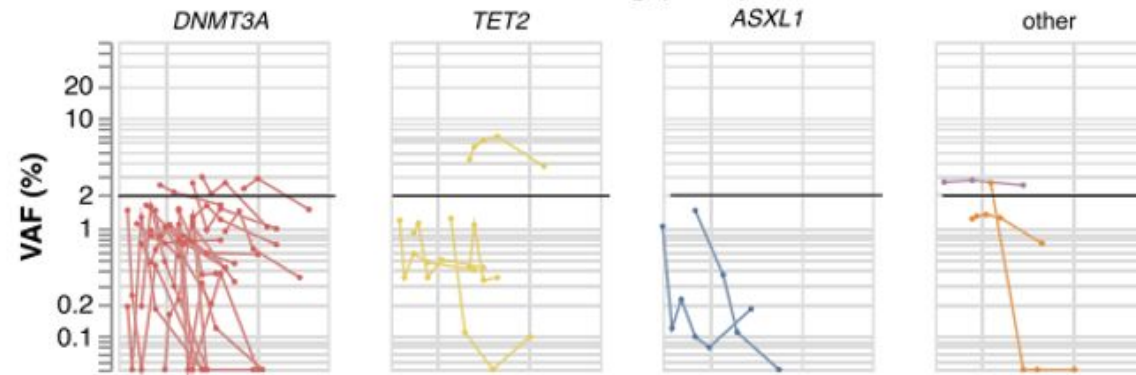
- How do CHIP mutants evolve?
- What are the selection pressures?
- Can we treat to create conditions that select against CHIP clones (evolutionary therapy)?

Lots of existing mathematical modeling work by e.g. Stiehl, Marciniak-Czochra , Mackey, Loeffler, Roeder

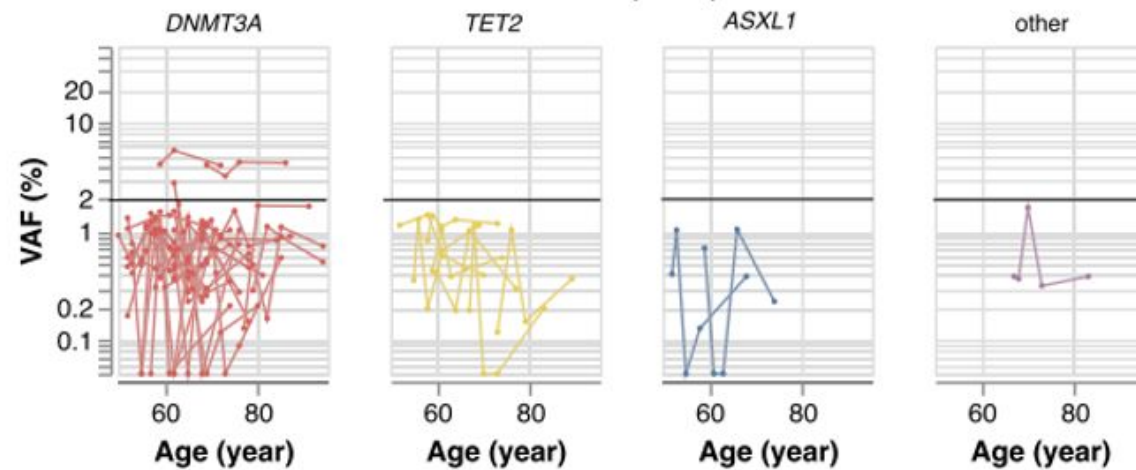
Growing (n=76)



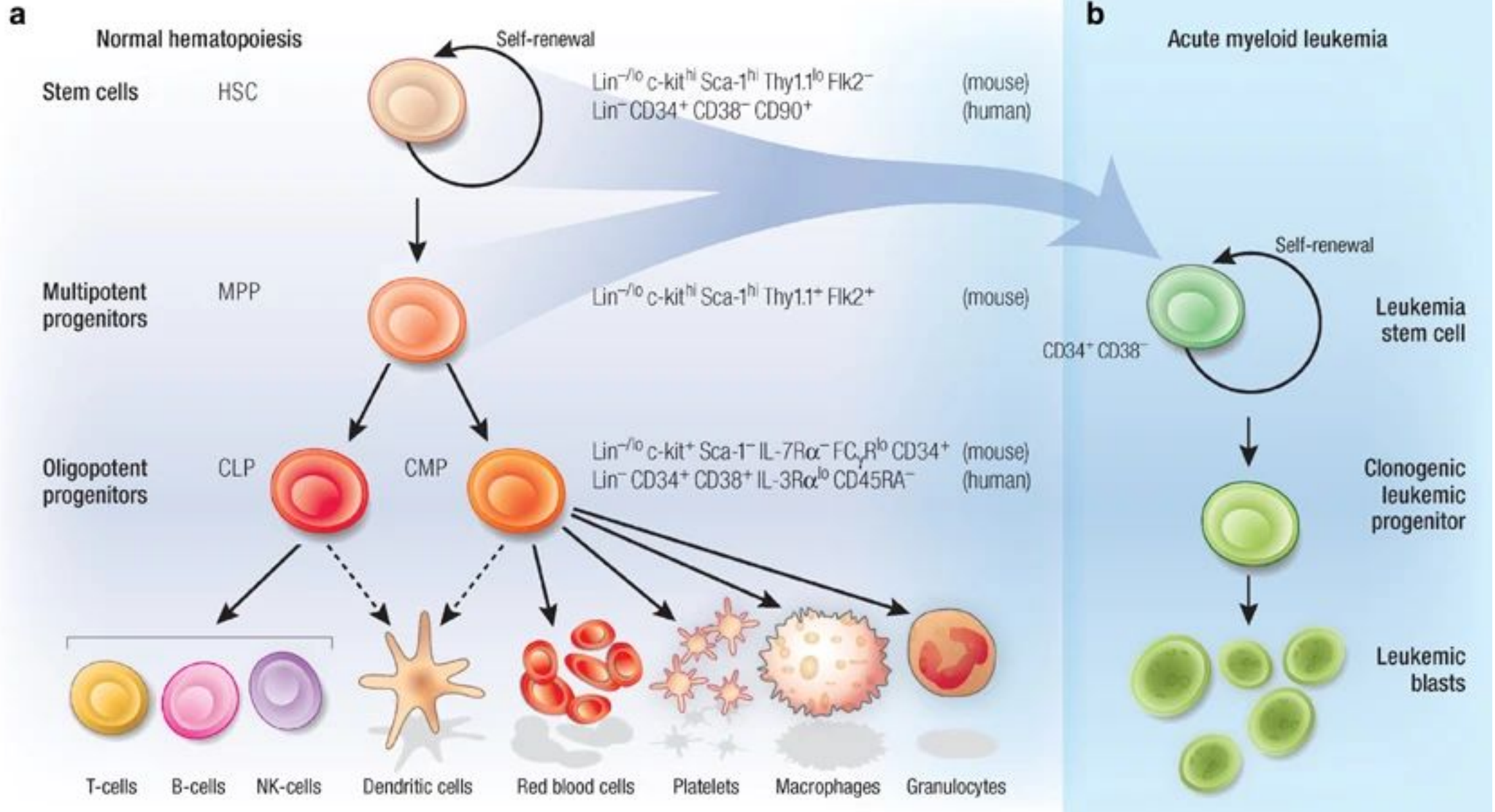
Shrinking (n=30)



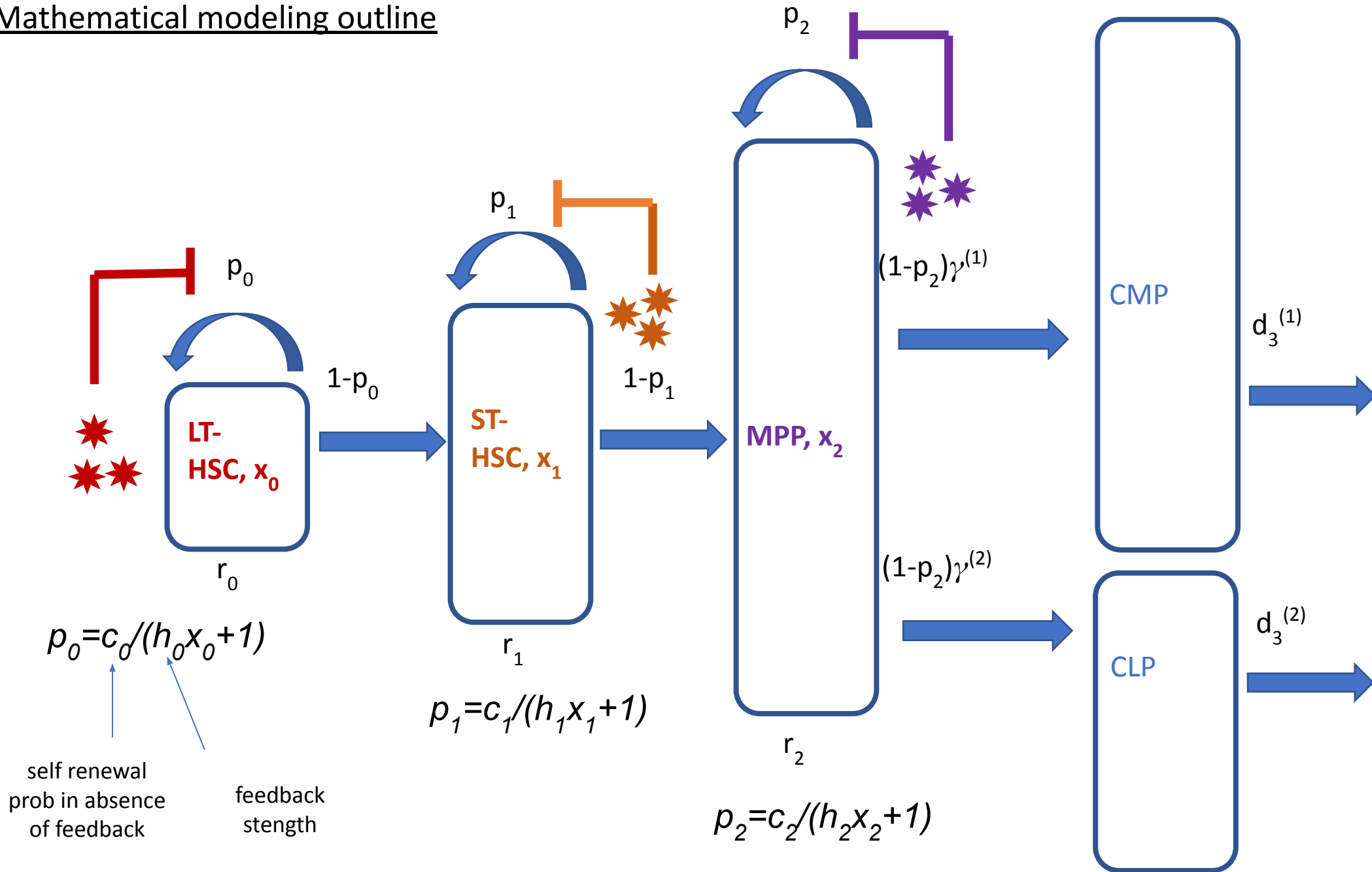
Static (n=40)



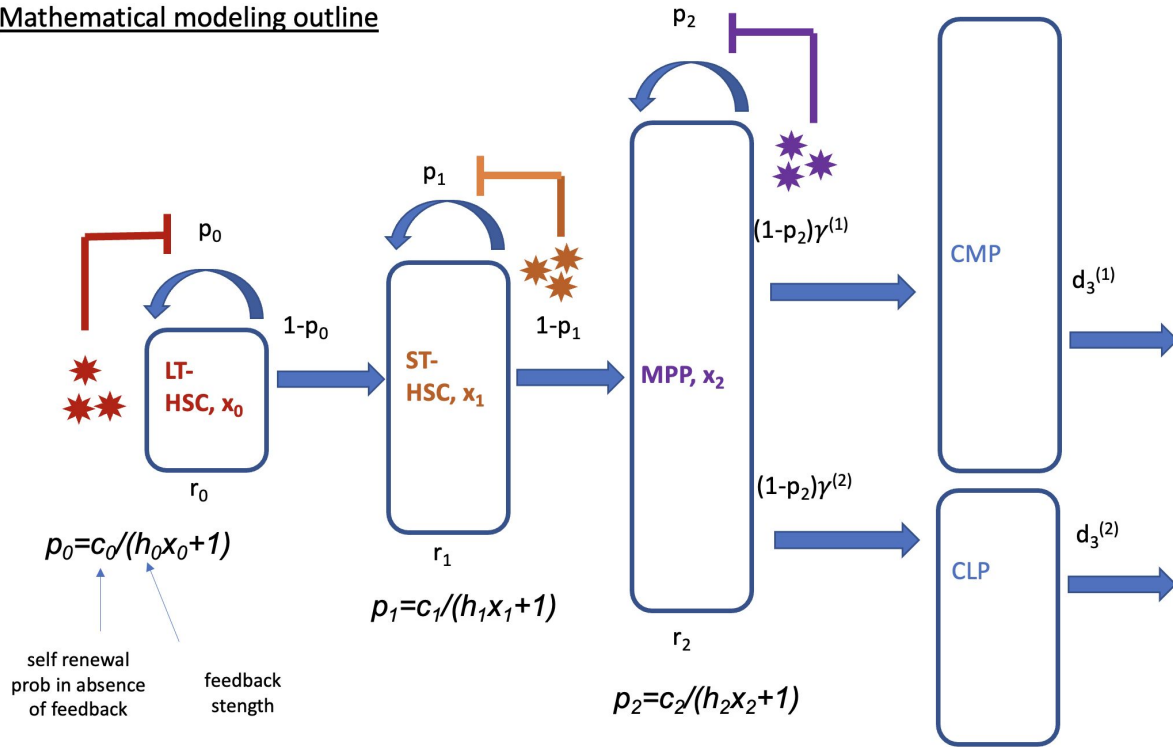
What is the fate of mutants arising in the different compartments?



Mathematical modeling outline



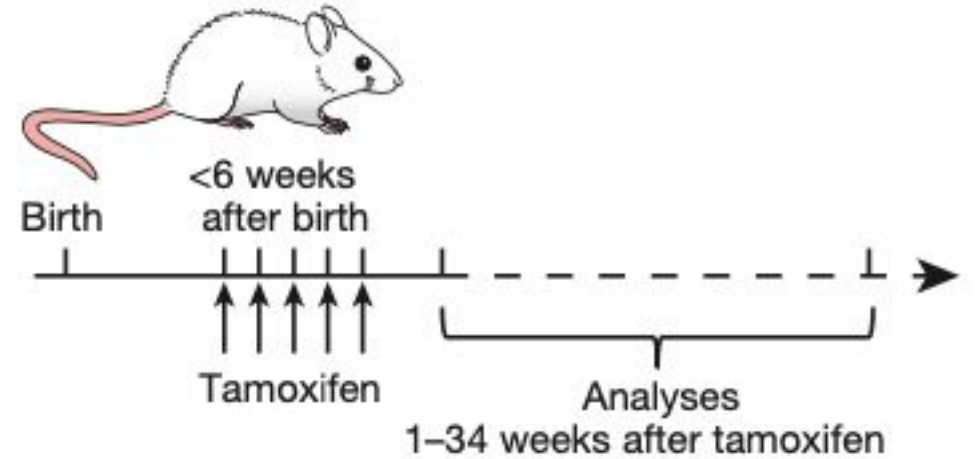
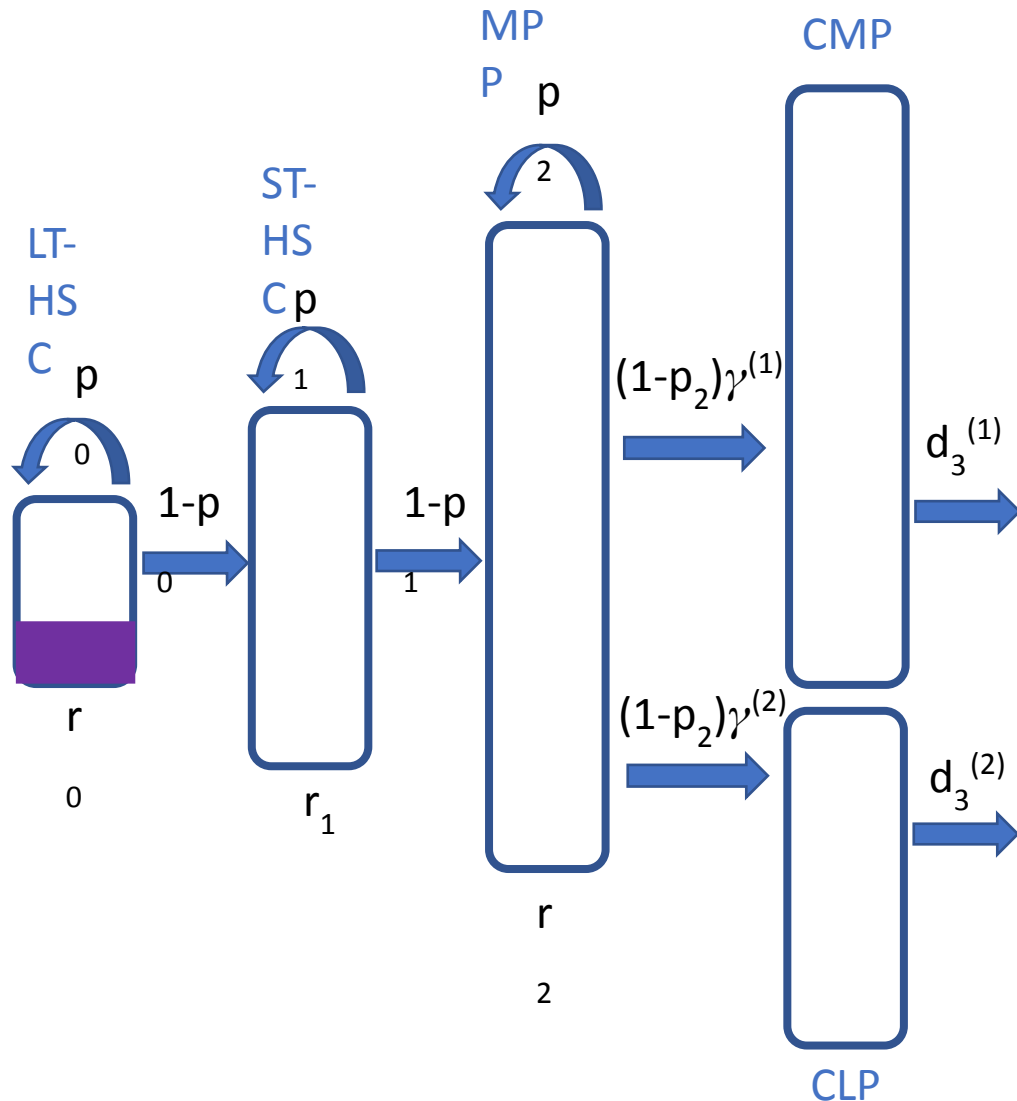
Mathematical modeling outline



$$\begin{aligned} \frac{dx_0}{dt} &= r_0 x_0 (2p_0 - 1), \\ \frac{dx_1}{dt} &= 2r_0 x_0 (1 - p_0) + r_1 x_1 (2p_1 - 1), \\ \frac{dx_2}{dt} &= 2r_1 x_1 (1 - p_1) + r_2 x_2 (2p_2 - 1), \\ \frac{dx_3^{(1)}}{dt} &= 2r_2 x_2 (1 - p_2) \gamma^{(1)} - d_3^{(1)} x_3^{(1)}, \\ \frac{dx_3^{(2)}}{dt} &= 2r_2 x_2 (1 - p_2) \gamma^{(2)} - d_3^{(2)} x_3^{(2)}, \end{aligned}$$

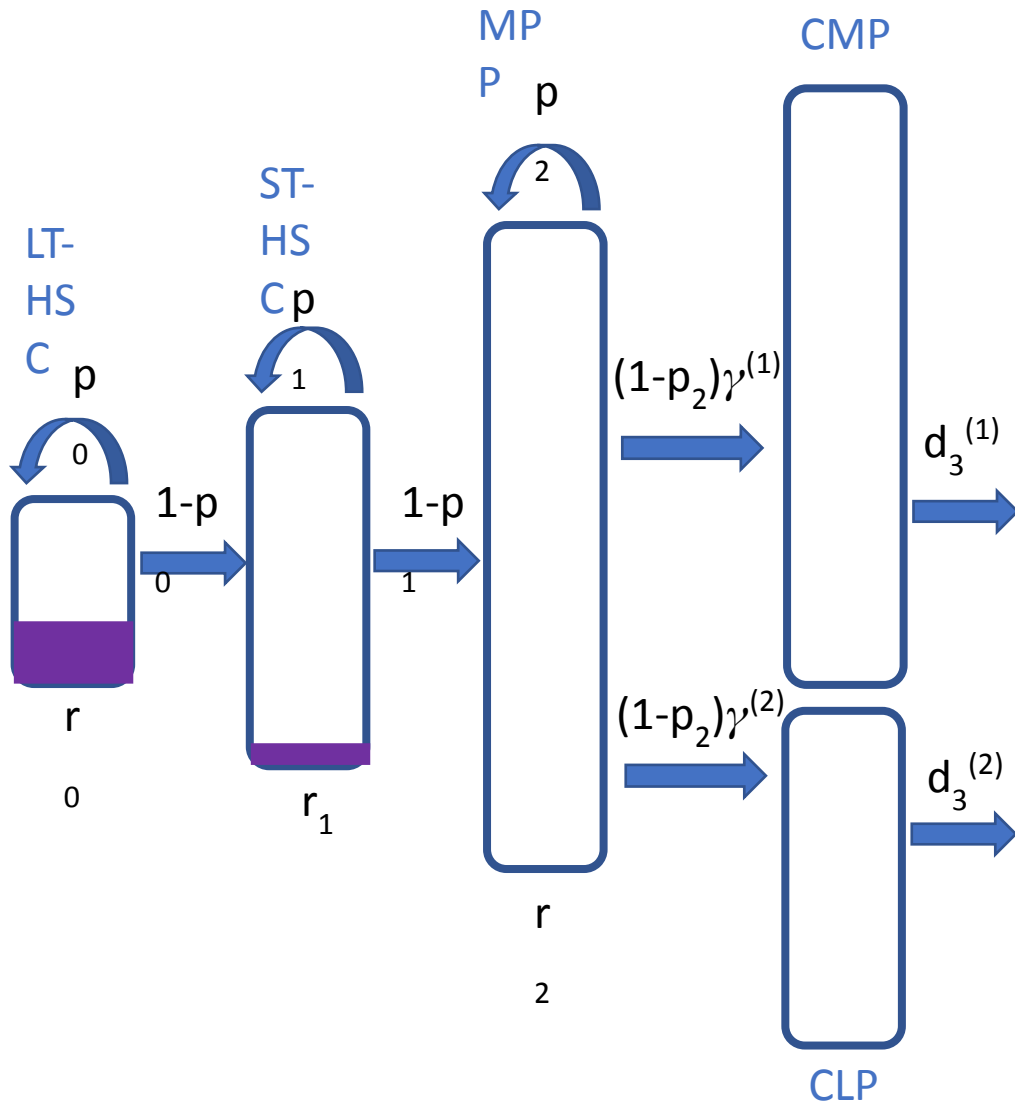
$$p_i = p_i(x_0, x_1, x_2, x_3^{(1)}, x_3^{(2)}), \quad 0 \leq i \leq 2.$$

Neutral label propagation



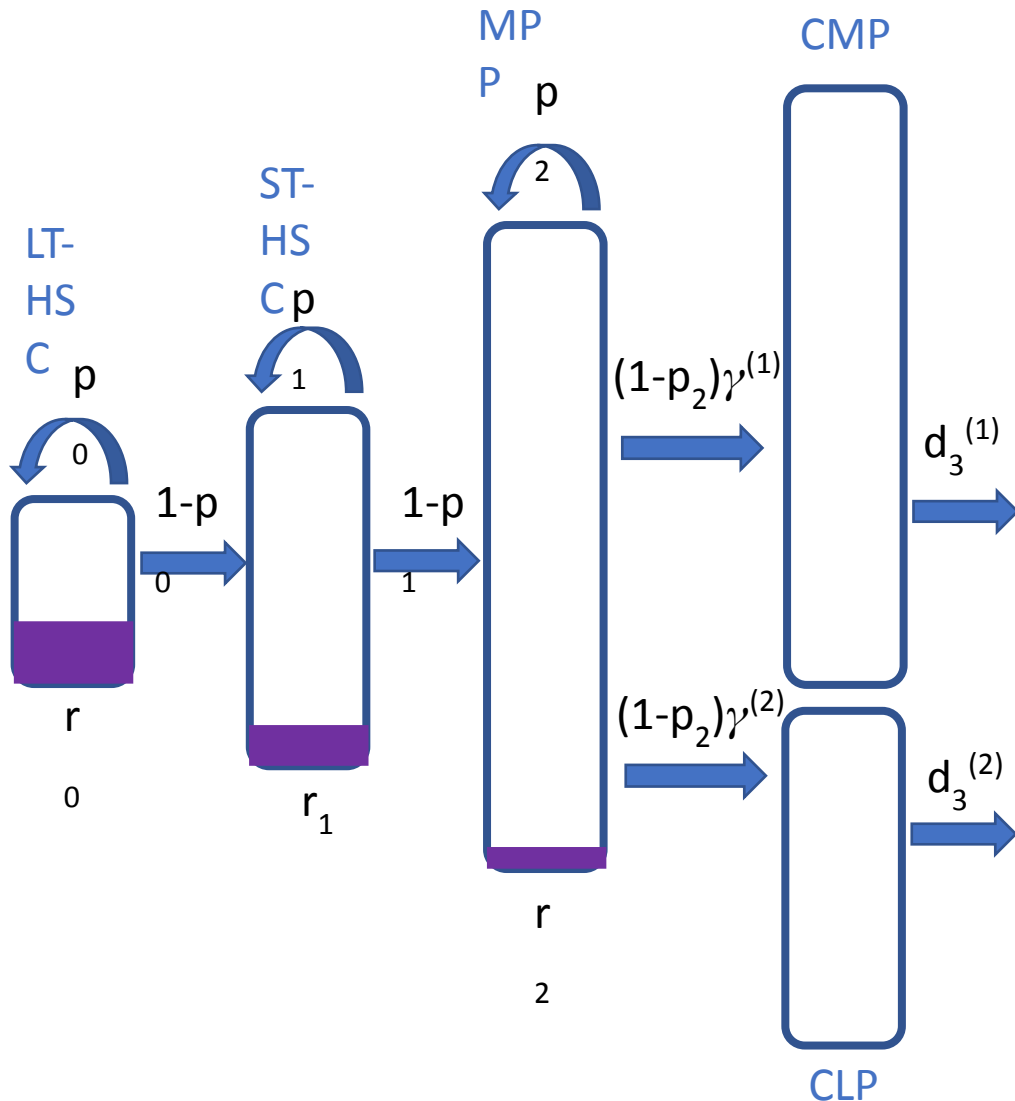
Busch, K., Klapproth, K., Barile, M., Flossdorf, M., Holland-Letz, T., Schlenner, S. M., ... & Rodewald, H. R. (2015). Fundamental properties of unperturbed haematopoiesis from stem cells in vivo. *Nature*, 518(7540), 542-546.

Neutral label propagation



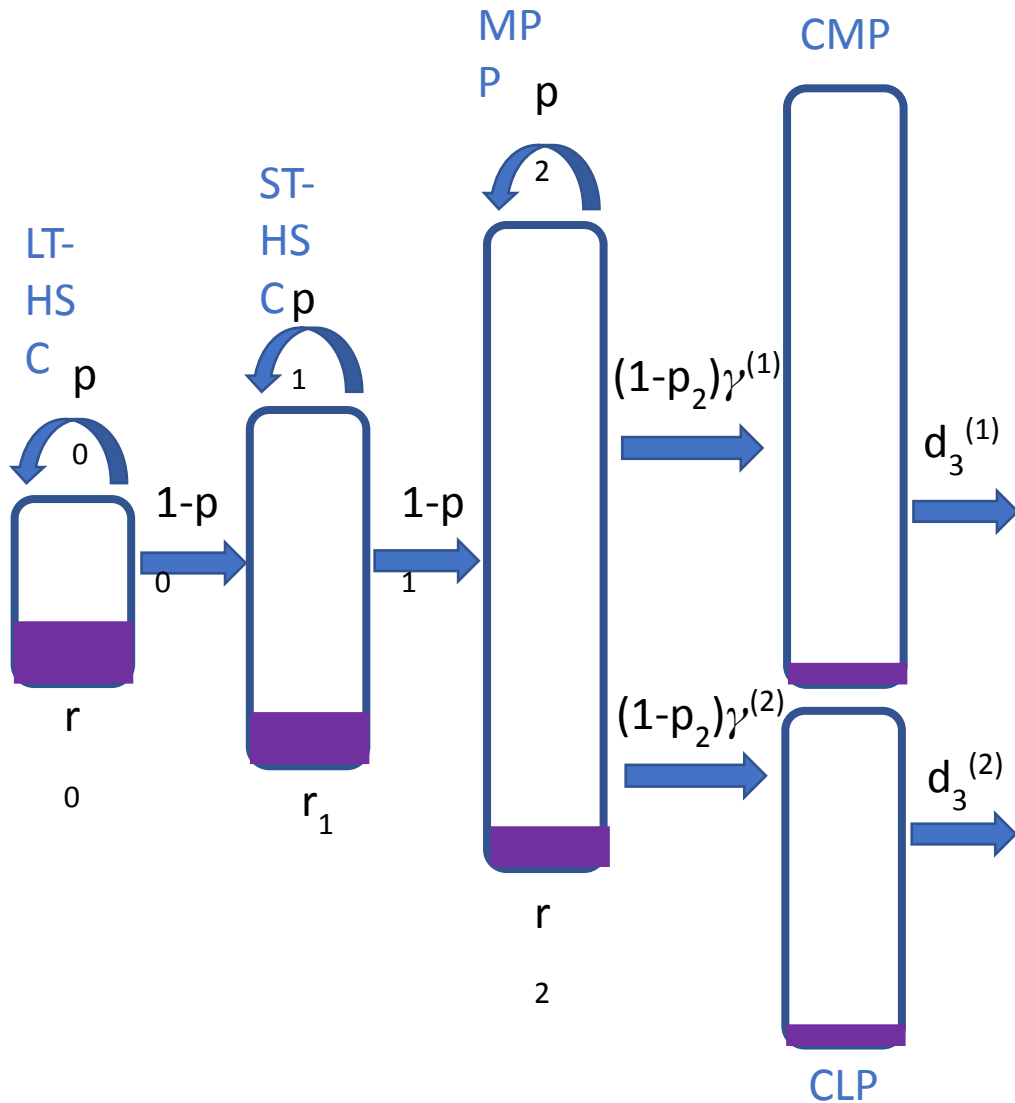
Busch, K., Klapproth, K., Barile, M., Flossdorf, M., Holland-Letz, T., Schlenner, S. M., ... & Rodewald, H. R. (2015). Fundamental properties of unperturbed haematopoiesis from stem cells in vivo. *Nature*, 518(7540), 542-546.

Neutral label propagation



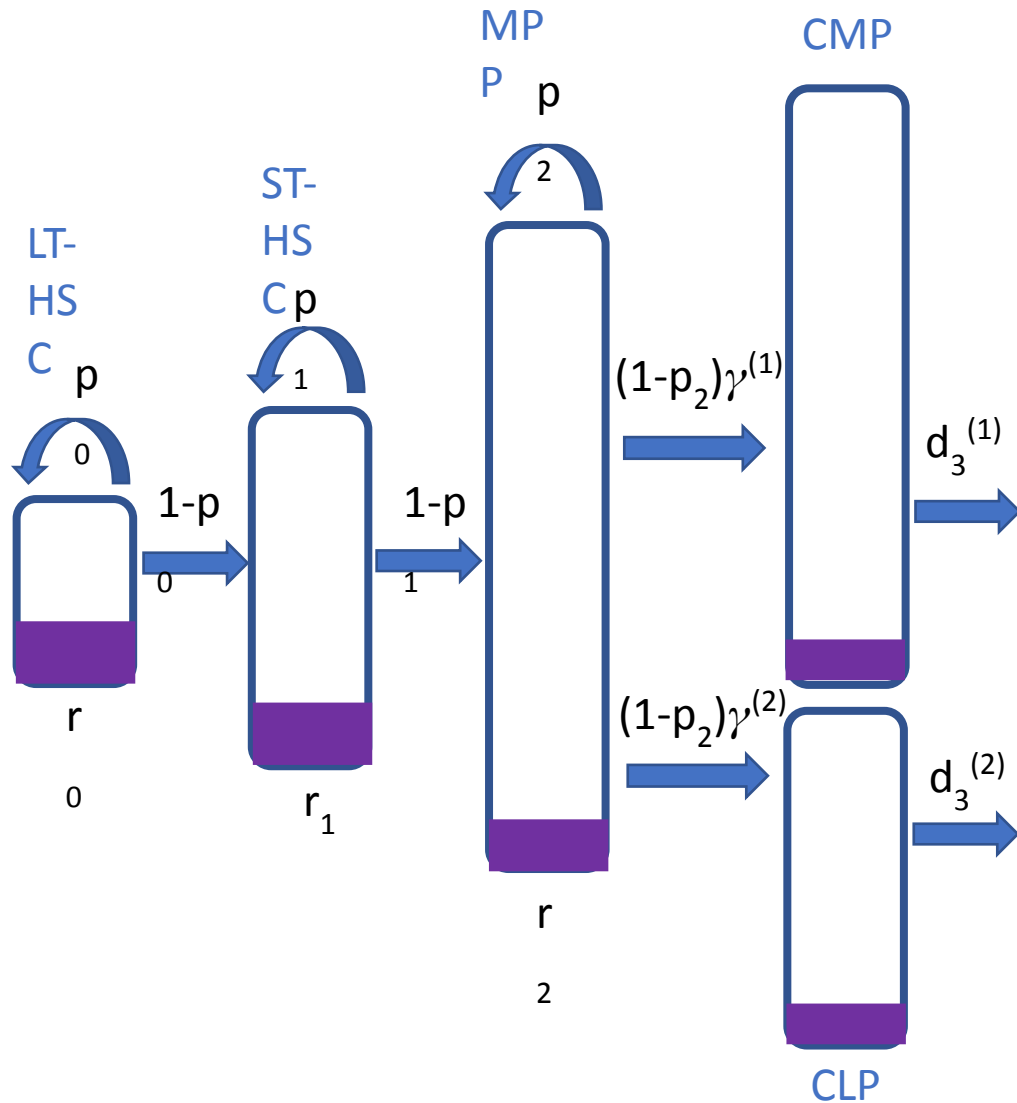
Busch, K., Klapproth, K., Barile, M., Flossdorf, M., Holland-Letz, T., Schlenner, S. M., ... & Rodewald, H. R. (2015). Fundamental properties of unperturbed haematopoiesis from stem cells in vivo. *Nature*, 518(7540), 542-546.

Neutral label propagation



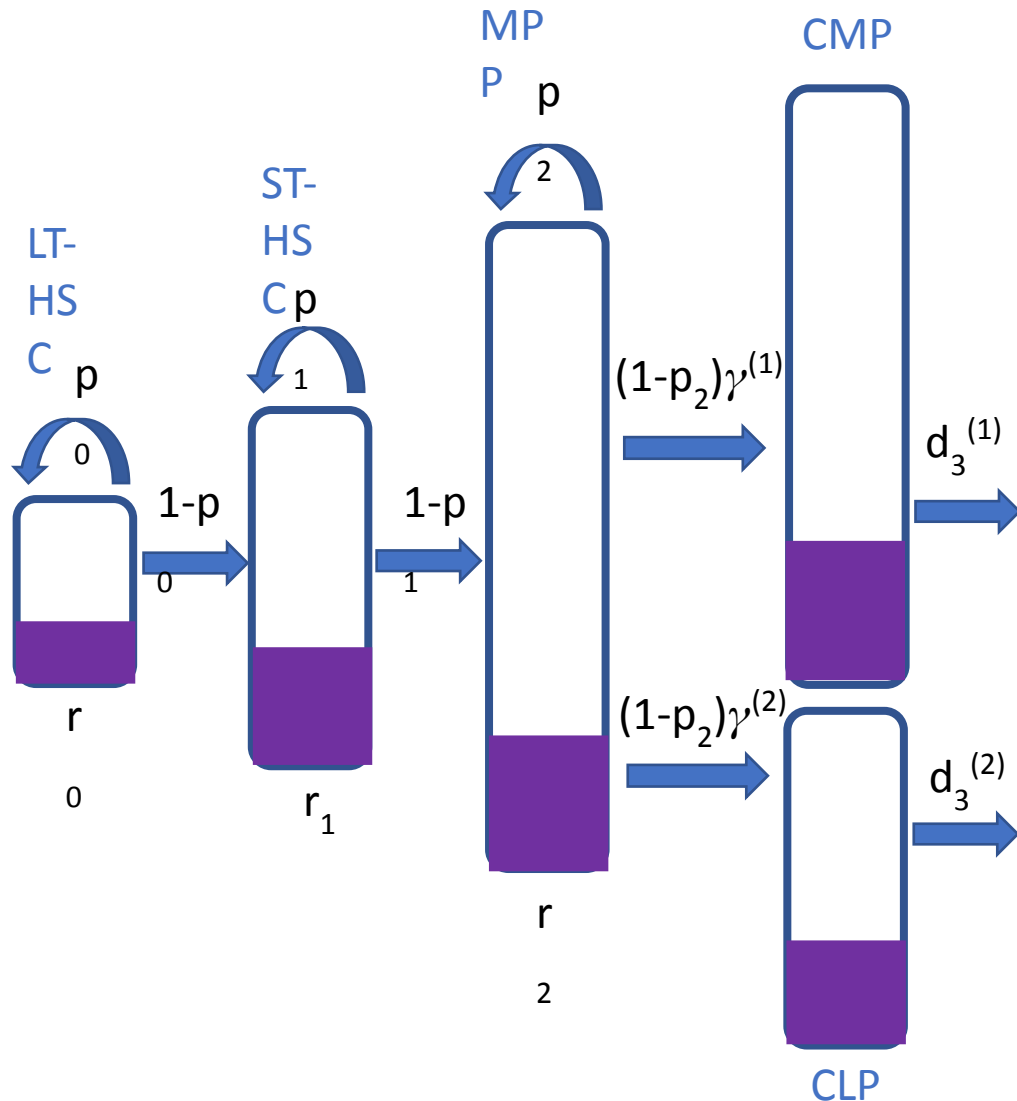
Busch, K., Klapproth, K., Barile, M., Flossdorf, M., Holland-Letz, T., Schlenner, S. M., ... & Rodewald, H. R. (2015). Fundamental properties of unperturbed haematopoiesis from stem cells in vivo. *Nature*, 518(7540), 542-546.

Neutral label propagation



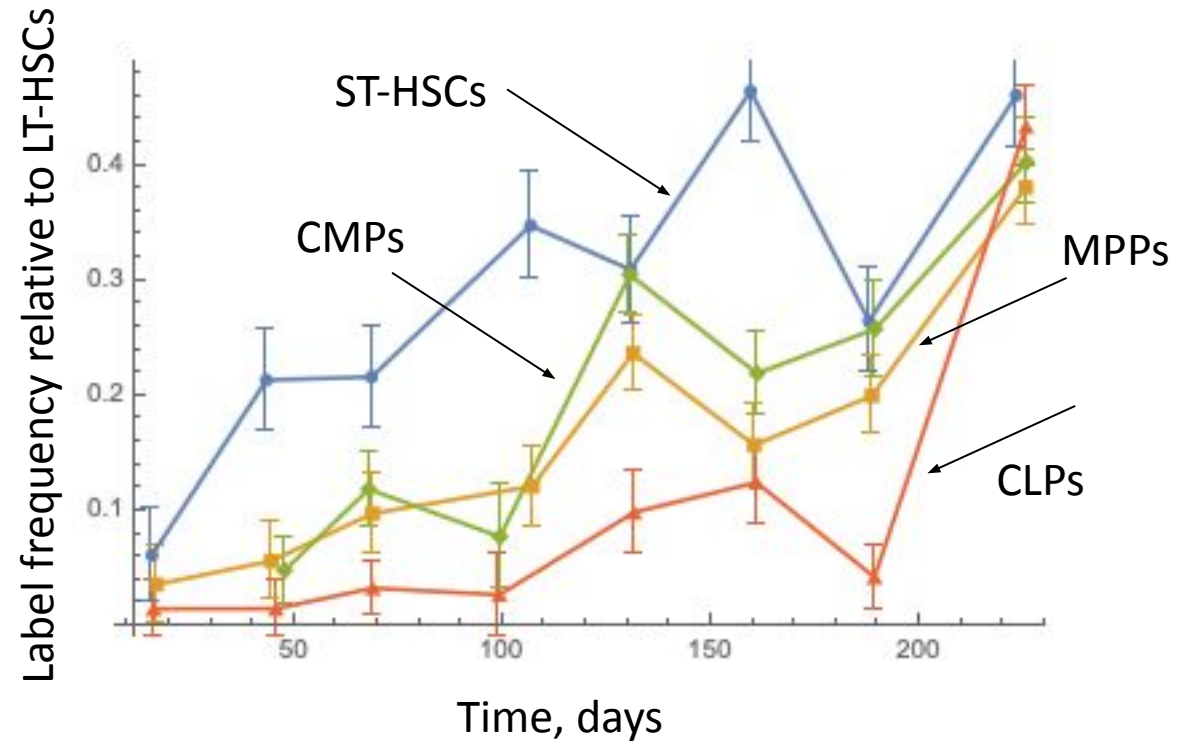
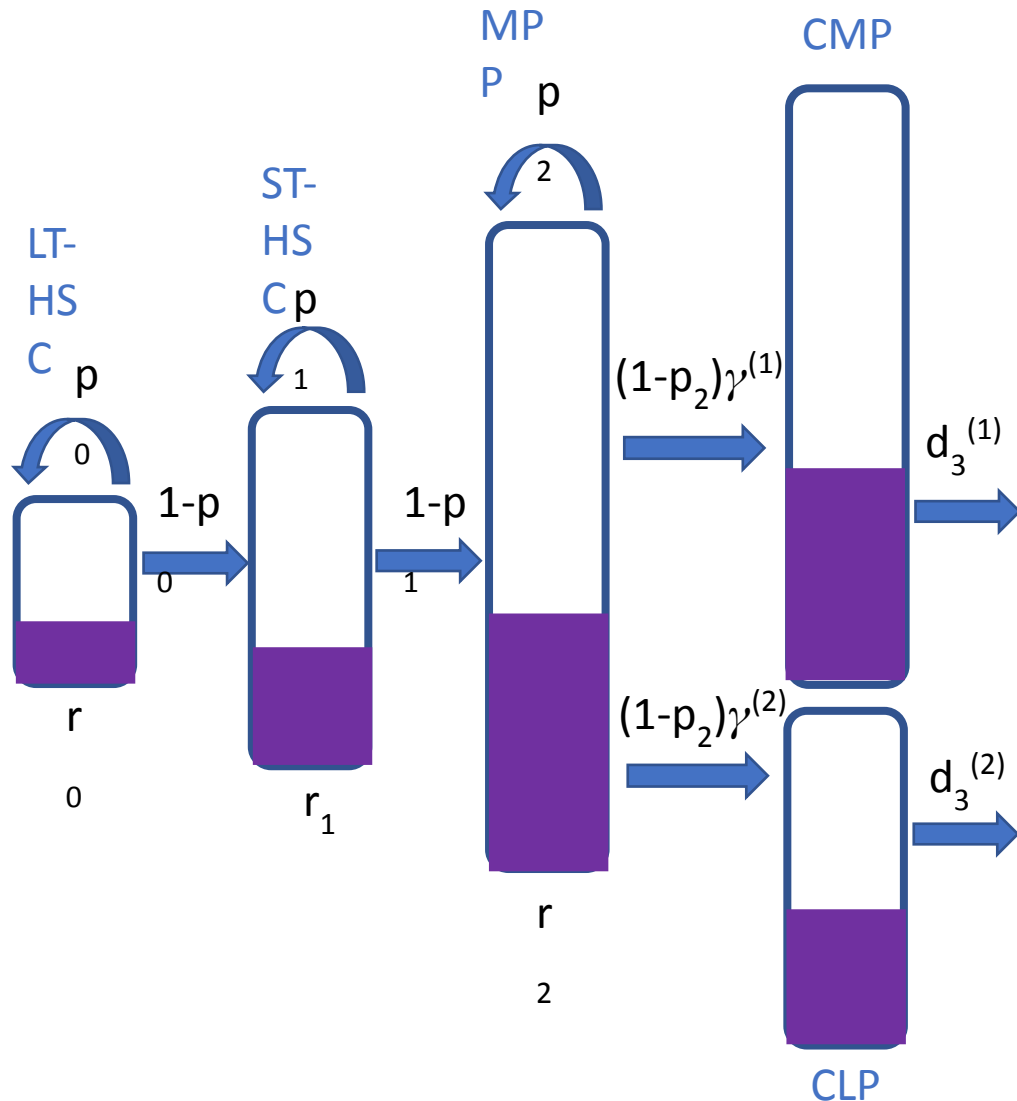
Busch, K., Klapproth, K., Barile, M., Flossdorf, M., Holland-Letz, T., Schlenner, S. M., ... & Rodewald, H. R. (2015). Fundamental properties of unperturbed haematopoiesis from stem cells in vivo. *Nature*, 518(7540), 542-546.

Neutral label propagation



Busch, K., Klapproth, K., Barile, M., Flossdorf, M., Holland-Letz, T., Schlenner, S. M., ... & Rodewald, H. R. (2015). Fundamental properties of unperturbed haematopoiesis from stem cells in vivo. *Nature*, 518(7540), 542-546.

Neutral label propagation



Busch, K., Klapproth, K., Barile, M., Flossdorf, M., Holland-Letz, T., Schlenner, S. M., ... & Rodewald, H. R. (2015). Fundamental properties of unperturbed haematopoiesis from stem cells in vivo. *Nature*, 518(7540), 542-546.

Model parameterization

Fraction of the neutral label in each compartment

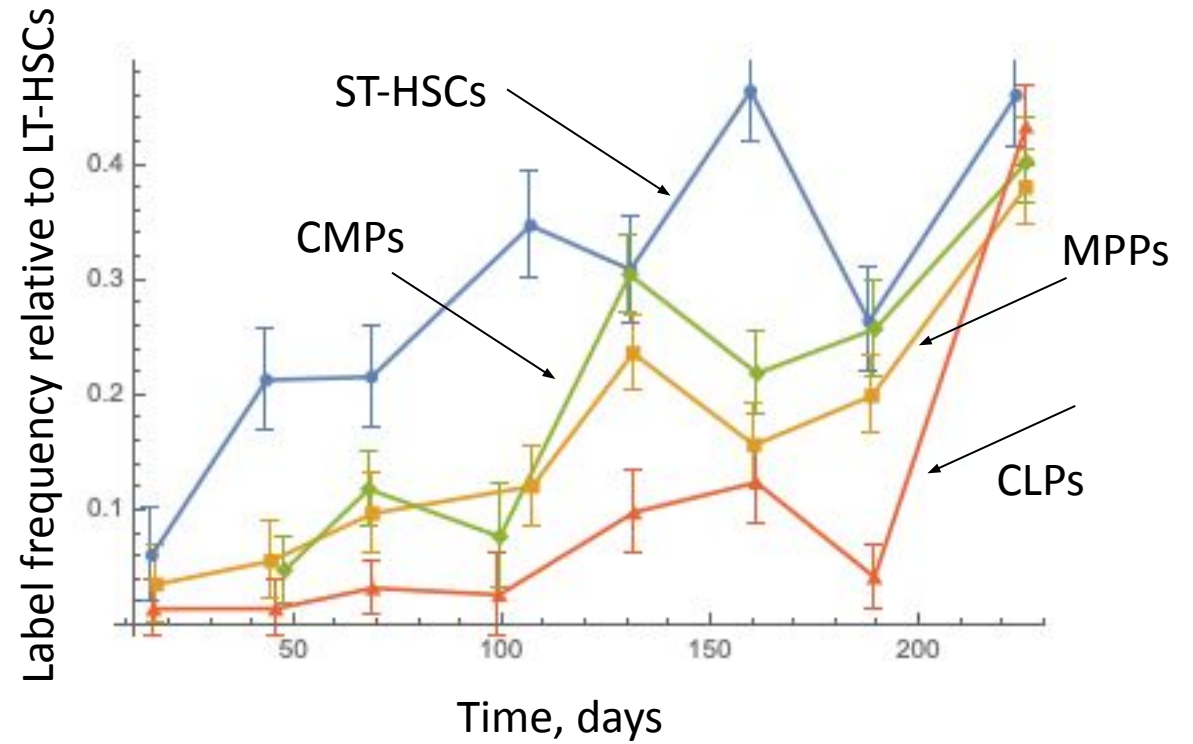
$$\begin{aligned} \dot{f}_0 &= 0, \\ \dot{f}_1 &= \frac{1}{\tau_1}(f_0 - f_1), \\ \dot{f}_2 &= \frac{1}{\tau_2}(f_1 - f_2), \\ \dot{f}_3^{(1)} &= \frac{1}{\tau_3^{(1)}}(f_2 - f_3^{(1)}), \quad \dot{f}_3^{(2)} = \frac{1}{\tau_3^{(2)}}(f_2 - f_3^{(2)}). \end{aligned}$$

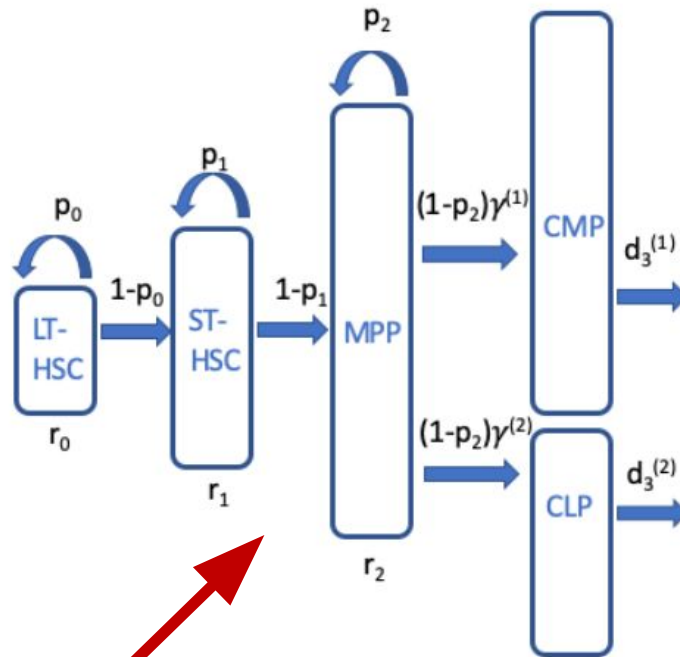
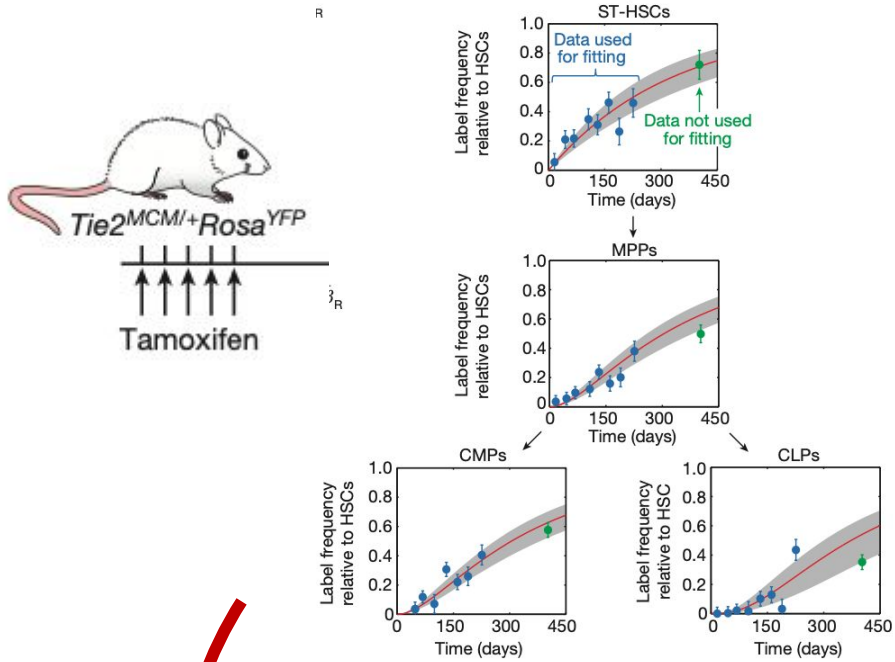
“Time to equilibrium”

$$\tau_1 = \frac{1}{r_1(1 - 2p_1)}, \quad \tau_2 = \frac{1}{r_2(1 - 2p_2)}, \quad \tau_3^{(1)} = \frac{1}{d_3^{(1)}}, \quad \tau_3^{(2)} = \frac{1}{d_3^{(2)}}.$$

Compartment size ratios:

$$\frac{X_1}{X_0} = \frac{r_0}{r_1(1 - 2\bar{p}_1)}, \quad \frac{X_2}{X_1} = \frac{2r_1(1 - \bar{p}_1)}{r_2(1 - 2\bar{p}_2)}, \quad \frac{X_3^{(1)}}{X_2} = \frac{2r_2\gamma_2^{(1)}}{d_3^{(1)}}, \quad \frac{X_3^{(2)}}{X_2} = \frac{2r_2\gamma_2^{(2)}}{d_3^{(2)}}.$$





$$\begin{aligned} \frac{dx_0}{dt} &= r_0 x_0 (2p_0 - 1), \\ \frac{dx_1}{dt} &= 2r_0 x_0 (1 - p_0) + r_1 x_1 (2p_1 - 1), \\ \frac{dx_2}{dt} &= 2r_1 x_1 (1 - p_1) + r_2 x_2 (2p_2 - 1), \\ \frac{dx_3^{(1)}}{dt} &= 2r_2 x_2 (1 - p_2) \gamma^{(1)} - d_3^{(1)} x_3^{(1)}, \\ \frac{dx_3^{(2)}}{dt} &= 2r_2 x_2 (1 - p_2) \gamma^{(2)} - d_3^{(2)} x_3^{(2)}, \end{aligned}$$

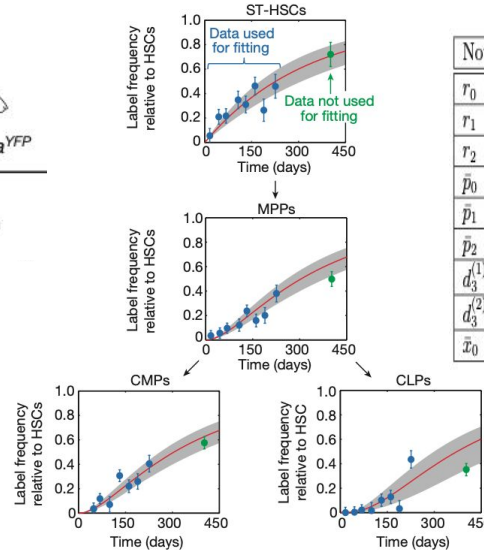
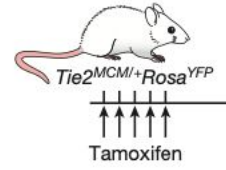
$$p_i = p_i(x_0, x_1, x_2, x_3^{(1)}, x_3^{(2)}), \quad 0 \leq i \leq 2.$$

First, parameter estimation without feedback

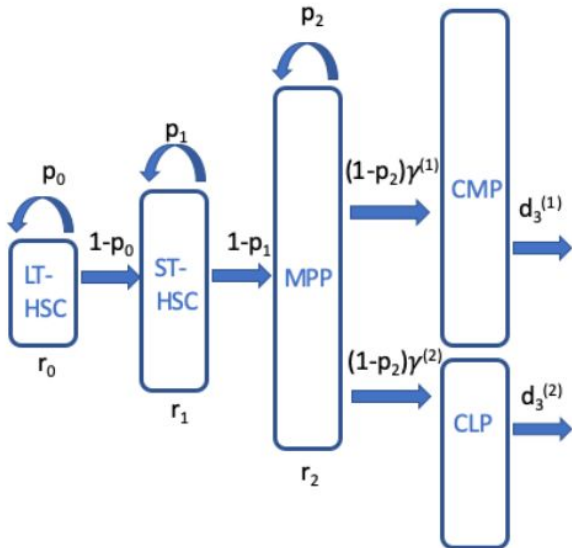
Notation	Parameter definition	Value	95% C.I.	Units
r_0	Division rate of LT-HSCs	0.0107	(0.0084, 0.014)	days ⁻¹
r_1	Division rate of ST-HSCs	0.067	(0.021, 0.10)	days ⁻¹
r_2	Division rate of MPPs	0.136	(0.066, 0.95)	days ⁻¹
\bar{p}_0	Self-renewal probability of LT-HSCs	0.5		1
\bar{p}_1	Self-renewal probability of ST-HSCs	0.473	(0.40, 0.48)	1
\bar{p}_2	Self-renewal probability of MPPs	0.416	(0.323, 0.49)	1
$d_3^{(1)}$	Removal rate of CMPs	0.034	(0.017, 0.22)	days ⁻¹
$d_3^{(2)}$	Removal rate of CLPs	0.007	(0.005, 0.017)	days ⁻¹
\bar{x}_0	Equilibrium number of LT-HSCs	17,000*		cells

Introduce mutants:

Under what conditions do mutants invade and when do they fail?



Notation	Parameter definition	Value	95% C.I.	Units
r_0	Division rate of LT-HSCs	0.0107	(0.0084, 0.014)	days ⁻¹
r_1	Division rate of ST-HSCs	0.067	(0.021, 0.10)	days ⁻¹
r_2	Division rate of MPPs	0.136	(0.066, 0.95)	days ⁻¹
\bar{p}_0	Self-renewal probability of LT-HSCs	0.5		1
\bar{p}_1	Self-renewal probability of ST-HSCs	0.473	(0.40, 0.48)	1
\bar{p}_2	Self-renewal probability of MPPs	0.416	(0.323, 0.49)	1
$d_3^{(1)}$	Removal rate of CMPs	0.034	(0.017, 0.22)	days ⁻¹
$d_3^{(2)}$	Removal rate of CLPs	0.007	(0.005, 0.017)	days ⁻¹
\bar{x}_0	Equilibrium number of LT-HSCs	17,000*		cells



$$\begin{aligned} \frac{dx_0}{dt} &= r_0 x_0 (2p_0 - 1), \\ \frac{dx_1}{dt} &= 2r_0 x_0 (1 - p_0) + r_1 x_1 (2p_1 - 1), \\ \frac{dx_2}{dt} &= 2r_1 x_1 (1 - p_1) + r_2 x_2 (2p_2 - 1), \\ \frac{dx_3^{(1)}}{dt} &= 2r_2 x_2 (1 - p_2) \gamma^{(1)} - d_3^{(1)} x_3^{(1)}, \\ \frac{dx_3^{(2)}}{dt} &= 2r_2 x_2 (1 - p_2) \gamma^{(2)} - d_3^{(2)} x_3^{(2)}, \end{aligned}$$

$$p_i = p_i(x_0, x_1, x_2, x_3^{(1)}, x_3^{(2)}), \quad 0 \leq i \leq 2.$$

Evolution \rightarrow

Wild-type cell populations

$$\begin{aligned} \frac{dx_0}{dt} &= r_0 x_0 (2p_0 - 1), \\ \frac{dx_1}{dt} &= 2r_0 x_0 (1 - p_0) + r_1 x_1 (2p_1 - 1), \\ \frac{dx_2}{dt} &= 2r_1 x_1 (1 - p_1) + r_2 x_2 (2p_2 - 1), \\ \frac{dx_3^{(1)}}{dt} &= 2r_2 x_2 (1 - p_2) \gamma^{(1)} - d_3^{(1)} x_3^{(1)}, \\ \frac{dx_3^{(2)}}{dt} &= 2r_2 x_2 (1 - p_2) \gamma^{(2)} - d_3^{(2)} x_3^{(2)}, \end{aligned}$$

Mutant cell populations

$$\begin{aligned} \frac{dy_0}{dt} &= r_0 y_0 (2p_0^{(m)} - 1), \\ \frac{dy_1}{dt} &= 2r_0 y_0 (1 - p_0^{(m)}) + r_1 y_1 (2p_1^{(m)} - 1), \\ \frac{dy_2}{dt} &= 2r_1 y_1 (1 - p_1^{(m)}) + r_2 y_2 (2p_2^{(m)} - 1), \\ \frac{dy_3^{(1)}}{dt} &= 2r_2 y_2 (1 - p_2^{(m)}) \gamma^{(1)} - d_3^{(1)} y_3^{(1)}, \\ \frac{dy_3^{(2)}}{dt} &= 2r_2 y_2 (1 - p_2^{(m)}) \gamma^{(2)} - d_3^{(2)} y_3^{(2)}. \end{aligned}$$

Evolution - Modeling Mutant Spread

Wild-type cell populations

$$\begin{aligned}\frac{dx_0}{dt} &= r_0 x_0 (2p_0 - 1), \\ \frac{dx_1}{dt} &= 2r_0 x_0 (1 - p_0) + r_1 x_1 (2p_1 - 1), \\ \frac{dx_2}{dt} &= 2r_1 x_1 (1 - p_1) + r_2 x_2 (2p_2 - 1), \\ \frac{dx_3^{(1)}}{dt} &= 2r_2 x_2 (1 - p_2) \gamma^{(1)} - d_3^{(1)} x_3^{(1)}, \\ \frac{dx_3^{(2)}}{dt} &= 2r_2 x_2 (1 - p_2) \gamma^{(2)} - d_3^{(2)} x_3^{(2)},\end{aligned}$$

Mutant cell populations

$$\begin{aligned}\frac{dy_0}{dt} &= r_0 y_0 (2p_0^{(m)} - 1), \\ \frac{dy_1}{dt} &= 2r_0 y_0 (1 - p_0^{(m)}) + r_1 y_1 (2p_1^{(m)} - 1), \\ \frac{dy_2}{dt} &= 2r_1 y_1 (1 - p_1^{(m)}) + r_2 y_2 (2p_2^{(m)} - 1), \\ \frac{dy_3^{(1)}}{dt} &= 2r_2 y_2 (1 - p_2^{(m)}) \gamma^{(1)} - d_3^{(1)} y_3^{(1)}, \\ \frac{dy_3^{(2)}}{dt} &= 2r_2 y_2 (1 - p_2^{(m)}) \gamma^{(2)} - d_3^{(2)} y_3^{(2)}\end{aligned}$$

Competition through shared feedback:

$$p_0 = c_0 / (h_0 (x_0 + y_0) + 1)$$

$$p_0^{(m)} = c_0^{(m)} / (h_0 (x_0 + y_0) + 1)$$

$$p_1 = c_1 / (h_1 (x_1 + y_1) + 1)$$

$$p_1^{(m)} = c_1^{(m)} / (h_1 (x_1 + y_1) + 1)$$

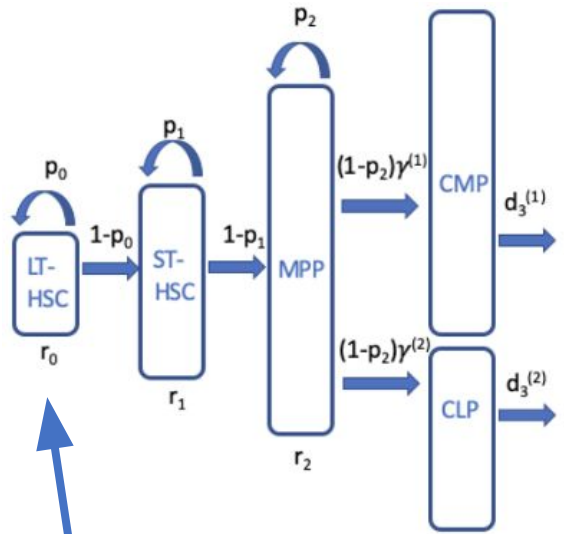
$$p_2 = c_2 / (h_2 (x_2 + y_2) + 1)$$

$$p_2^{(m)} = c_2^{(m)} / (h_2 (x_2 + y_2) + 1)$$

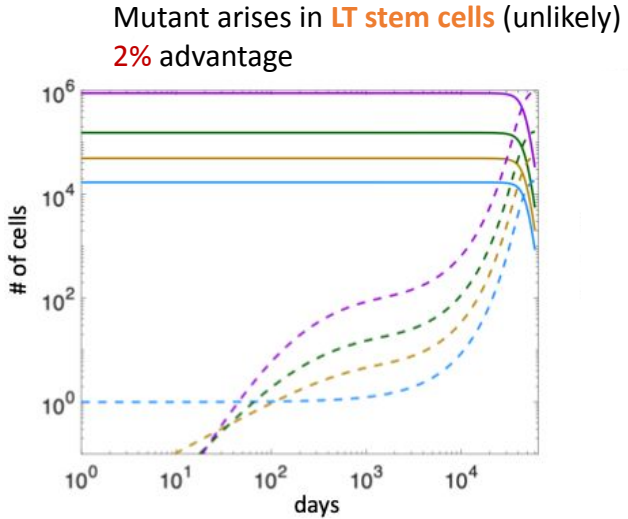
Advantageous mutants:

$$p_i^{(m)} = (1 + s)p_i > p_i$$

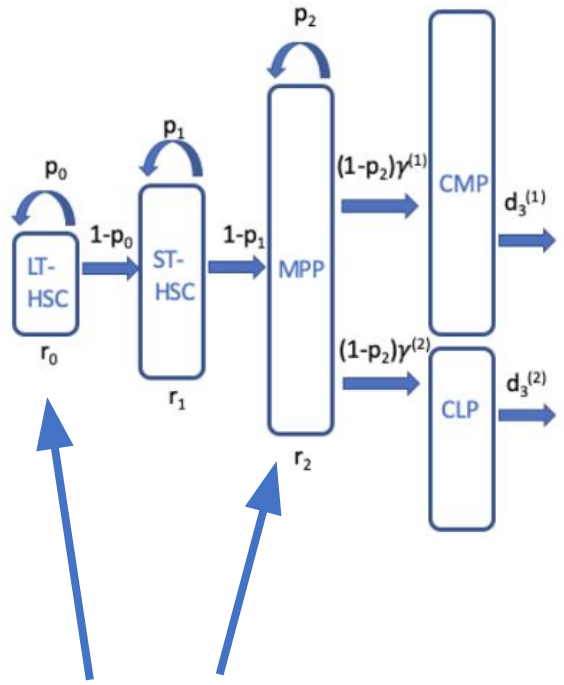
Insights from evolutionary computer simulations



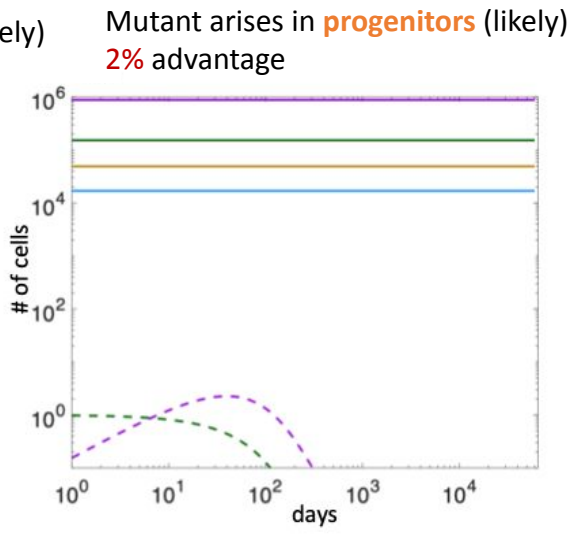
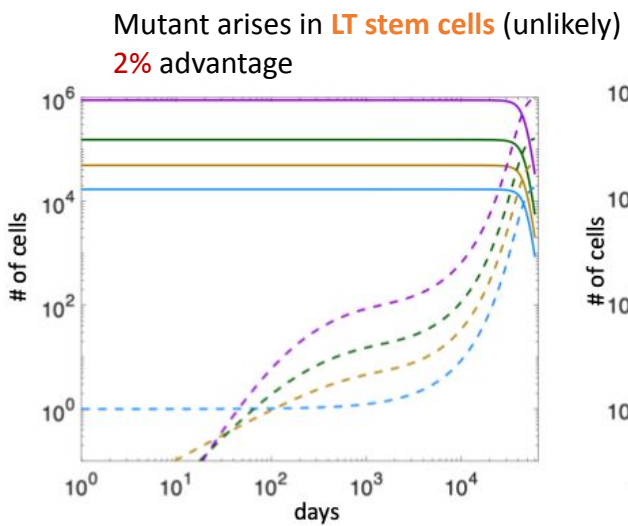
Where does the mutant arise?



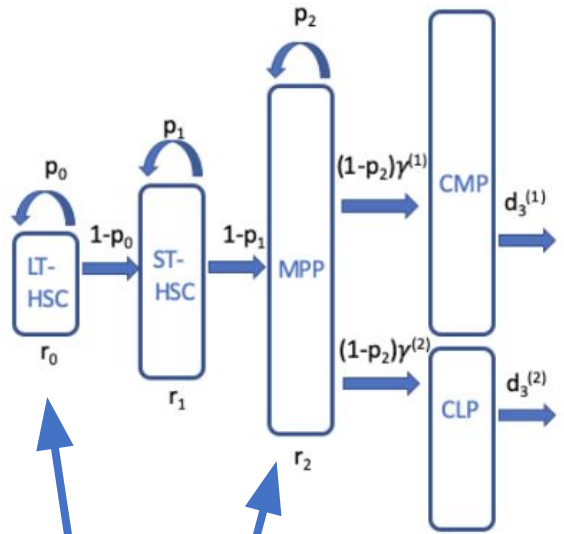
Insights from evolutionary computer simulations



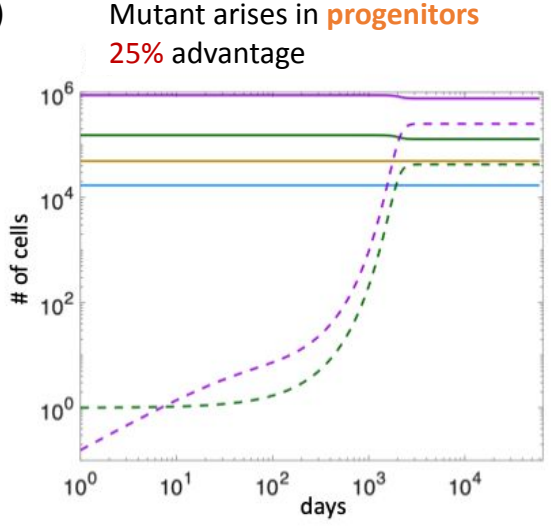
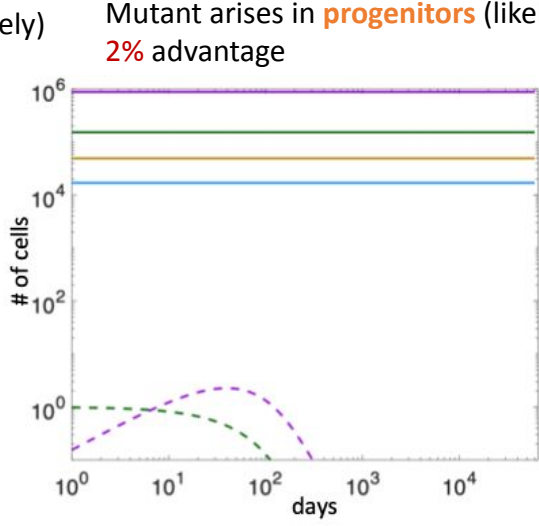
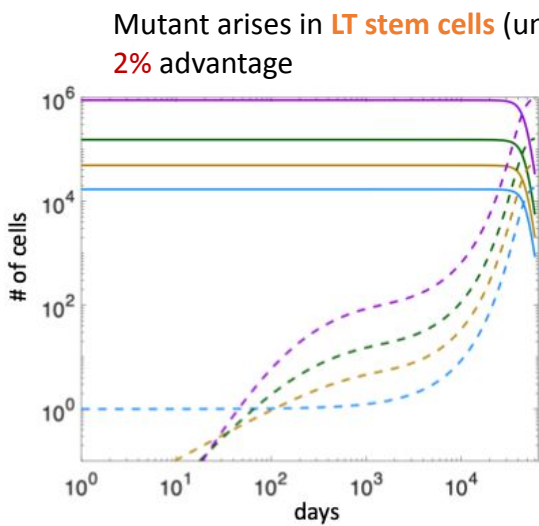
Where does the mutant arise?



Insights from evolutionary computer simulations



Where does the mutant arise?

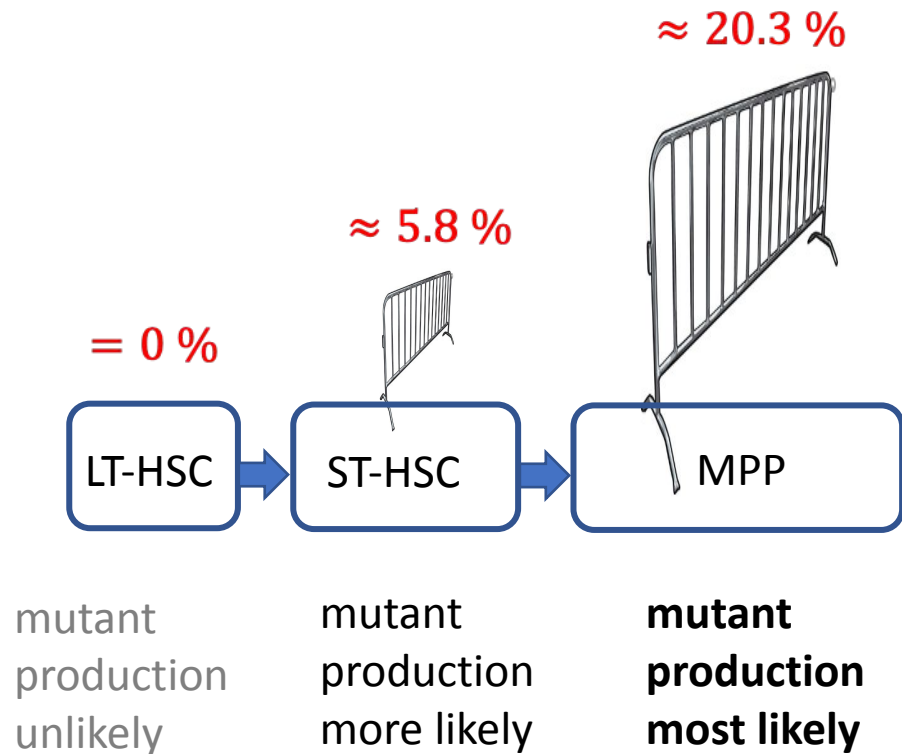


Mutants matter only when they arise in the downstream, progenitor compartments

But there, successful invasion requires a massive mutant advantage

⇒ Barrier to mutant invasion

Hematopoietic hierarchy protects against mutations



Mutant invasion barrier:

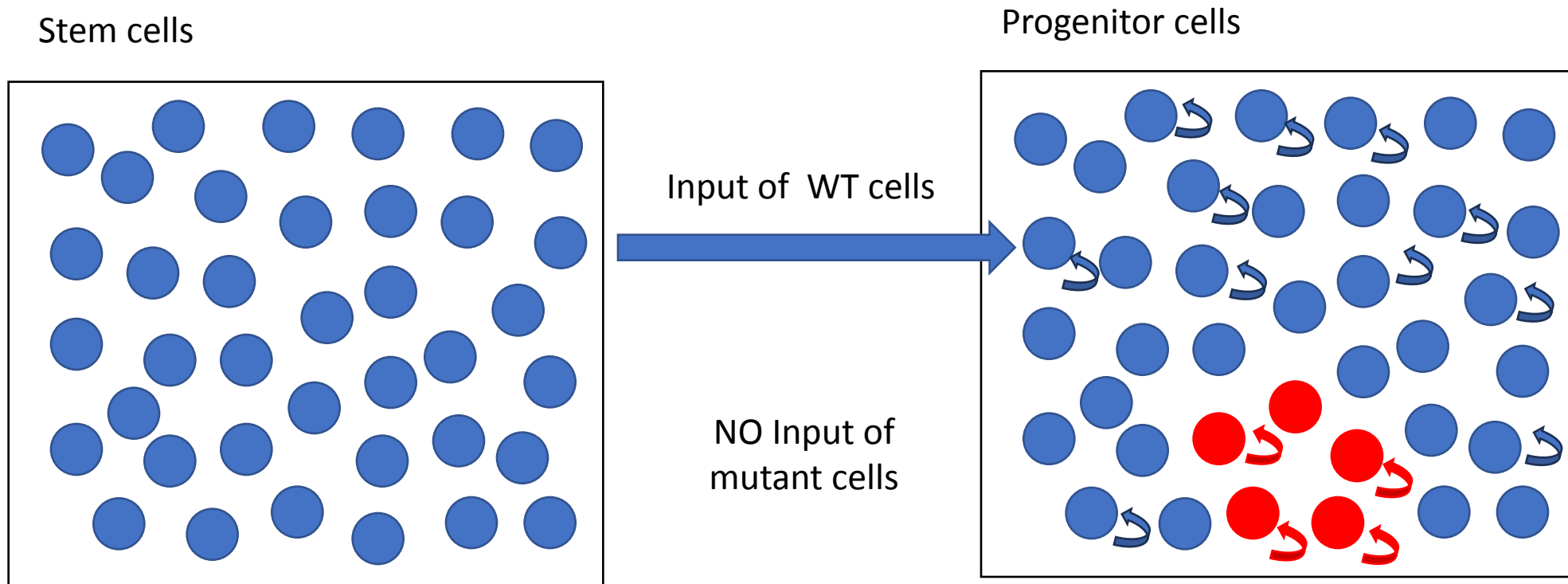
$$s > s_c = \frac{1}{2\bar{p}_i} - 1$$

Advantageous mutants:

$$p_i^{(m)} = (1 + s)p_i > p_i$$

Evolutionary compromise between

- tissue amplification and
- invasion barrier



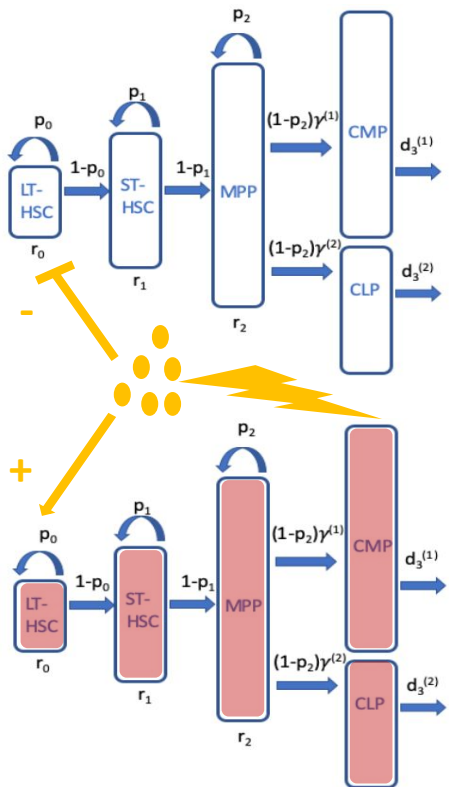
Fitness of cells in progenitor compartment:

WT cells: local division + input from upstream compartment

mutant cells: local division only

=> Hence advantage in division must be large to overcome WT fitness

What can facilitate mutant invasion?

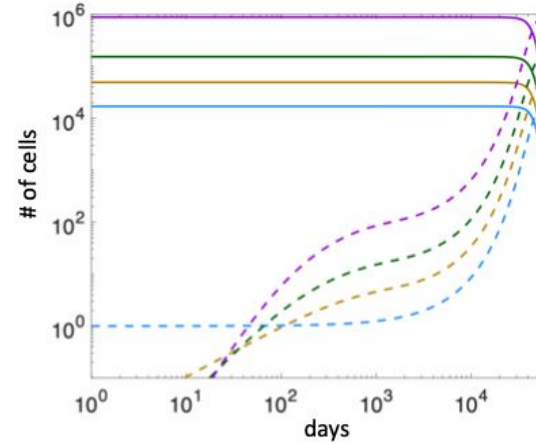


Mutants generate inflammation

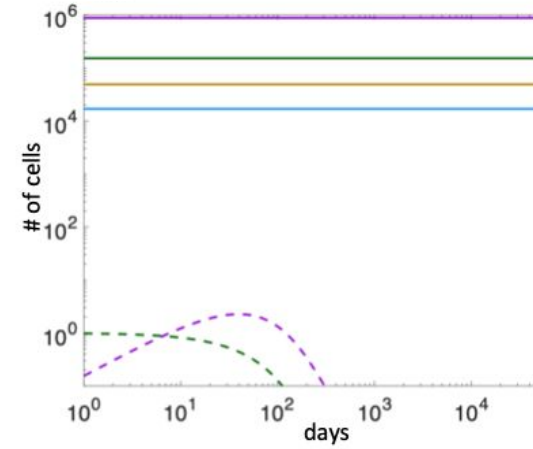
Inflammation creates environment that is beneficial for mutants

=> Evolutionary niche construction

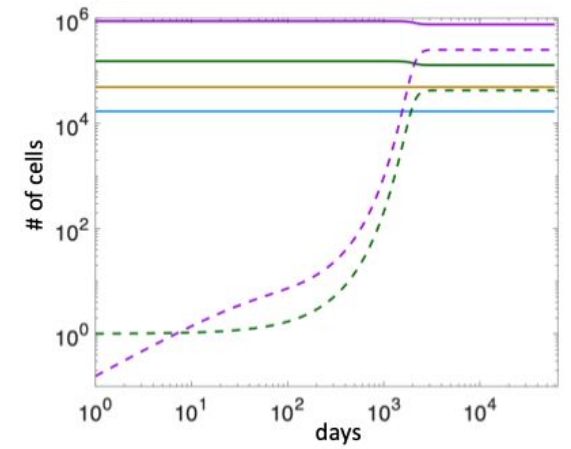
Mutant arises in **LT stem cells** (unlikely)
2% advantage



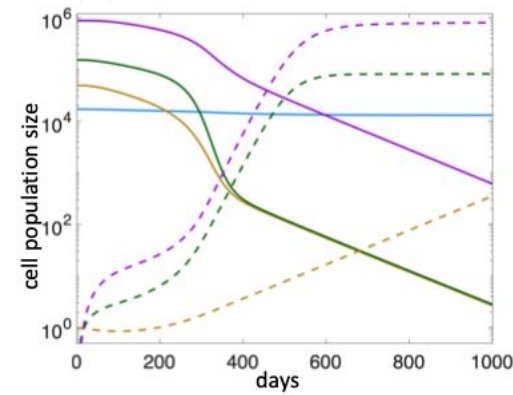
Mutant arises in **progenitors** (likely)
2% advantage



Mutant arises in **progenitors**
25% advantage



Mutant arises in progenitors
2% advantage

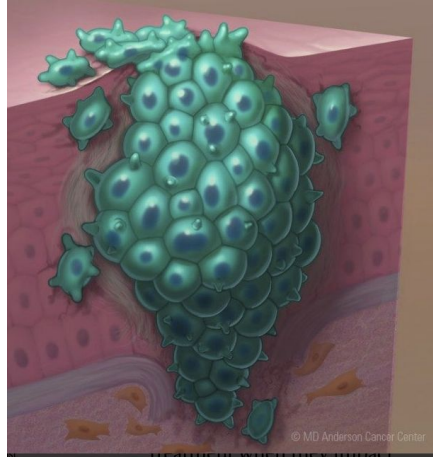


Fast mutant emergence

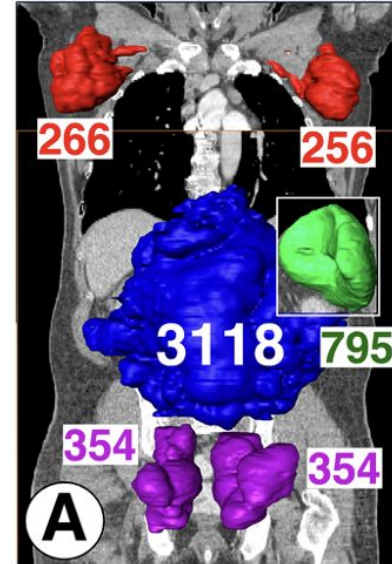
3. Cell evolution in spatially structured populations:



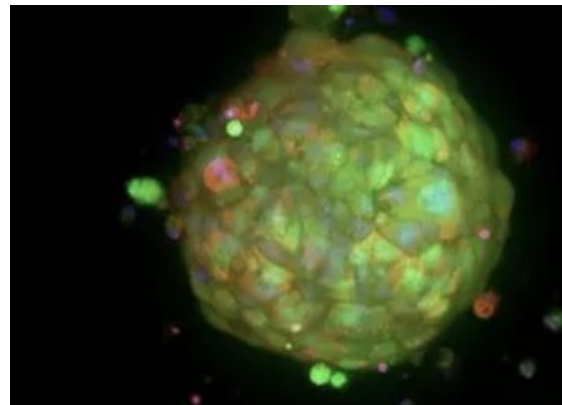
Everything is spatial



tumors arising in patients
are spatially structured



Lymph nodes packed
with leukemia cells



patient-derived tumor organoid

Some spatial modeling approaches

Partial Differential Equations (PDEs)

Continuous mathematical models using reaction-diffusion-taxis equations to describe cell populations and molecular concentrations across space and time.

- Continuous cell densities
- Deterministic dynamics
- Computationally efficient
- Analytical tractability

Agent-Based Models (ABMs) & Cellular Automata (CA)

Discrete models that simulate individual cells as autonomous agents with explicit behaviors and local interactions.

- Lattice-based CA (fixed grid)
- Off-lattice ABM (free movement)
- Stochastic cell behaviors
- Cell heterogeneity

Cellular Potts Model (CPM)

Lattice-based, energy-minimization approach where cells are extended objects with explicit shapes spanning multiple lattice sites.

- Multi-pixel cell representation
- Adhesion & surface tension
- Explicit cell shapes & volumes
- Monte Carlo dynamics

Lattice Gas Cellular Automata (LGCA)

Multiple cells can occupy a single lattice site, tracking cell movement through channels between sites rather than individual trajectories.

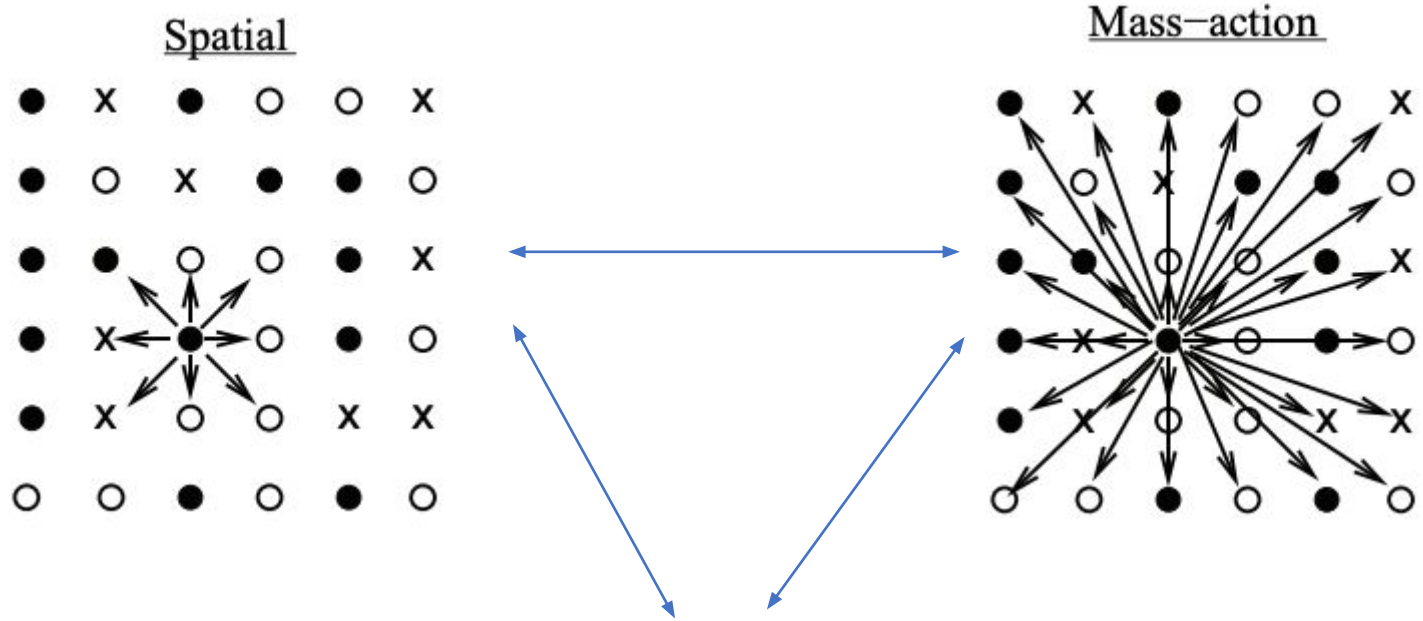
- Multiple cells per site
- Statistical mechanics framework
- Large-scale simulations
- Links to continuum models

Hybrid & Multiscale Models

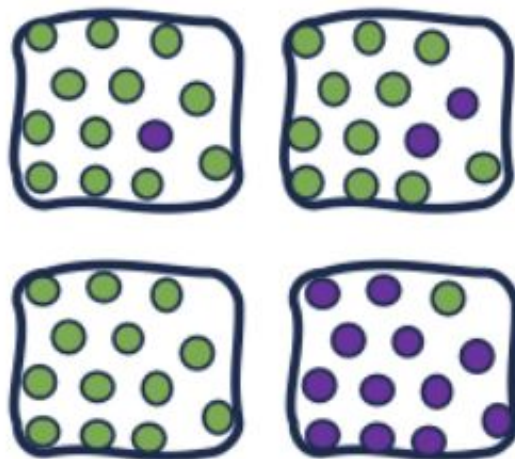
Combine multiple modeling approaches to span spatial and temporal scales—discrete cells coupled with continuous chemical fields.

- PDE + ABM coupling
- Intracellular signaling networks
- Tissue-level phenomena
- Drug pharmacokinetics

Mixed vs ABM vs deme models – similarities and differences



Demes, e.g. lymph nodes



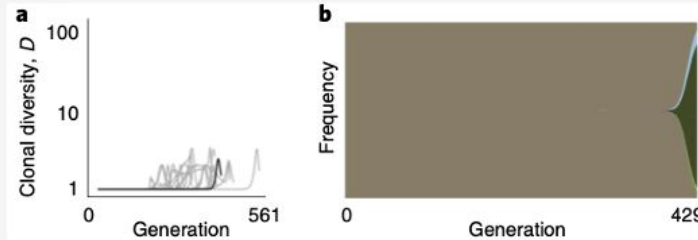
Study examples that show important roles of space for tumor evolution

1. Non-Spatial



Mode: Rapid Clonal Expansion

- Well-mixed population
- Fast selective sweeps
- Few dominant clones
- Low diversity ($D < 10/3$)

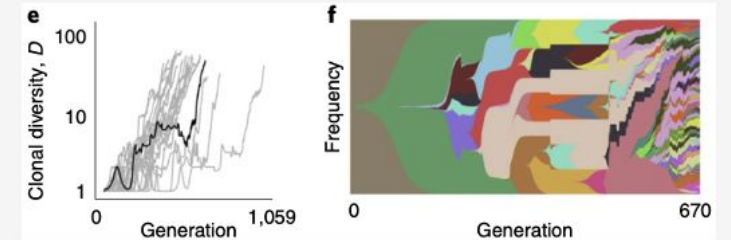


2. Gland Fission (Adenoma)



Mode: Progressive Diversification

- Growth by bifurcation
- Localized sweeps
- Highly branched tree
- High diversity ($D > 20$)

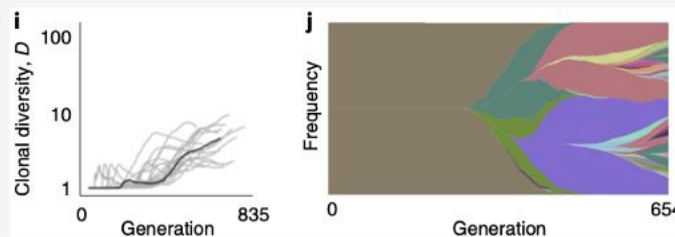


3. Invasive Glandular



Mode: Branching Evolution

- Invades normal tissue
- Clonal interference
- Multiple long branches
- Moderate diversity ($3 < D < 20$)

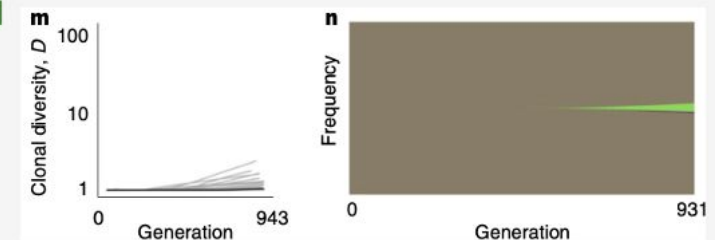


4. Boundary Growth



Mode: Effectively Neutral

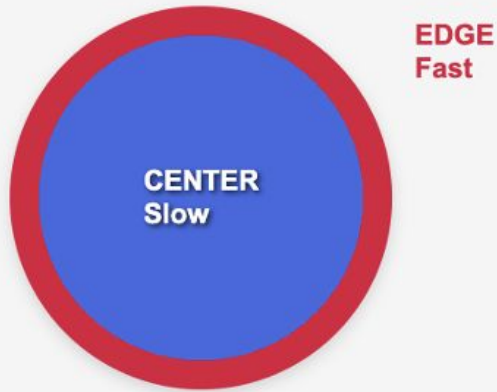
- Proliferation at edge only
- Genetic drift dominates
- Star-shaped tree
- Low drivers per cell ($n < 2$)



Boundary-Driven Growth in Hepatocellular Carcinoma

Lewinsohn et al 2023, Nature Ecology & Evolution

Tumor Architecture



- **Edge:** High division rate
- **Center:** Low division rate

🎯 Key Finding

Tumor 1

6.4×

faster division on edge vs center

Tumor 2

2.8×

faster division on edge vs center

📊 Data Used

- Multi-region sequencing from 2 HCC tumors
- 9-16 spatially-labeled biopsies per tumor
- Genetic sequences + spatial locations (edge/center)
- SDevo model links mutation rate to division rate

✓ Biological Interpretation

Boundary-driven growth confirmed in vivo:

- Cell divisions concentrated at tumor periphery
- Center cells division-limited (crowding, hypoxia, nutrient depletion)
- Spatial structure shapes tumor evolution

💡 **Conclusion: Clinical tumors exhibit strong boundary-driven growth with most proliferation occurring at the tumor surface, validating predictions from spatial models**

Spatial Sampling Determines Clonality Inference

Opasic et al., BMC Cancer (2019)

Research Question: How many Convert to SmartArt Graphic needed to correctly identify truly clonal (truncal) mutations from spatially heterogeneous tumors?

Methodology

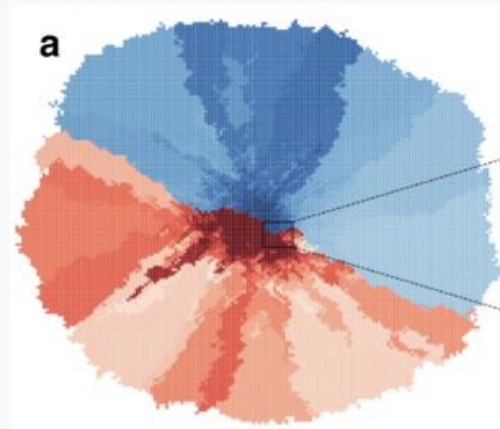
1. Spatial Tumor Model (2D Lattice)



- Cells grow on 2D lattice
- Mutations create spatial heterogeneity
- First sub-clone (■) branches from ancestral (■)

2. Sampling & Analysis

- Take n biopsies (single-cell or bulk)
- Reconstruct mutational profiles
- 10,000 iterations per simulation
- Compare: random vs. pattern sampling



Key equation:

$$\text{Probability of correct classification} = 1 - f^n$$

where f = proportion of largest sub-clone

Key Results

1. Samples Needed (98% confidence)

$f = 0.1$: ~2 samples ✓

$f = 0.5$: ~6 samples

$f = 0.9$: >38 samples

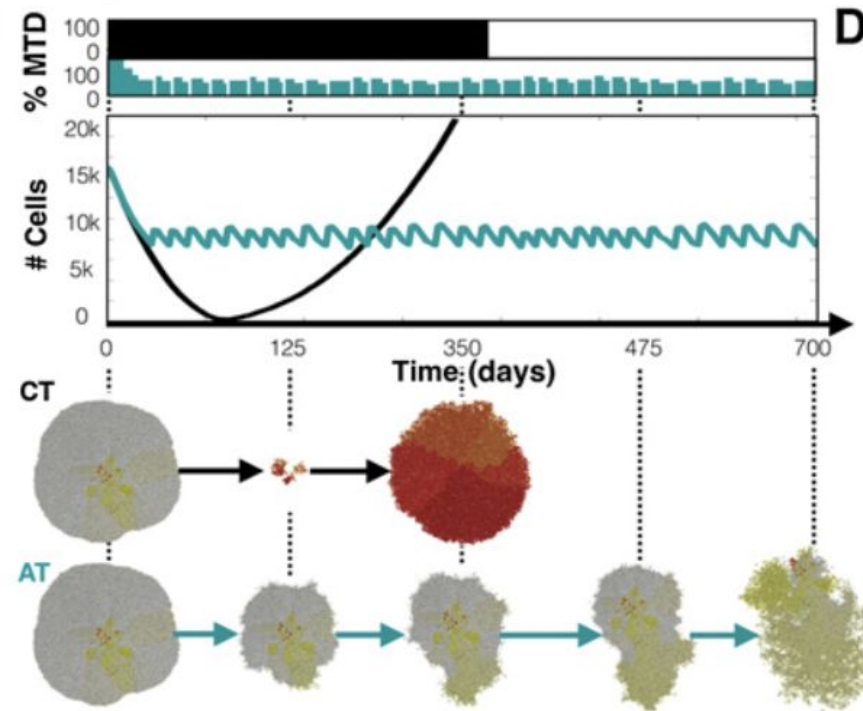
where f = proportion of largest sub-clone

2. Pattern Sampling > Random Sampling

Strategy: Sample from tumor periphery at equidistant locations (e.g., North, South, East, West positions)

Benefit: Maximizes spatial dispersion → increases probability of sampling different clonal regions → higher accuracy with fewer samples

Spatial structure can be important for the competition between resistant and sensitive cells



Convergence and Technologies

Cancer
Research

Spatial Heterogeneity and Evolutionary Dynamics Modulate Time to Recurrence in Continuous and Adaptive Cancer Therapies

Jill A. Gallaher¹, Pedro M. Enriquez-Navas², Kimberly A. Luddy², Robert A. Gatenby¹, and Alexander R.A. Anderson¹



ARTICLE

Received 21 Apr 2016 | Accepted 28 Jul 2016 | Published 3 Oct 2016

DOI: 10.1038/ncomms12760 OPEN

Excess of mutational jackpot events in expanding populations revealed by spatial Luria-Delbrück experiments

Diana Fusco^{1,2}, Matti Gralka¹, Jona Kayser^{1,2}, Alex Anderson¹ & Oskar Hallatschek^{1,2}

More mutants in spatially growing colonies compared to non-spatially growing colonies at the same population size

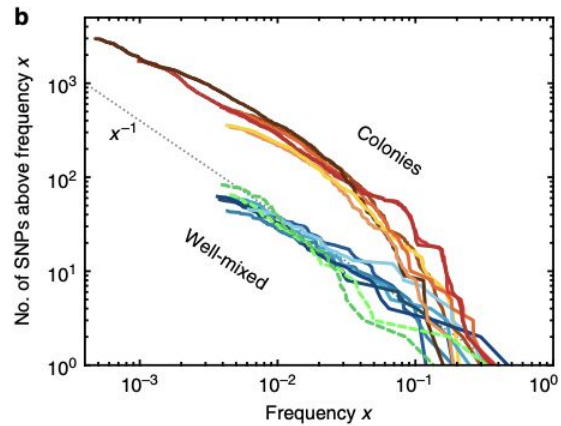
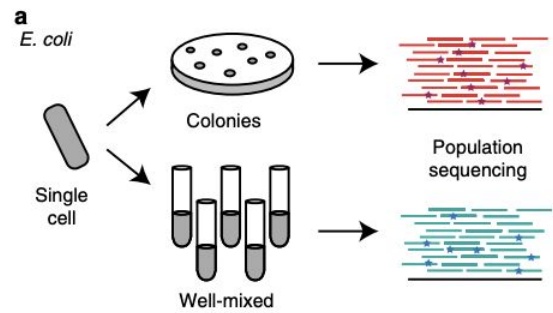
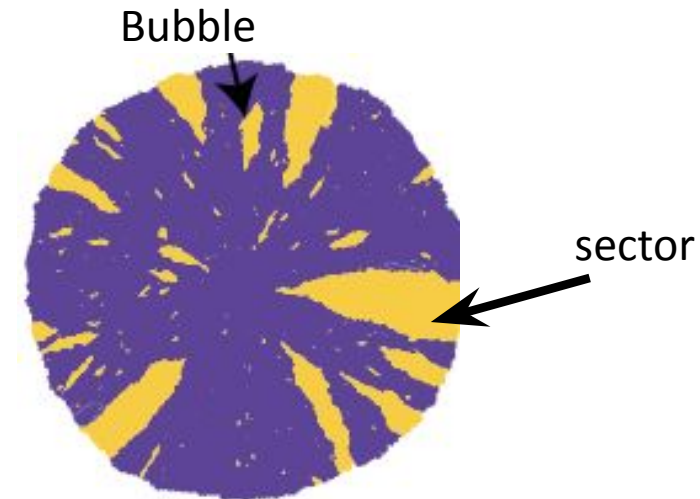
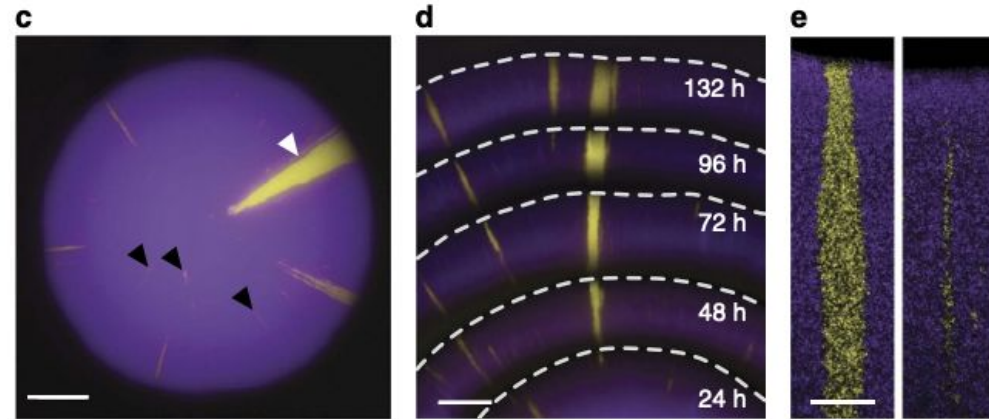
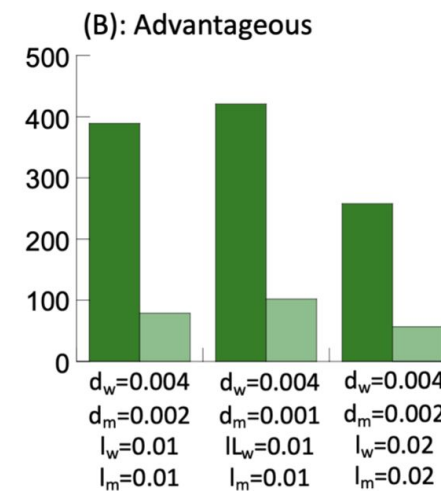
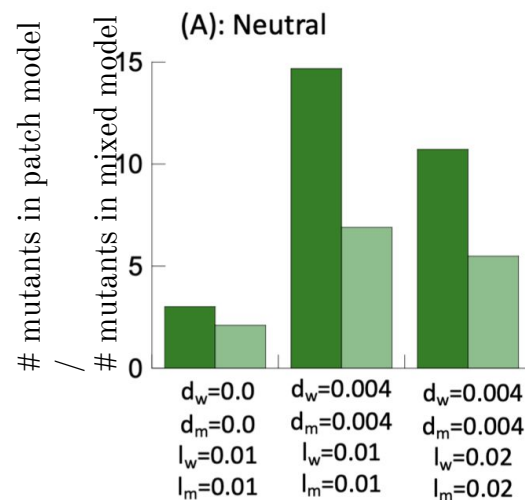
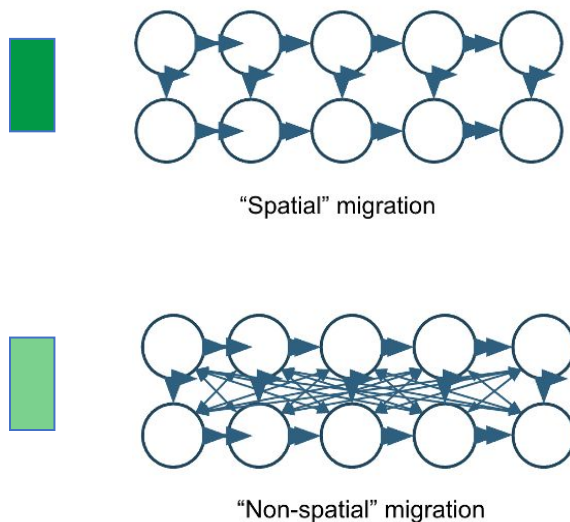
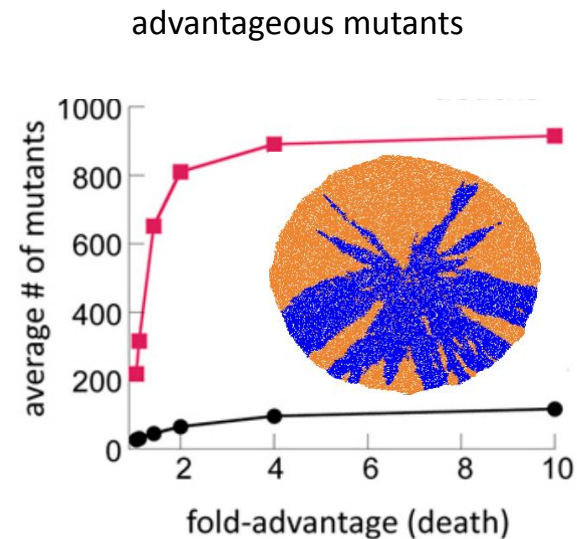
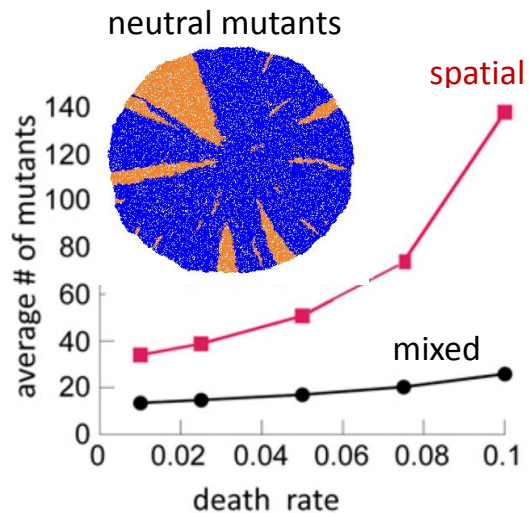
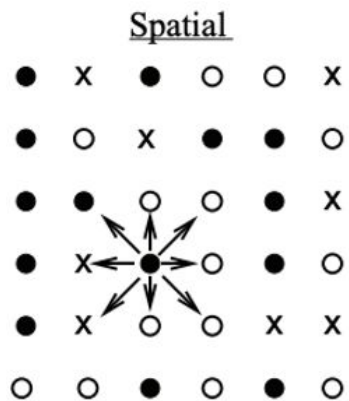


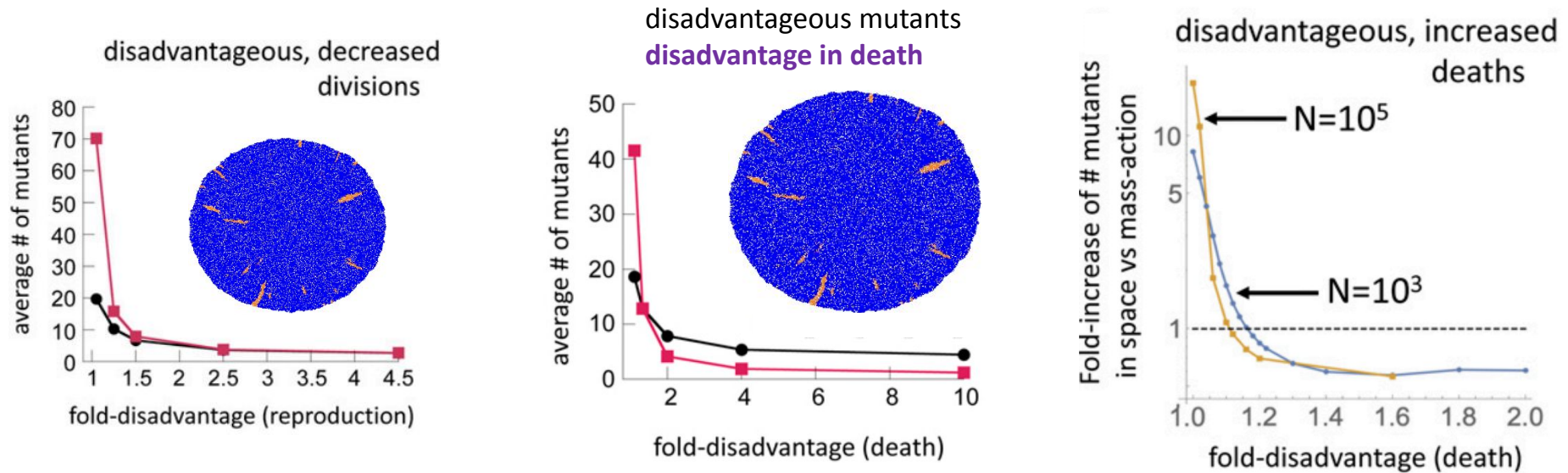
Figure 1 | Population sequencing reveals an excess of jackpot events in spatially growing populations. (a) Starting from few cells of a mutator



At population size N
how many mutants?
(crucial question for resistance evolution)



Complexity of Disadvantageous Mutants



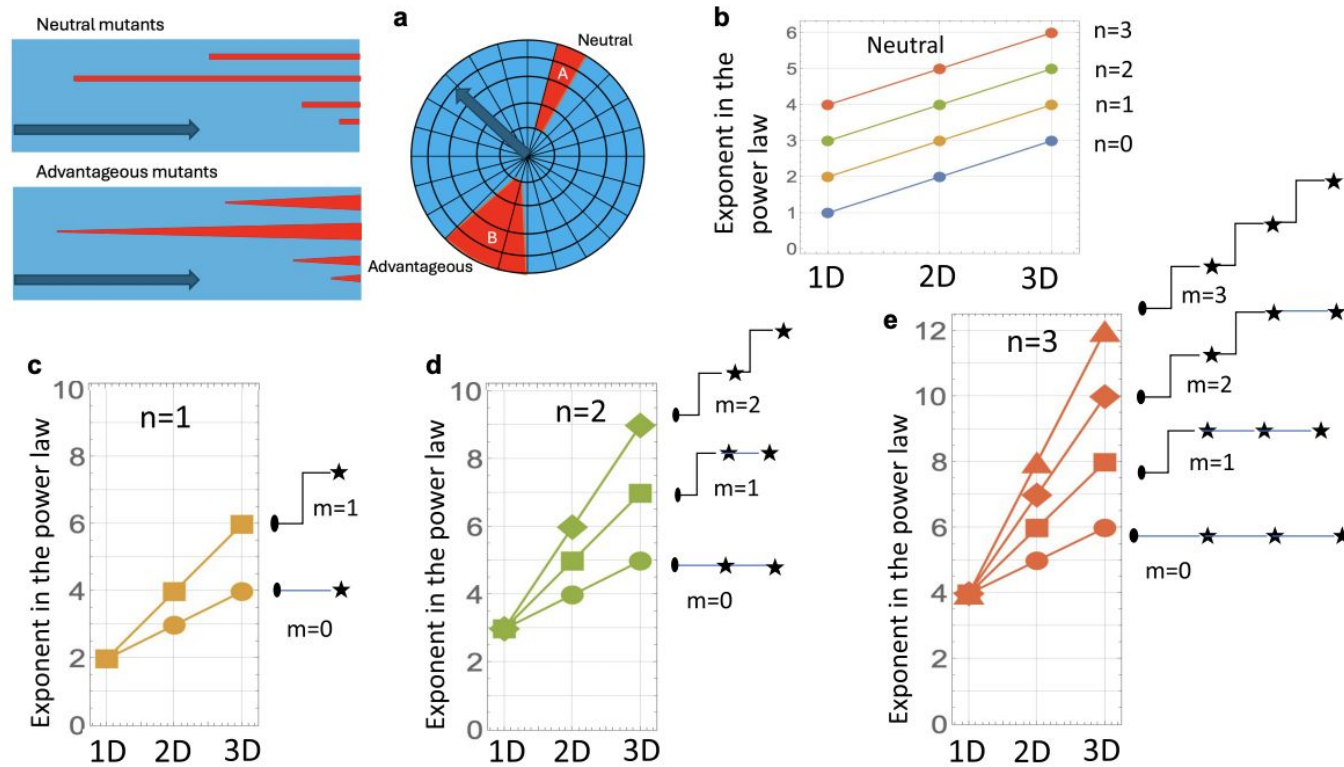
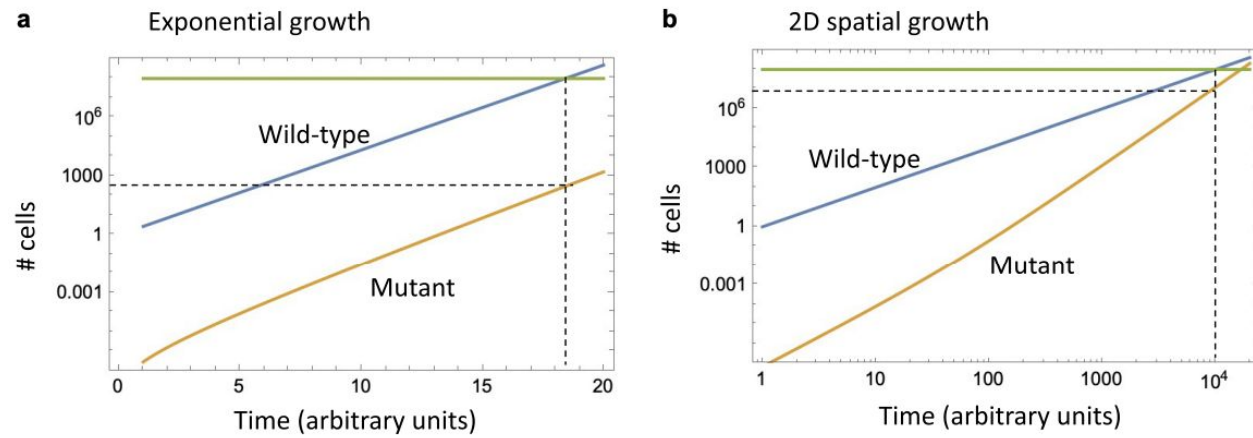
If mutant disadvantage is in less birth: more mutants in spatial compared to mixed system

If mutant disadvantage is in more death: less mutants in spatial compared to mixed system

Same patterns observed in

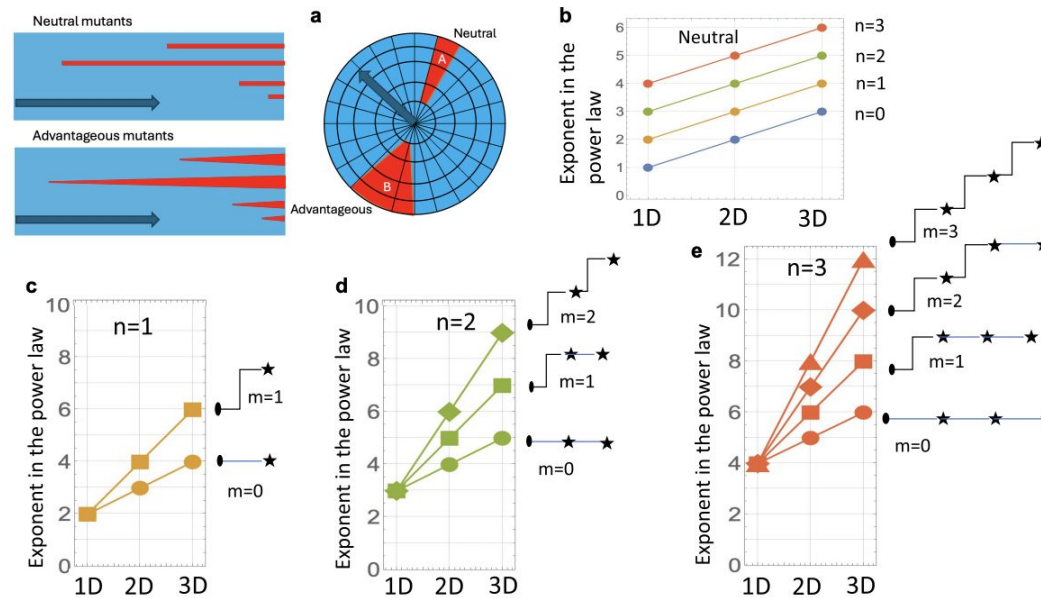
- ABM
- Deme model with **migration to nearest neighbors**
- Deme model with **non-spatial migration**

Scaling laws for n-hit mutants in 1, 2, and 3 dimensional spatial growth

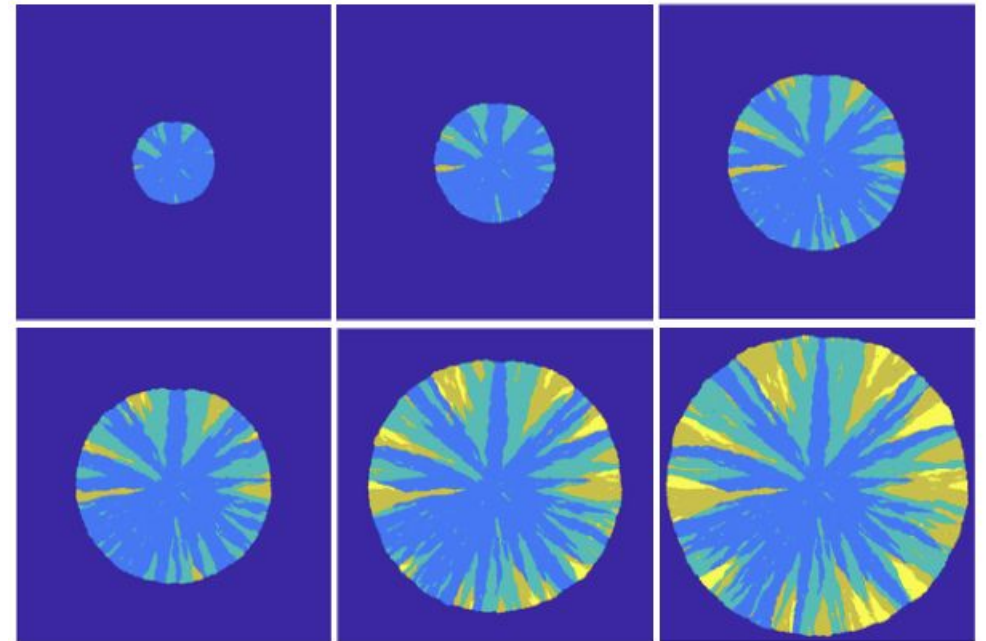
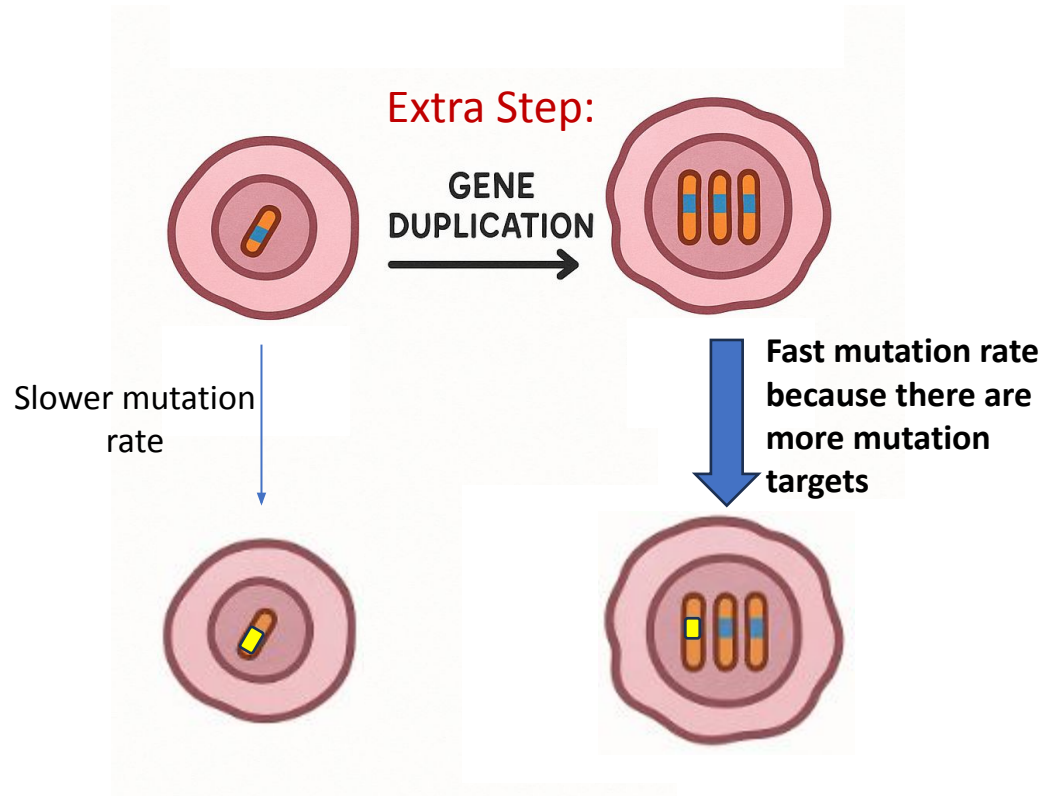


Why are mutant scaling laws useful?

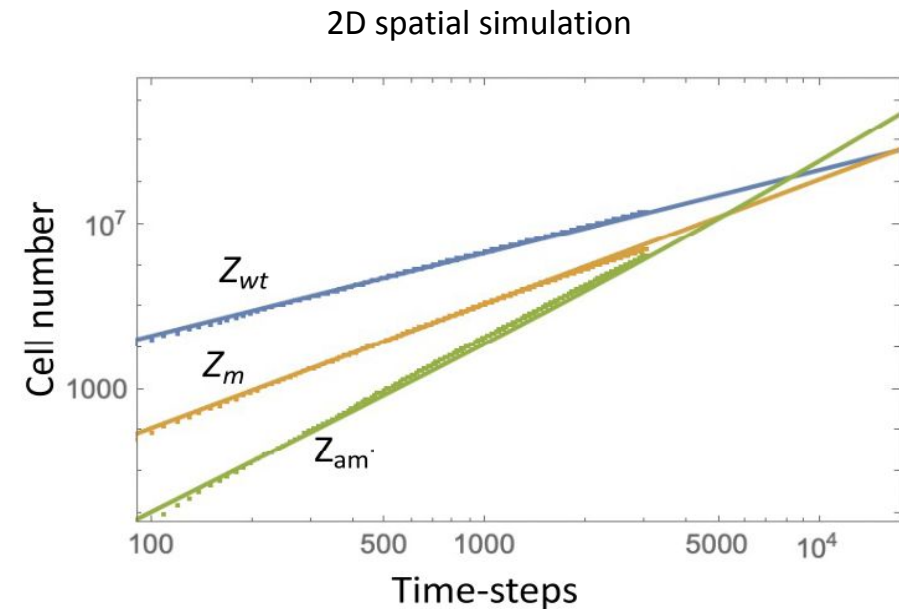
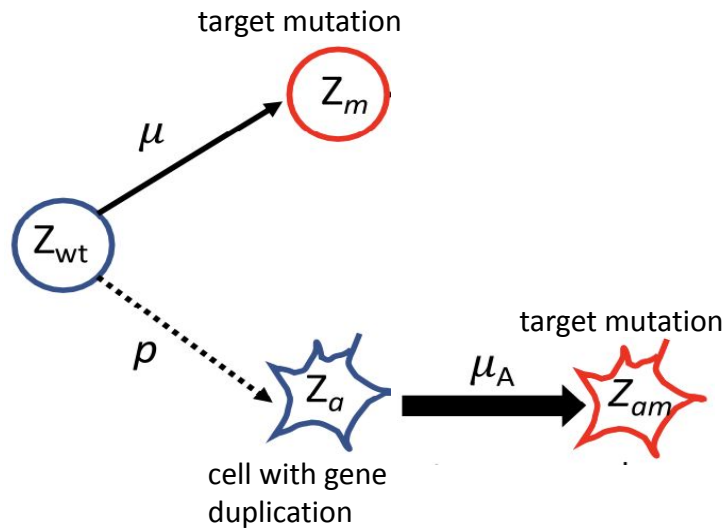
- Tumors are large cell populations, up to 10^{12} or 10^{13} cells.
- Simulating growth to such sizes with stochastic ABMs to determine mutant burden is very slow
- With scaling laws, you can extrapolate mutant burden to large population sizes without the need to simulate up to these huge population sizes



Application: Role of gene amplifications

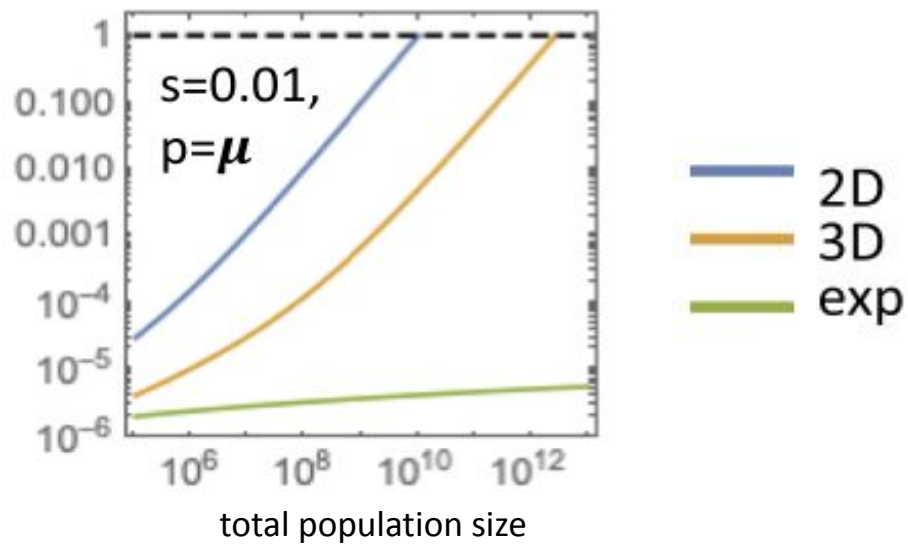


Spatial structure is required for cells with gene amplifications to contribute to mutant evolution

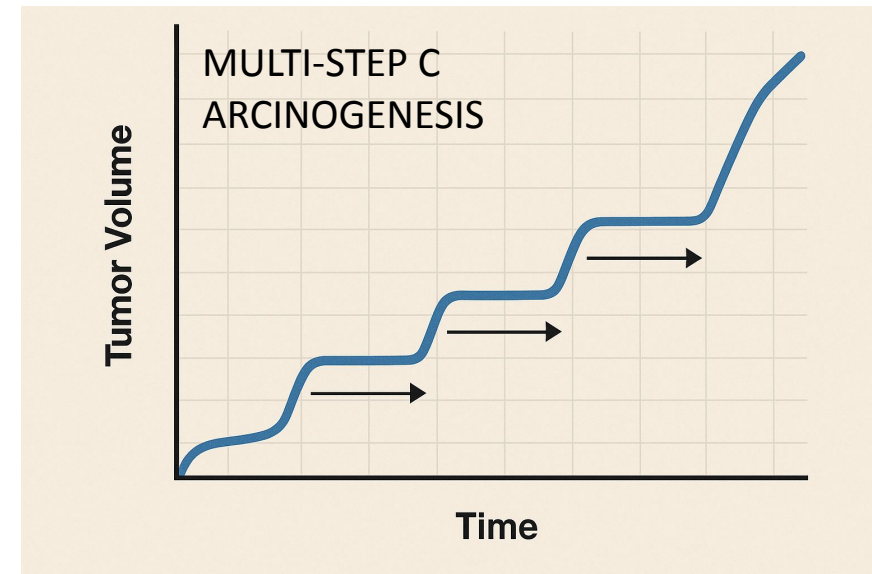
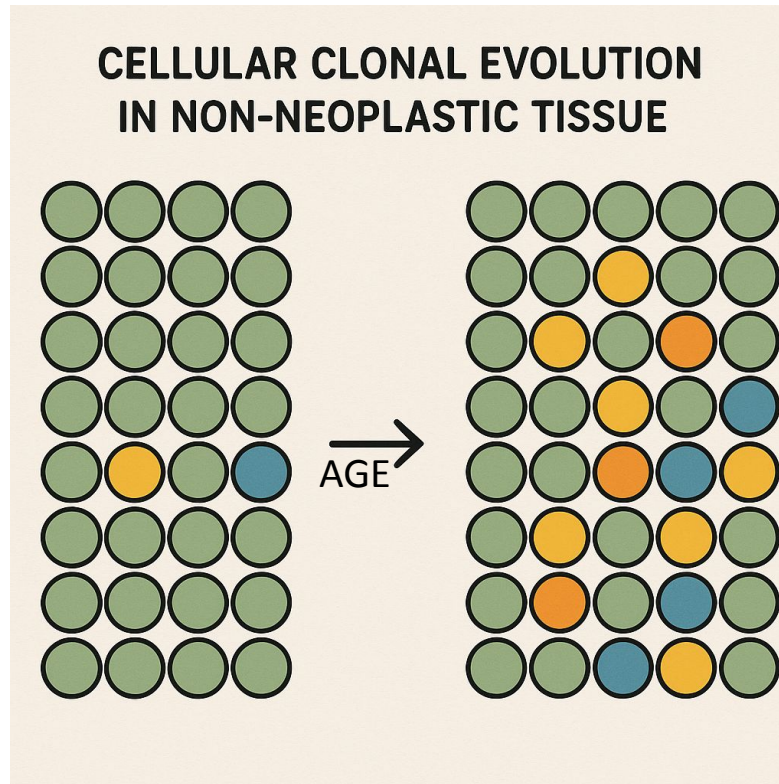


Relative contribution of duplicated cells to target mutant generation

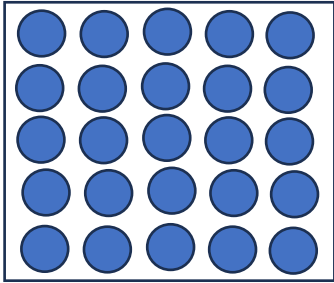
comparing population structures



Spatial mutant evolution and selection at steady state

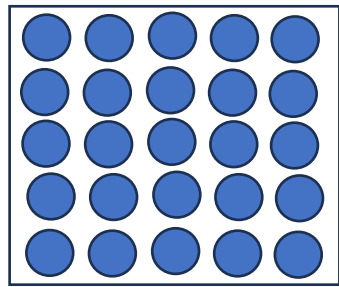


FIXATION PROBABILITY as a measure of fitness

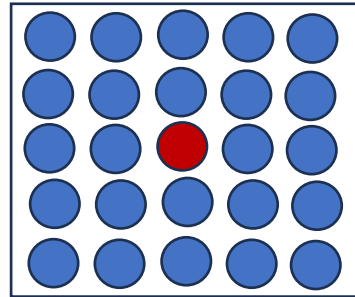


WT population at equilibrium

Fixation probability as a measure of fitness

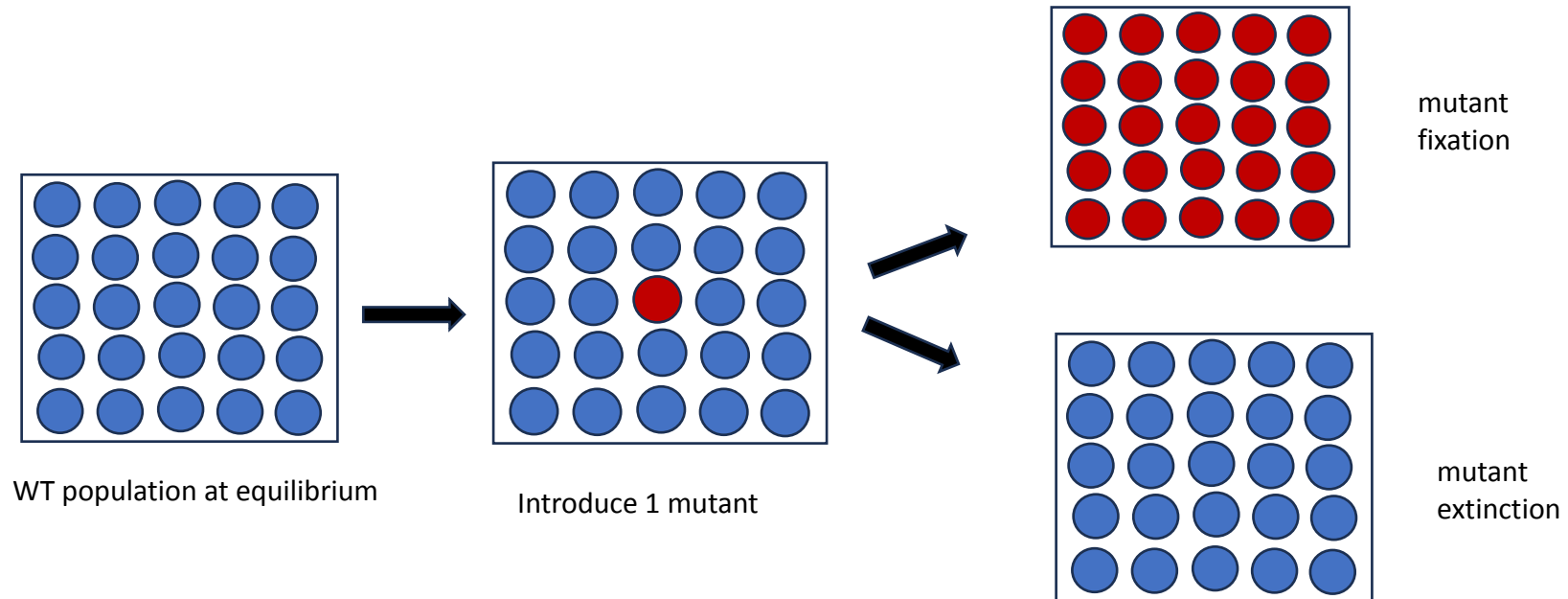


WT population at equilibrium



Introduce 1 mutant

Fixation probability as a measure of fitness



Mutants can be

- neutral
- disadvantageous
- advantageous

Fixation probability

$$p(\text{fix}) = 1/N$$

$$p(\text{fix}) = \frac{1 - \left(\frac{1}{r}\right)^i}{1 - \left(\frac{1}{r^n}\right)}$$

Moran process

Advantage or disadvantage typically expressed through the change of one parameter, such as a changed birth rate or a changed death rate

Correlations Between Apoptotic and Proliferative Indices in Malignant Non-Hodgkin's Lymphomas

Faster cell division rates often correlate with faster cell death rates

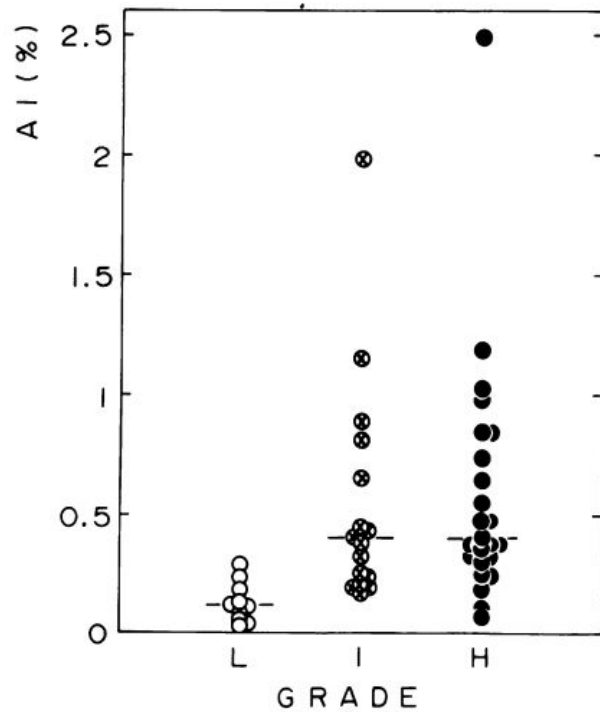


Figure 2. Mean apoptotic indices per case (AI) of low (L, open circles), intermediate (I, crossed circles), and high (H, closed circles) malignancy grade NHLs according to the Working Formulation.²⁰ Bars represent median AIs per group.

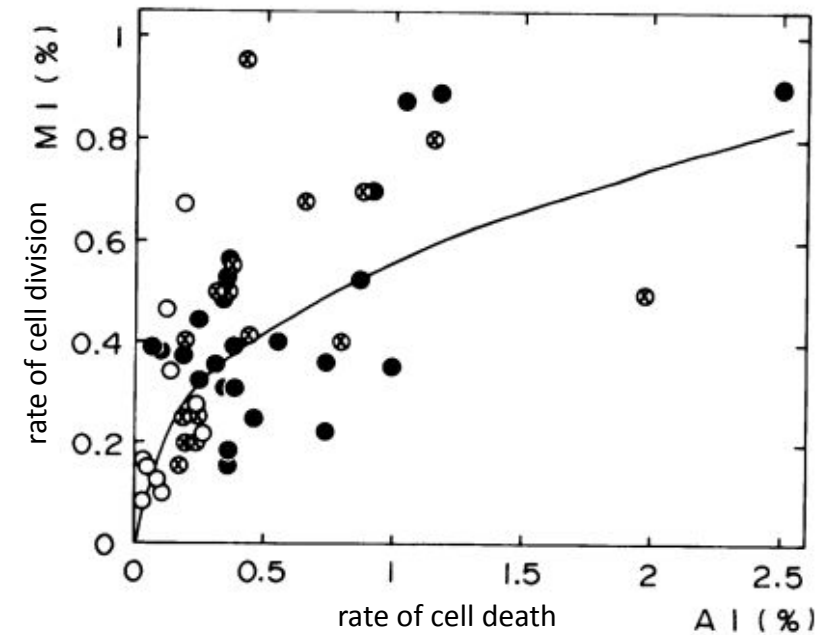


Figure 3. Mean mitotic indices per case (MI) plotted against AIs of NHLs. Regression analysis: nonlinear model, $y = ax^b$. The correlation coefficient (CC) is 0.659. See also legend to Figure 2.

The concept of Quasi-Neutral Mutants

JOURNAL ARTICLE

Some Consequences of Demographic Stochasticity in Population Genetics

Todd L Parsons, Christopher Quince, Joshua B Plotkin ✉

Genetics, Volume 185, Issue 4, 1 August 2010, Pages 1345–1354,

<https://doi.org/10.1534/genetics.110.115030>

reproduction rate of mutant and WT

$$r_m = \tau r_w$$

death rate of mutant and WT

$$d_m = \tau d_w$$

**MUTANT AND WT HAVE IDENTICAL
LIFE-TIME REPRODUCTIVE SUCCESS**

$\tau > 1$: higher turnover mutant

$\tau < 1$: lower turnover mutant

	reproduction rate	death rate	life-time repr. output
	r	d	r/d
wt	0.1	0.01	10
mutant	1.0	0.1	10

Fixation probability of quasi-neutral mutants in *well-mixed populations*

WT cells $\frac{dx}{dt} = r_w x \left(1 - \frac{x+y}{K}\right) - d_w x$

Mutant cells $\frac{dy}{dt} = \tau r_w y \left(1 - \frac{x+y}{K}\right) - \tau d_w y$



stochastic process

Fixation probability of quasi-neutral mutants in *well-mixed populations*

WT cells $\frac{dx}{dt} = r_w x \left(1 - \frac{x+y}{K}\right) - d_w x$

Mutant cells $\frac{dy}{dt} = \tau r_w y \left(1 - \frac{x+y}{K}\right) - \tau d_w y$



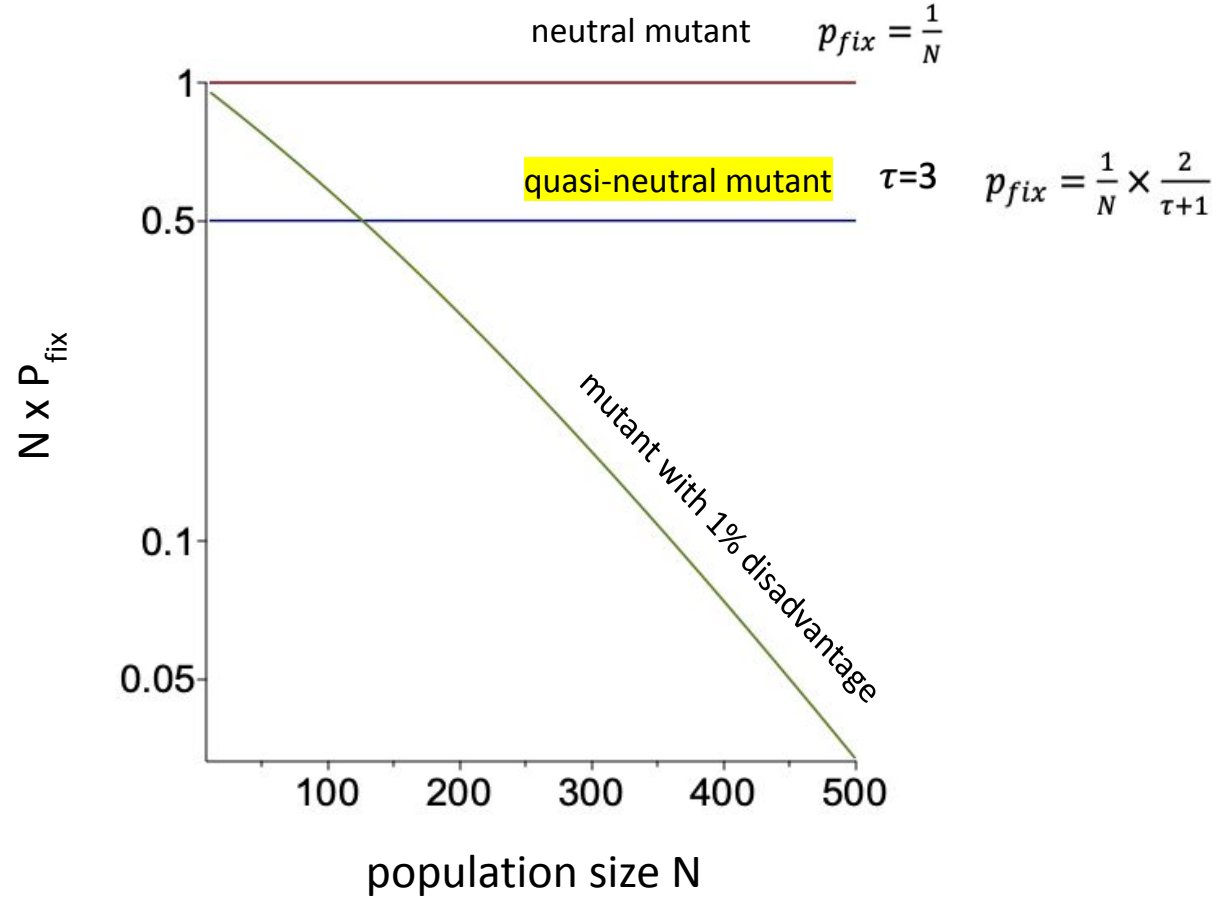
stochastic process

$$p_{fix} = \frac{1}{N} \times \frac{2}{\tau+1}$$

rather than

$$p_{fix} = \frac{1}{N}$$

Fixation probability of quasi-neutral mutants in *well-mixed populations*

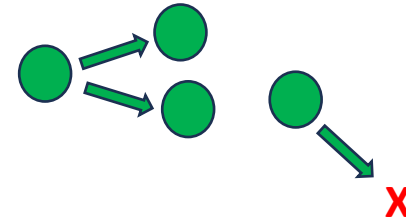


Reason for deviation from neutrality

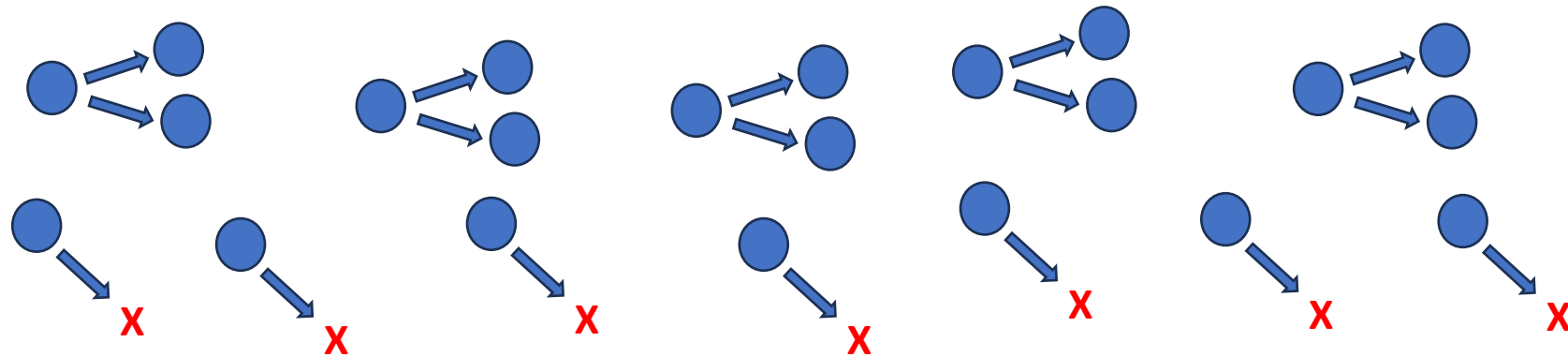
time frame



slow turnover



fast turnover

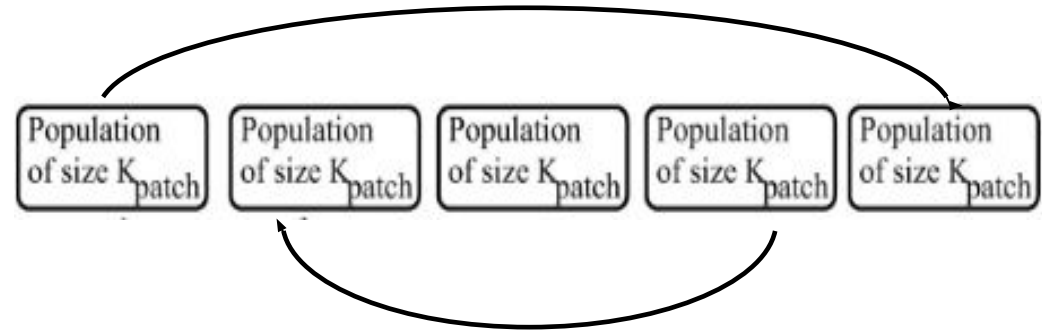


Spatial Dynamics

Dynamics of quasi-neutral mutants in **deme structured** populations

Komarova & Wodarz 2025, Nature Communications

Deme / patch model with non-spatial migration



In each deme, Gillespie simulations are performed for the ODE mode:

$$\text{WT cells} \quad \frac{dx}{dt} = r_w x \left(1 - \frac{x+y}{K}\right) - d_w x$$

$$\text{Mutant cells} \quad \frac{dy}{dt} = \tau r_w y \left(1 - \frac{x+y}{K}\right) - \tau d_w y$$

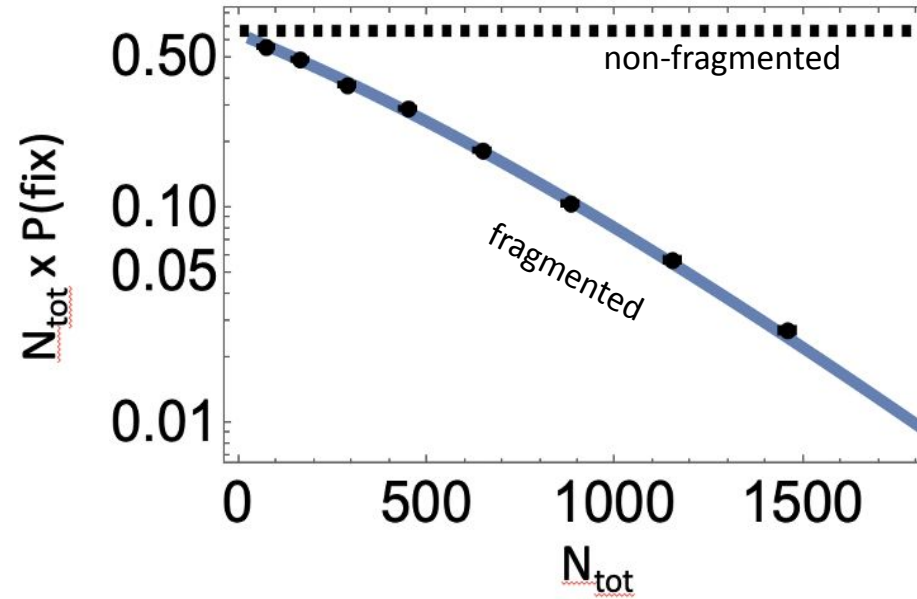
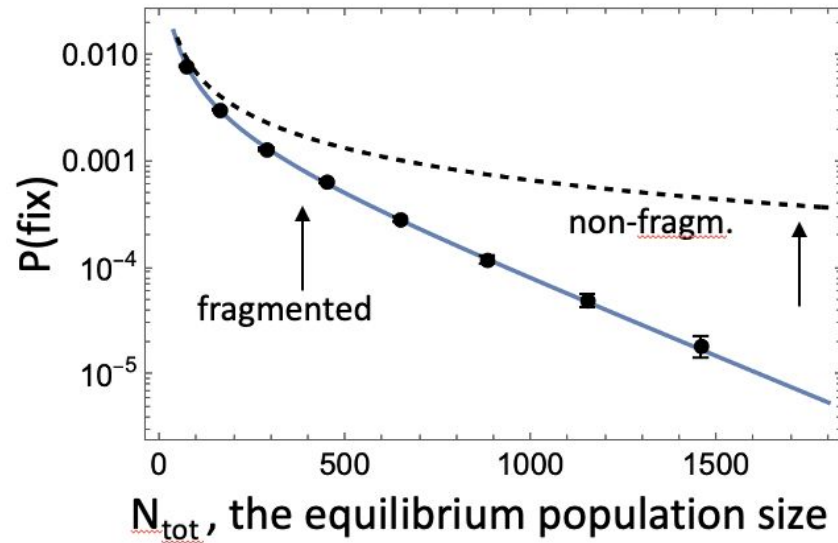
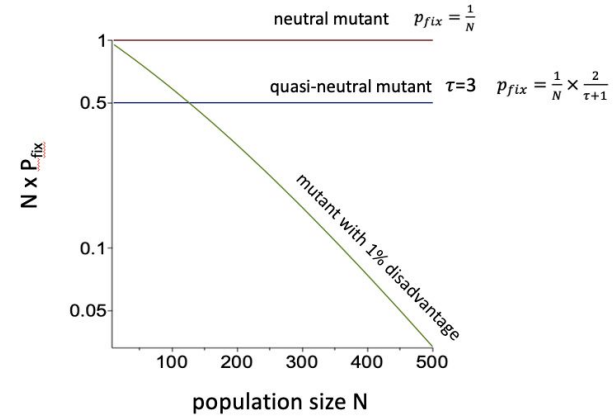
Reproduction can lead to the offspring being placed into a randomly chosen deme with a certain probability.
i.e. migration is coupled to reproduction.

=> WT population is at equilibrium. Introduce 1 mutant into a randomly chosen deme

SPATIAL STRUCTURE MAKES A QUASI-NEUTRAL MUTANT TRULY DISADVANTAGEOUS

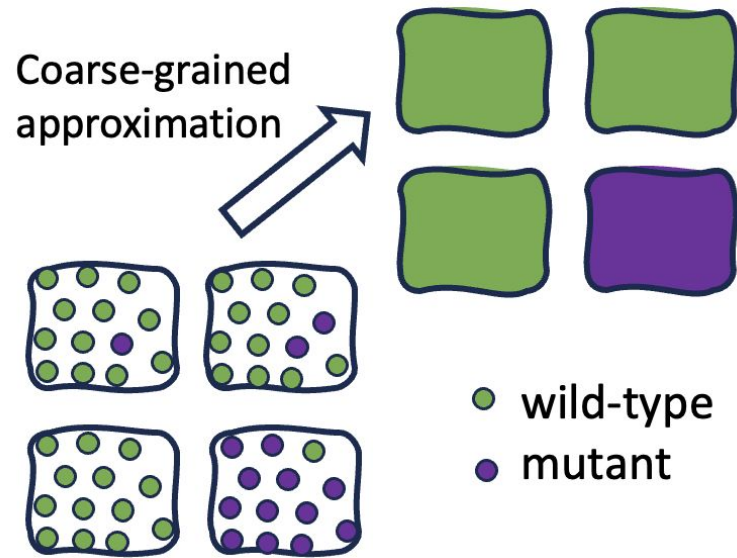
DESPITE IDENTICAL REPRODUCTIVE SUCCESS

non-spatial



In a deme-structured model, the quasi-neutral mutant becomes truly disadvantageous, even though it has the same life-time reproductive success compared to WT

Calculating stuff



assumptions:

1. mutation rate is sufficiently low such that individual demes are typically homogeneous with respect to the type
2. Small deme population size

ρ_m probability of a single mutant to fixate in an isolated wild-type deme

ρ_w probability of a single wild-type individual to fixate in an isolated mutant deme.

$$\Pi_1^{frag} \approx \rho_m \frac{1 - \frac{1}{\mathcal{F}}}{1 - \frac{1}{\mathcal{F}D}}$$

$\mathcal{F} = \tau \frac{\rho_m}{\rho_w}$ = relative fitness of a mutant deme

defined by the ratio of the 2 deme conversion rates

For large populations, we have $\frac{\rho_m}{\rho_w} = \frac{1}{\tau}$ and hence $\mathcal{F}=1$
so the effect is lost

A BIOLOGICALLY MORE REALISTIC SCENARIO: A MUTANT WITH A CHANGED LIFE-TIME REPRODUCTIVE OUTPUT & ALSO PROPORTIONALLY SCALED BIRTH AND DEATH RATES

$$r_m = \tau (1+s)r_w$$

$$d_m = \tau d_w$$

$s > 1$: mutant has higher reproductive output than WT

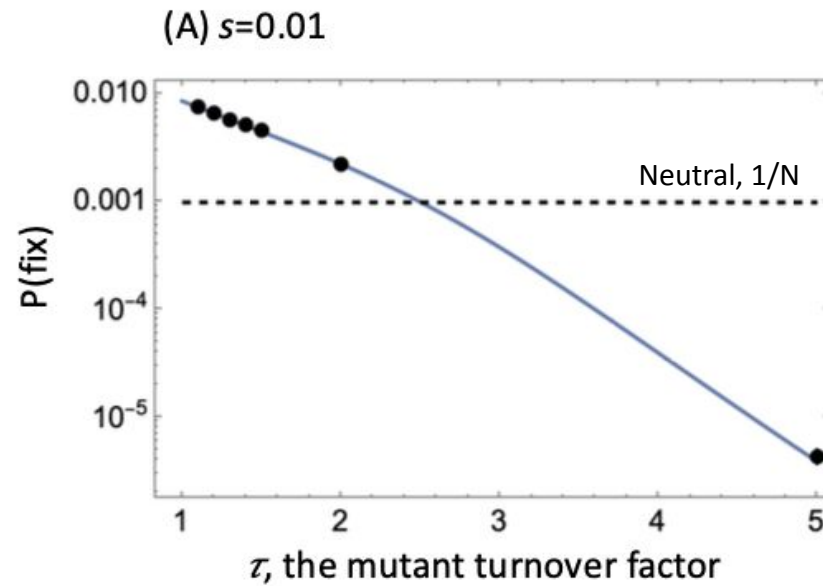
$s < 1$: mutant has lower reproductive output than WT

When the turnover parameter $\tau=1$, a mutant is advantageous if $s>1$ and disadvantageous if $s<1$.

What happens if the turnover parameter, τ , deviates from 1?

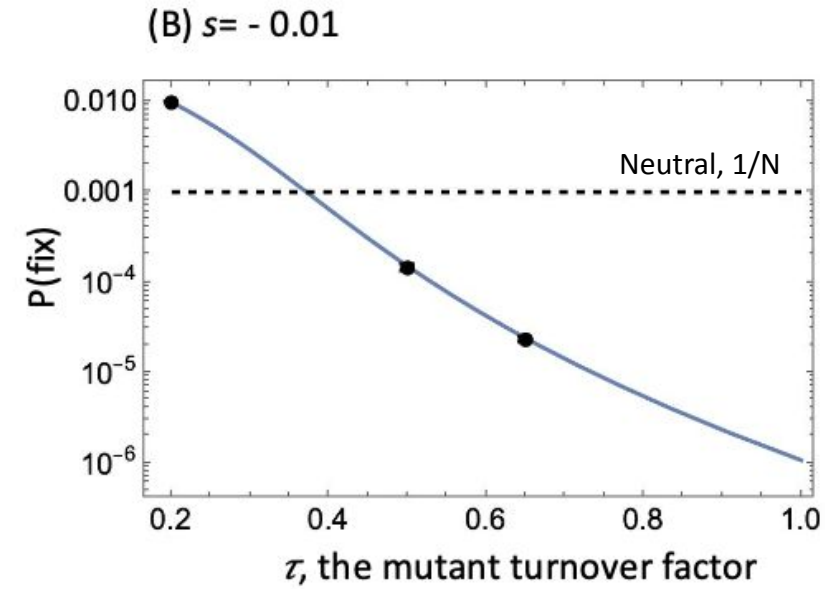
SPATIAL STRUCTURE REVERSES SELECTION

Mutant with higher reproductive output



A mutant with a **higher reproductive output** than WT can become **strongly disadvantageous** if it also has higher turnover

Mutant with lower reproductive output



A mutant with a **lower reproductive output** than WT can become **advantageous** if it also has lower turnover

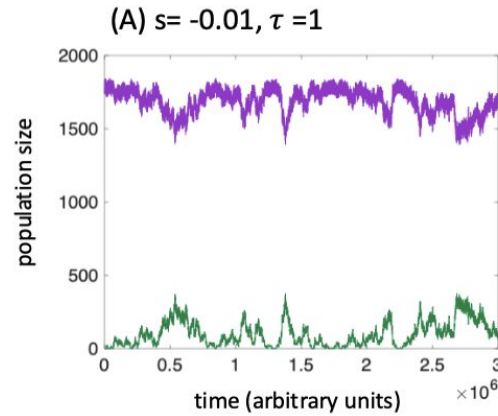
Relationship between life-time reproductive success and Darwinian fitness is more complex than previously appreciated

MOVE AWAY FROM FIXATION PROBABILITIES:

Assume that mutant is generated by WT a certain rate

Mutant with lower
life-time reproductive
output

mutant with **LOWER** life-time
reproductive output than WT



WT wins for $\tau = 1$ (identical turnover)

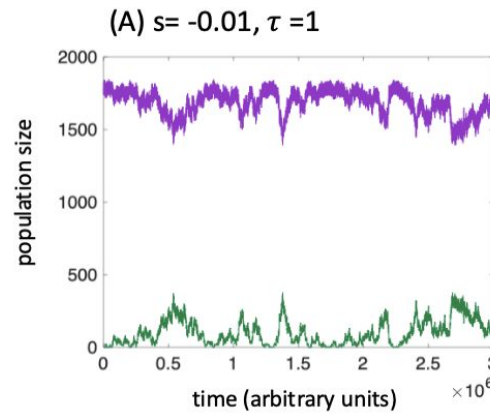
mutant persists at
mutation-selection balance

MOVE AWAY FROM FIXATION PROBABILITIES:

Assume that mutant is generated by WT a certain rate

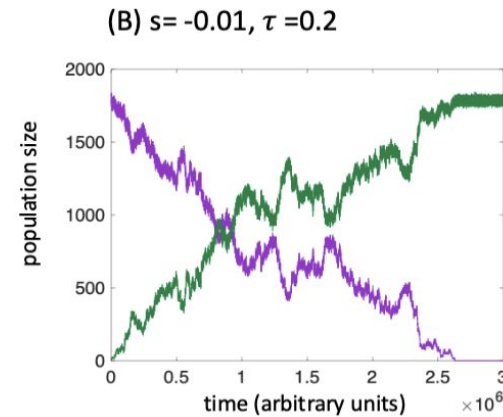
Mutant with lower
life-time reproductive
output

mutant with **LOWER** life-time
reproductive output than WT



WT wins

mutant persists at
mutation-selection balance



mutant invades and takes over
with reduced turnover ($\tau < 1$)

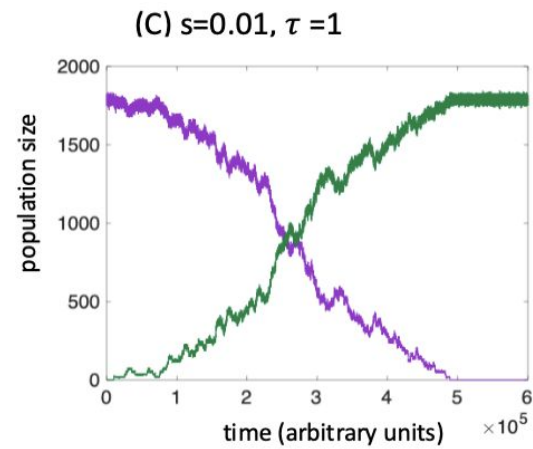
MOVE AWAY FROM FIXATION PROBABILITIES:

Assume that mutant is generated by WT a certain rate

Mutant with higher
life-time reproductive
output

mutant with **HIGHER** life-time
reproductive output than WT

mutant takes over if it has
identical turnover ($\tau = 1$)



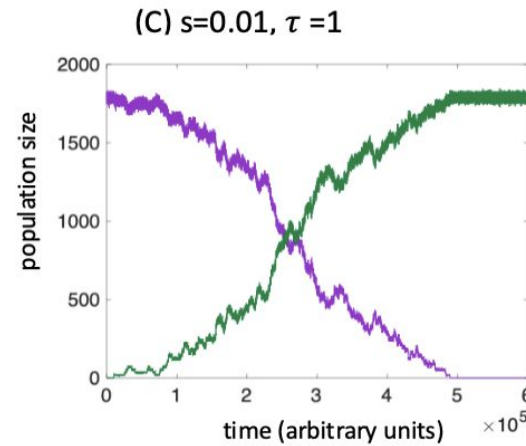
MOVE AWAY FROM FIXATION PROBABILITIES:

Assume that mutant is generated by WT a certain rate

Mutant with higher
life-time reproductive
output

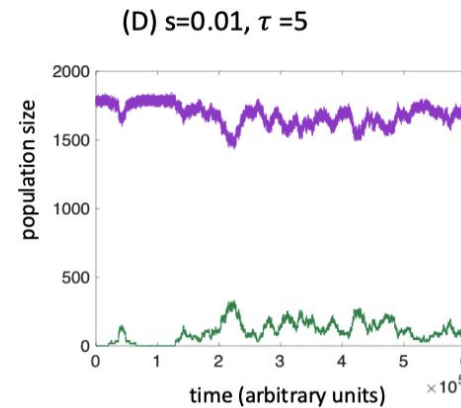
mutant with **HIGHER** life-time
reproductive output than WT

mutant takes over if it has
identical turnover ($\tau = 1$)

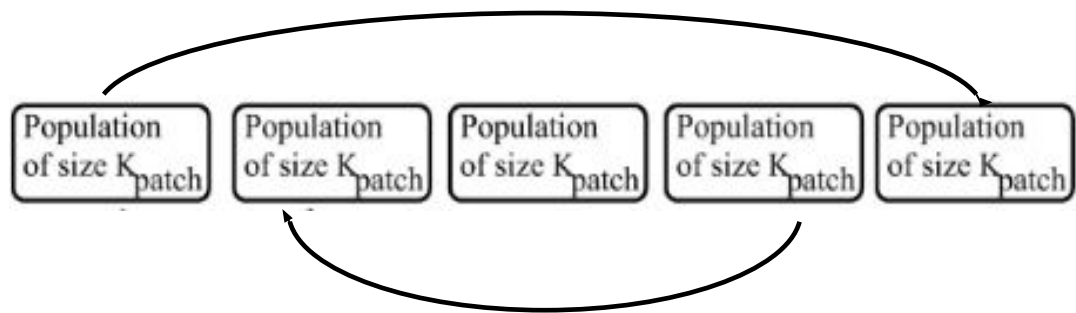


mutant becomes disadvantageous
if it also has a higher turnover ($\tau > 1$)

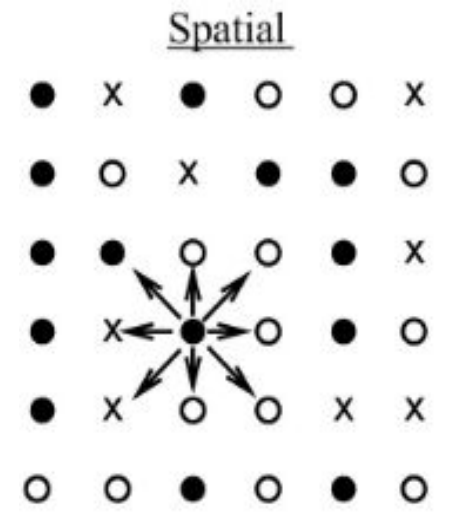
mutant persists at
mutation-selection balance



deme model with non-spatial migration



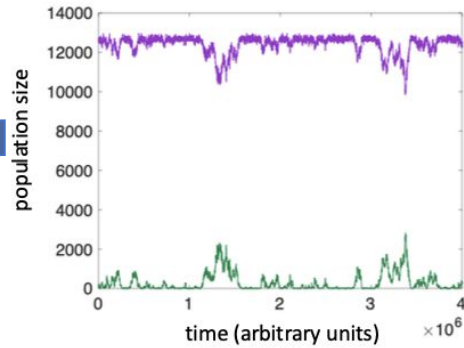
Agent-based model



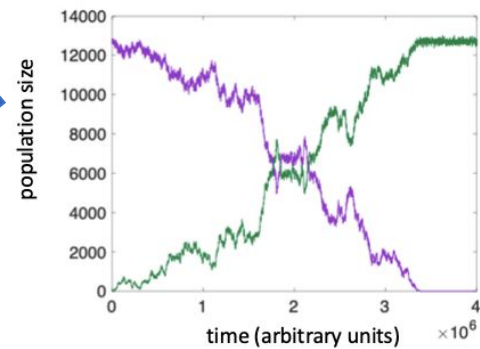
Spatial agent-based model has same basic properties as deme model with non-spatial migration

Mutant with LOWER reproductive output

(A) $s = -0.001, \tau = 1$

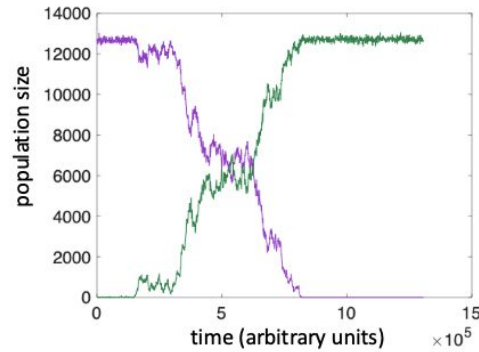


(B) $s = -0.001, \tau = 0.1$

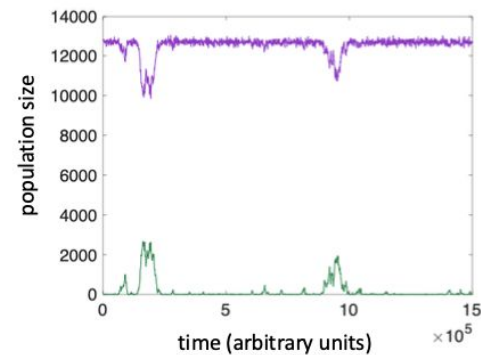


Mutant with HIGHER reproductive output

(C) $s = 0.001, \tau = 1$



(D) $s = 0.001, \tau = 3$



Mutant and WT have identical turnover

Mutant has changed turnover

Takeaway messages

Spatial structure can have important consequence on evolutionary dynamics

These can be found in relatively simple models of spatial cell dynamics

Such insights inform computational models that describe specific cancers and take into account the higher biological complexities seen in the spatial organization of tumors (eg cancer stem cells, differentiated cells, microenvironment)

Lab at UCSD



Samrat Sohel Mondal
Postdoctoral Scholar



Sydney Ackermann
PhD Student



Ramanarayanan Kizhuttill
PhD Student



Abhinav Kannan
Masters Student

Collaborators

Justin Pritchard (Penn State)
Angela Fleischman (UC Irvine)
Natalia Komarova (UC San Diego)

Former Lab members

Yufei Zhang
Peter Uhl
Wen-Jian Chung
Yifan Wang
Ignacio Rodriguez-Brenes
Shaun Stipp
Jesse Kreger
Elvira Kadaub
John Lau
Dustin Phan
Sarah Roy
Zhiying Sun

